

**KARADENIZ TECHNICAL UNIVERSITY  
THE GRADUATE SCHOOL OF NATURAL AND APPLIED SCIENCES**

**ELECTRICAL AND ELECTRONICS ENGINEERING GRADUATE PROGRAM**

**DEVELOPMENT OF NOVEL PHYSIOLOGICAL ANALYSIS METHODS BASED ON  
DUAL-WAVELENGTH PHOTOPLETHYSMOGRAPHIC SIGNALS TIME DIFFERENCES**

**Ph.D. THESIS**

**Nader VAHDANI MANAF, M.Sc.E.**

**JANUARY 2016**

**TRABZON**



**KARADENİZ TEKNİK ÜNİVERSİTESİ**

**THE GRADUATE SCHOOL OF NATURAL AND APPLIED SCIENCES**

**ELECTRICAL AND ELECTRONICS ENGINEERING GRADUATE PROGRAM**

**DEVELOPMENT OF NOVEL PHYSIOLOGICAL ANALYSIS METHODS BASED ON  
DUAL-WAVELENGTH PHOTOPLETHYSMOGRAPHIC SIGNALS TIME  
DIFFERENCES**

**Nader VAHDANI MANAF, M.Sc.E.**

**This Thesis is Accepted to Give the Degree of**

**"DOCTOR OF PHILOSOPHY IN ELECTRONIC ENGINEERING"**

**By The Graduate School of Natural and Applied Sciences**

**at Karadeniz Technical University**

**The date of Submission : 15/12/2015**

**The date of examination : 20/01/2016**

**Thesis Supervisor : Prof. Dr. Temel KAYIKÇIOĞLU**

**Trabzon 2016**

**KARADENİZ TECHNICAL UNIVERSITY  
THE GRADUATE SCHOOL OF NATURAL and APPLIED SCIENCES**

**Electrical and Electronics Engineering Graduate Program**

**The thesis entitled:**

**DEVELOPMENT OF NOVEL PHYSIOLOGICAL ANALYSIS METHODS  
BASED ON DUAL-WAVELENGTH PHTOPLETHYSMOGRAPHIC SIGNALS  
TIME DIFFERENCES**

**Prepared by Nader Vahdani Manaf**

**has been accepted as a thesis of**

**DOCTOR OF PHILOSOPHY**

**after the examination by the jury assigned by the Administrative Board of the  
Graduate School of Natural and Applied Sciences with the decision number  
1631**

**dated 15/12/2015**

**Examining Committee Members**

**Supervisor : Prof. Dr. Temel KAYIKÇIOĞLU .....**

**Member : Prof. Dr. Ali GANGAL .....**

**Member : Prof. Dr. Cemal KÖSE .....**

**Member : Prof. Dr. Osman EROĞUL .....**

**Member : Prof. Dr. Ziya TELATAR .....**

**Prof. Dr. Sadettin KORKMAZ  
Director**

## FOREWORD

I would like to express my appreciation to my supervisors Temel KAYIKÇIOĞLU for his indefatigable enthusiasm and piquancy. This research was conducted in the Department of Electronic Engineering at Karadeniz Technical University and I would like to take the opportunity to thank the administrative, technical, and academic staff, as well as the postgraduate researchers of the department.

To all member of the Department of Electrical and Electronics Engineering, both past and present, I want to give very sincere thanks to them for their support of my research and continuing friendship. I enjoyed every minute of working with them and wish them all the best. I especially would like to thank Önder aydemir and Mehmet Öztürkfor all of the good times, both in and out of the department.

Finally, my greatest thanks go to my family for their ongoing love and encouragement; I could not have done this without you.

Nader Vahdani Manaf  
Trabzon 2015

## **THESIS STATEMENT**

I declare that, this PhD thesis, I have submitted with the title “Development of novel physiological analysis methods based on dual-wavelength photoplethysmographic signals time differences” has been completed under the guidance of my PhD supervisor Prof. Dr. Temel KAYIKÇIOĞLU. All the data used in this thesis were obtained experimental works done as parts of this thesis in our research labs. All referred information used in the thesis has been indicated in the text and cited in reference list. I have obeyed all research and ethical rules during my research and I accept all responsibility if proven otherwise.15/12/2015

Nader Vahdani Manaf

## TABLE OF CONTENTS

|   | <u>PAGE NO</u> |
|---|----------------|
| FOREWORD.....                                     | III            |
| THESIS STATEMENT.....                             | IV             |
| TABLE OF CONTENTS.....                            | V              |
| ÖZET.....   | IX             |
| SUMMARY.....                                      | X              |
| LIST OF FIGURES.....                              | XI             |
| LIST OF TABLES.....                               | XIII           |
| LIST OF SYMBOLS.....                              | XIV            |
| 1. GENERAL INFORMATION.....                       | 1              |
| 1.1. Introduction.....                            | 1              |
| 1.2. The Main Applications of PPG.....            | 4              |
| 1.2.1. Blood Pressure Estimation.....             | 4              |
| 1.2.2. Respiratory Monitoring.....                | 5              |
| 1.2.3. Apnea Detection.....                       | 6              |
| 1.2.4. Pulse Oximetry.....                        | 6              |
| 1.2.5. Assessment of Arterial Disease.....        | 7              |
| 1.3. The Basics of PPG Pulse.....                 | 8              |
| 1.4. Optimum Placement of LED and Photodiode..... | 10             |
| 1.5. Suitable Wavelengths.....                    | 10             |
| 1.6. Characteristic Parameters of PPG Pulses..... | 11             |
| 1.7. Photoplethysmographic Signals.....           | 12             |
| 1.8. Artifacts in PPG.....                        | 13             |
| 1.9. Methods of Light Detection.....              | 14             |
| 1.10. Simple and Complex PPG.....                 | 15             |
| 1.10.1. Simple PPG.....                           | 15             |
| 1.10.2. Complex (Multi-Wavelength) PPG.....       | 15             |
| 1.10.3. Time Division Multiplexing (TDM).....     | 16             |
| 1.10.4. Disadvantages of TDM Method.....          | 18             |
| 1.11. Aims and Objectives.....                    | 18             |
| 1.12. Thesis overview.....                        | 19             |
| 2. MATERIALS and METHODS.....                     | 20             |

|          |  |    |
|----------|--|----|
| 2.1.     | Planning of the Studies .....  | 20 |
| 2.1.1.   | Study (1): New method to Obtain Dual-Wavelength PPG Signals .....      | 20 |
| 2.1.2.   | Study (2): Bio-Physiological Analysis Based on TD Variations .....     | 20 |
| 2.1.3.   | Study (3): Using TDs to Assess Respiratory System .....                | 21 |
| 2.1.4.   | Study (4): Biological Assessments by Using of Multi-Wavelength TDs.... | 21 |
| 2.1.5.   | Study (5): Apnea Detection Using TDs.....                              | 21 |
| 2.1.6.   | Study (6): Use of TDs for Wake/Sleep Classification.....               | 21 |
| 2.1.7.   | Study (7): Comparing PTTs Obtained from ECG and Different PPGs.....    | 22 |
| 2.1.8.   | Study (8): Compare Simultaneous TDs and PTTs in Exercise Test.....     | 22 |
| 2.2.     | Sensor Systems .....   | 22 |
| 2.2.1.   | Proposed Dual-Wavelength PPG Sensor System .....                       | 23 |
| 2.2.2.   | Dual-Element Photodiode.....   | 25 |
| 2.2.3.   | RGB and IR LEDs .....  | 25 |
| 2.2.4.   | ECG System .....   | 27 |
| 2.2.5.   | Acquiring Data Using Audio Codec.....                                  | 28 |
| 2.3.     | Host Computer Installed Program .....                                  | 29 |
| 2.4.     | Experimental Setup to Collect PPG Data.....                            | 29 |
| 2.5.     | Experimental Protocols.....  | 30 |
| 2.5.1.   | Experimental Protocol for the Study (1).....                           | 30 |
| 2.5.2.   | Experimental Protocol for the Study (2).....                           | 31 |
| 2.5.3.   | Experimental Protocol for the Study (3).....                           | 32 |
| 2.5.4.   | Experimental Protocol for the Study (4).....                           | 32 |
| 2.5.5.   | Experimental Protocol for the Study (5).....                           | 33 |
| 2.5.6.   | Experimental Protocol for the Study (6).....                           | 33 |
| 2.5.7.   | Experimental Protocol for the Study (7).....                           | 34 |
| 2.5.8.   | Experimental Protocol for the Study (8).....                           | 34 |
| 2.6.     | Preprocessing.....   | 34 |
| 2.6.1.   | Filtering and Noise Cancelation .....                                  | 35 |
| 2.6.1.1. | Band pass filtering.....   | 35 |
| 2.6.1.2. | Smoothing and Detrending .....   | 38 |
| 2.6.2.   | Removal of DC Component .....  | 39 |
| 2.6.3.   | Normalization .....  | 42 |
| 2.6.4.   | Peak Detection .....   | 43 |
| 2.7.     | Calculation of TDs.....  | 44 |

|          |  |    |
|----------|--|----|
| 2.8.     | Features and Specifications Used in Each Study.....    | 48 |
| 2.8.1.   | Features Used in the Study (1) .....                   | 49 |
| 2.8.2.   | Features Used in the Study (2) .....                   | 49 |
| 2.8.3.   | Features Used in the the the the Study (3).....        | 50 |
| 2.8.4.   | Features Used in the the Study (4).....                | 51 |
| 2.8.5.   | Features Used in the Study (5) .....                   | 52 |
| 2.8.6.   | Features Used in the Study (6) .....                   | 52 |
| 2.8.7.   | Features Used in the Studies (7 and 8) .....           | 55 |
| 2.9.     | Analysis and Classification Methods.....               | 56 |
| 2.9.1.   | Statistical Analysis.....                              | 56 |
| 2.9.1.1. | T-test .....   | 56 |
| 2.9.2.   | Classification methods.....                            | 58 |
| 2.9.2.1. | k-Nearest Neighbor (k-NN) classifier .....             | 58 |
| 2.9.2.2. | Classifier Training Methods .....                      | 59 |
| 2.10.    | Analysis/Classification Method Used in Each Study..... | 60 |
| 2.10.1.  | Study (1); Statistical Analysis .....                  | 60 |
| 2.10.2.  | Study (2); Statistical Analysis .....                  | 60 |
| 2.10.3.  | Study (3); Statistical Analysis .....                  | 61 |
| 2.10.4.  | Study (4); Statistical Analysis .....                  | 61 |
| 2.10.5.  | Study (5); k-NN classifier.....                        | 61 |
| 2.10.6.  | Study (6); k-NN classifier.....                        | 62 |
| 2.10.7.  | Studies (7 and 8); Statistical Analysis .....          | 62 |
| 3.       | RESULTS .....  | 63 |
| 3.1.     | The Results of the Study (1) .....                     | 63 |
| 3.2.     | The Results of the study (2).....                      | 64 |
| 3.3.     | The Results of the Study (3) .....                     | 69 |
| 3.4.     | The Results of the Study (4) .....                     | 73 |
| 3.5.     | The Results of the Study (5) .....                     | 75 |
| 3.6.     | The Results of the Study (6) .....                     | 77 |
| 3.7.     | The Results of the Study (7) .....                     | 80 |
| 3.8.     | The Results of the Study (8) .....                     | 82 |
| 4.       | DISCUSSION.....  | 83 |
| 5.       | CONCLUSIONS AND FUTURE WORKS.....                      | 86 |
| 6.       | REFERENCES .....                                       | 89 |



7. APPENDIX .....99  
CURRICULUM VITAE

Doktora Tezi

ÖZET

ÇİFT DALGABOYLU FOTOPLETİSMOGRAF İŞARETLERİNİN ZAMAN FARKI  
DEĞİŞİMLERİNE DAYALI YENİ FİZYOLOJİK ANALİZ YÖNTEMLERİNİN  
GELİŞTİRMESİ

Nader Vahdani Manaf

Karadeniz Teknik Üniversitesi  
Fen Bilimleri Enstitüsü  
Elektrik-Elektronik Mühendisliği Anabilim dalı  
Danışman: Prof. Dr. Temel KAYIKÇIOĞLU  
2015, 98 Sayfa, 16 Ek Sayfa

Fotopletismografi (PPG) sinyali, kalp faaliyetleri kaynaklı arteriyel kan miktarının değişimine bağlıdır. PPG, biyolojik ve fizyolojik değerlendirmelerde avantajlı bir ölçüm tekniği olarak kullanılmaktadır. Literatürde PPG analizlerinin çoğu, tek dalga boylu PPG darbesinin zaman ve frekans karakteristiklerine veya darbe şekline dayalıdır. Bu tezde, ilk kez olarak iki ayrı dalga boylu fotopletismografi (PPG) işareti arasındaki zaman farkları çıkarılmıştır ve bu farklar çift dalga boylu PPG sinyallerinin analizi için yeni bir yöntem olarak önerilmiştir. Çalışmada, öncelikle olarak veri kaydı ve işlemesi için bilgisayara bağlanabilen iki-dalga boylu PPG sensor sistemi geliştirilmiştir. Daha sonra her kalp atımı için oluşan PPG çiftleri arasındaki zaman farkları elde edilmiştir ve çeşitli fizyolojik durumların izlenmesinde kullanılmıştır. Elde edilen zaman farkı öznelikleri farklı çalışmalarla incelenmiştir. Verilerin analizi için istatistiksel analizler ve sınıflandırma algoritmaları kullanılmıştır. Sonuçlar incelendiğinde, değişik durumlarda farklı dalga boylu PPG işaretleri arasındaki zaman farklarının anlamlı bir değişim gösterdiği gözlemlenmiştir. Daha önce varılmamış (bildirilmemiş) olan bu olgu, yeni ve ilginç bir bulgu olarak tanımlanmıştır. Ayrıca, sınıflandırma sonuçlarında kullanılan zaman farkı özelliklerinin çeşitli fizyolojik durumların sınıflandırmasında yüksek bir potansiyele sahip olduğunu görülmüştür.

**Anahtar Kelimeler:** Çift-dalga boylu PPG işaretleri, Zaman farkı, Fizyoloji, Sınıflandırma

PhD. Thesis

SUMMARY

DEVELOPMENT of NOVEL PHYSIOLOGICAL ANALYSIS METHODS BASED ON  
DUAL-WAVELENGTH PHOTOPLETHYSMOGRAPHIC SIGNALS TIME  
DIFFERENCES

Nader Vahdani Manaf

Karadeniz Technical University  
The Graduate School of Natural and Applied Sciences  
Electrical and Electronics Engineering Program  
Supervisor: Prof. Dr. Temel KAYIKÇIOĞLU  
2015, 98 Pages, 16 Appendix Pages

Photoplethysmographic (PPG) signals are obtained by changes in the amount of arterial blood, which in turn depends on the heart activities. PPG has been used as an advantageous measurement technique in biological and physiological assessments. Most previous analyses of PPG signal were based on time and frequency domain characteristics or shape of the simple PPG signal with a unique wavelength of light. In the present thesis, for the first time, time difference variations between two simultaneous unlike PPG signals were extracted and proposed as a new strategy for the analysis of dual-wavelength PPG signals. An improved dual-channel PPG biosensor was developed to obtain simultaneous PPG signals with different wavelengths. Then, time differences between the obtained PPG pairs were extracted in each heartbeat and used for various physiological conditions monitoring. The extracted time difference features were analyzed in different studies. Statistical analysis and classification algorithms were used to analyze the obtained data. Results showed that different PPG signals had significant time difference variations (time shifts relative to each other) with changes in a psychophysical state of investigated subjects. This earlier unreported phenomenon would have been a novel and interesting finding. In addition, analyses and classification results showed that the used time difference features had very good potential to classify various bio-physiological conditions.

**Key Words:** Dual-wavelength PPG signals, Time difference, Physiology, Classification

## LIST OF FIGURES

### PAGE NO

|   |    |
|---|----|
| Figure 1.1. Simultaneous ECG and PPG signals and obtained PTT .....                 | 5  |
| Figure 1.2. A commercial pulse oximeter .....                                       | 7  |
| Figure 1.3. Light absorbance concept in pulse oximetry.....                         | 9  |
| Figure 1.4. Characteristic parameters of a single PPG pulse.....                    | 11 |
| Figure 1.5. (a) A sample short-term PPG signal (b) A sample.....                    | 12 |
| Figure 1.6. (a) Transmission and (b) reflection mode PPG sensors .....              | 14 |
| Figure 1.7. Instance timing for driving two different light sources.....            | 16 |
| Figure 1.8. Dual-wavelength PPG sensor using TDM method .....                       | 17 |
| Figure 1.9. Expanding dual-wavelength PPG sensor to four separate wavelengths ..... | 17 |
| Figure 2.1. Position of sensors and connections.....                                | 23 |
| Figure 2.2. A proposed block diagram for dual-wavelength PPG sensor .....           | 24 |
| Figure 2.3. Circuit diagram of the developed sensor system.....                     | 26 |
| Figure 2.4. Spectral response of S8753 photodiode [82] .....                        | 27 |
| Figure 2.5. Peak wavelength spectrum of used LEDs .....                             | 27 |
| Figure 2.6. Schematic diagram of 3-lead ECG recording system .....                  | 28 |
| Figure 2.7. Experimental setup.....   | 30 |
| Figure 2.8. (a) Time multiplexed PPG signals (b) Filtered PPG signals.....          | 37 |
| Figure 2.9. (a) Recorded PPG and (b) filtered PPG signals .....                     | 40 |
| Figure 2.10. PPG signals without DC component cancelling .....                      | 41 |
| Figure 2.11. PPG signals after cancelling DC component .....                        | 41 |
| Figure 2.12. Normalized PPG signals .....   | 42 |
| Figure 2.13. Peak points of PPG pulses and their time difference .....              | 44 |
| Figure 2.14. TDs between unlike PPG signals .....                                   | 45 |
| Figure 2.15. The algorithm to extract TDs .....                                     | 48 |
| Figure 2.16. TDs obtained in (a) wake and (b) deep sleep situations .....           | 50 |
| Figure 2.17. Scatter plot for (a) mean and (b) SD of TDs.....                       | 51 |
| Figure 2.18. Feature space formed by mean and SD of TDs .....                       | 51 |
| Figure 2.19. Feature space formed by $A_{FWHM}-\Delta t_r-\Delta t_f$ .....         | 53 |
| Figure 2.20. Red-IR PPG pulse pairs in (a) wake and (b) sleep conditions .....      | 54 |

|   |    |
|---|----|
| Figure 2.21. Sample EEG and dual-wavelength PPG signals obtained from two consequent heartbeats ..... | 55 |
| Figure 2.22. A simple example for $k$ -NN method .....  | 59 |
| Figure 2.23. Leave one-out cross-validation with N samples .....                                      | 60 |
| Figure 3.1. Bar plot for the mean and SE of TDs for both of the methods .....                         | 64 |
| Figure 3.2. TDs obtained from nonsmoking-smoking experiment .....                                     | 66 |
| Figure 3.3. TDs obtained from wakefulness-sleep experiment.....                                       | 66 |
| Figure 3.4. TD series obtained from rest-run experiment .....   | 67 |
| Figure 3.5. Error plot of quantitative analysis (means and SD) .....                                  | 68 |
| Figure 3.6. Means versus SD in (a) wake-sleep experiment (b) breath holding experiment .....          | 71 |
| Figure 3.7. Box-and-whisker diagram obtained from (a) mean and (b) SD of TDs .....                    | 72 |
| Figure 3.9. The mean of TDs for both breathing conditions .....                                       | 75 |
| Figure 3.10. (a) Training and (b) test data sets .....  | 78 |
| Figure 3.11. Error plot to compare PTTs obtained from ECG and different PPGs.....                     | 80 |
| Figure 3.12. ECG and dual-wavelength PPG (a) before and (b) during exercise test....                  | 82 |

## LIST OF TABLES

|   | <u>PAGE NO</u> |
|---|----------------|
| Table 1.1. Extinction coefficient with respect to wavelength .....                            | 10             |
| Table 2.1. The basic information of experimental protocols.....                               | 36             |
| Table 2.2. Used features and analysis/classification methods in each study.....               | 62             |
| Table 3.1. Results of t-test to compare proposed and TDM.....                                 | 64             |
| Table 3.2. Obtained TDs in various conditions (first iteration of the experiments).....       | 67             |
| Table 3.3. Obtained TDs in various conditions (second iteration of the experiments) ..        | 68             |
| Table 3.4. Results of t-test for the different experiments; study (2).....                    | 69             |
| Table 3.5. Obtained TDs in each experiment of the study (3).....                              | 70             |
| Table 3.6. The results of the t-test for the first experiment of study (3).....               | 72             |
| Table 3.7. The results of the t-test for the second experiment of study (3).....              | 73             |
| Table 3.8. Mean, SD and SE of TDs obtained in study (4).....                                  | 74             |
| Table 3.9. <i>P</i> value of the t-test for PPG pairs .....                                   | 75             |
| Table 3.10. Classification results in 10 separate data mixing; study (5).....                 | 76             |
| Table 3.11. Classification results in 10 separate data mixing; study (6).....                 | 79             |
| Table 3.12. Average±SD of classification results and the best <i>k</i> parameter .....        | 79             |
| Table 3.13. The mean, SD and SE of PTTs obtained by ECG and PPGs in different conditions..... | 81             |
| Table 3.14. The t-test results to compare PTTs in normal and apneateic breathing .....        | 81             |
| Table 3.15. PTTS and TDs (ms) obtained before and after the exercise test .....               | 82             |

## LIST OF SYMBOLS

|                  |   |   |
|------------------|---|---|
| $A_{FWHM}$       | : | Average Full Width Half Max                     |
| BP               | : | Blood Pressure                                  |
| $C_{Hb}$         | : | Concentration of Oxyhemoglobin                  |
| $C_{HbO_2}$      | : | Concentration of Reduced Hemoglobin             |
| $D_{PH}$         | : | Difference of Pulse Heights                     |
| ECG              | : | Electrocardiography                             |
| FWHM             | : | Full Width Half Max                             |
| Hb               | : | Reduced Hemoglobin                              |
| HbO <sub>2</sub> | : | Oxyhemoglobin                                   |
| HR               | : | Heart Rate                                      |
| HRV              | : | Heart Rate Variability                          |
| IR               | : | Infrared  |
| $k$ -NN          | : | $k$ Nearest Neighbor                            |
| LED              | : | Light Emitting Diode                            |
| PH               | : | Pulse Height                                    |
| PPG              | : | Photoplethysmography                            |
| PRV              | : | Pulse Rate Variability                          |
| PTT              | : | Pulse Transit Time                              |
| RGB              | : | Red-Green-Blue                                  |
| RIIV             | : | Respiratory Induced Intensity Variation         |
| RR               | : | Respiratory Rate                                |
| SD               | : | Standard Deviation                              |
| TDM              | : | Time Division Multiplexing                      |
| TD               | : | Time Difference                                 |
| USB              | : | Universal Serial Bus                            |
| $\Delta tp$      | : | Time difference between peak pointes            |
| $\Delta tr$      | : | Time difference between rising edges of pulses  |
| $\Delta tf$      | : | Time difference between falling edges of pulses |
| $\mu$            | : | Mean  |

## **1. GENERAL INFORMATION**

Photoplethysmography (PPG) is a noninvasive method to evaluate physiological parameters. Providing simple and continuous monitoring are some advantages of this technique. Tissue blood volume is changed in each heartbeat due to pumping of blood by the heart. PPG measures blood volume variations from the skin surface and is usually obtained non-invasively by biomedical devices such as pulse oximeters in which a photodetector is used to detect blood volume changes.

The arterial pulse waveform carries biological information about the blood properties, cardiovascular system and peripheral arteries. Thus, PPG signal could be employed to obtain information about the cardiac conduction and circulatory system. The most usual information extracted from the PPG signals are the pulse rate and pulse rate variability (PRV). Other important information such as heart rate (HR) and heart rate variability (HRV), respiratory rate (RR), blood pressure (BP) and blood glucose could be estimated using PPG.

Due to the existing of principal biological information in the PPG, analyzing the PPG signal can be an important procedure to assessment the status of human physiology. Until to now, many properties of PPG were studied, but attributes, physiological characteristics and different aspects of PPG not fully discovered yet and researches in this field continues unabated.

### **1.1. Introduction**

Providing noninvasive, simple and continuous biological monitoring are important goals in biomedical applications. Optical measurement of vital signs is one of the main noninvasive biomedical techniques and photoplethysmography is a most applicable instance of these technologies [1]. Photoplethysmography (PPG) is a photo-electric technique and PPG signals are obtained by using a light source and a photodetector simultaneously with changes in the amount of arterial blood, which in turn depends on the heart activities. Until recent decades, PPG was used for the evaluation of some biological parameters such as PR and PRV. However, need for reliable and inexpensive clinical



assessment techniques has led to further utilization of PPG based methods. PPG signals are carefully achieved and recorded by using suitable optical sensors which help researchers and clinicians for assessment of bio-physiological conditions or diagnosis and therapy of a variety of diseases. A detailed explanation about PPG principles will be revealed in 1.3 Section.

PPG is easy to use and strongly correlated with circulatory system and heart activities. The output of a PPG sensor is a signal called PPG signal and it has cardiovascular system related waveform named pulse waveform. This signal arises from the interaction of light with tissues. The complex interplay between light and biological tissue includes some optical processes such as scattering, absorption, reflection, transmission and fluorescence [2].

PPG characteristics such as pulse width [3], wave shape [4], and some other variables have been used in literature and there are many studies on these issues. For instance, Hertzman introduced some important properties of PPG signals [5]. He also, described that PPG pulses have two phases of rising pulse edge (anacrotic phase) and falling pulse edge (catacrotic phase) [6]. Measuring of blood oxygen saturation using PPG signals is another field of PPG applications and it is actually a well consolidated and widely adopted in the clinical routine technique known as pulse oximetry [7]. In the mentioned field, amplitude ratios of separate PPG signals with different wavelengths are used and blood oxygen saturation is obtained from the amplitude ratio of the signals. There are some other studies in which respiratory related amplitude modulated oscillations [8], respiratory rate [9] and fluorescence characteristics of human blood [1] were studied using PPG signals. There are also some researches which report a high correlation between HRV and PRV [10]. Furthermore, PPG could contain some other significant cardiovascular features, such as arterial stiffness [11] and cardiac output and systemic vascular resistance [12]. Use of derivatives of photoplethysmographic signals as biometric identification technique was another interesting application of PPG signals [13].

A diversity of procedures have been utilized to process PPG signals, the most usual of which are applying wavelet transform [14], digital filtering, feature extraction and time domain averaging [15-20], variety of motion artifact decreasing methods [21], using artificial neural networks [22, 23], types of modeling approaches [24, 25], principal

components analysis [26-28], chaos theory [29], correlation [30], and wave form derivatives [31]. In general, major features of PPG signals were as follows:

- Time and frequency domain characteristics of single wavelength PPG signal
- PPG features according to the wave shape (turning points and slope of the curve)
- Amplitudes ratio of different PPG signals with different wavelengths

In fact, important specifications of PPG signal that previously were used to biological measurements could be divided to the pulse-morphology-based methods and the pulse-occurrence-based methods.

Parametric modeling and classification of the photoplethysmographic signals were other research subjects. Classification accuracy is key issue in the corresponding applications and it depends largely upon the extracted features. A variety of approaches have been proposed to feature extraction from PPG signals, the most common of which are eigenvector methods [32], wavelet transform based feature extraction [33], system identification and transfer function modeling [34], features extraction in second derivative [35], frequency domain and spectral features [36]. In addition to above mentioned studies, morphological features of PPG signal have also been used in some other studies. The morphological techniques allowed the detection of many bio-physiological parameters by monitoring how the shape of each PPG pulse was changed over time [37]. Changes in the morphology of PPG pulse have been investigated in some cases such as detecting Hypovolemia [38], detection of the hemodynamic stress of exercise [39] and measuring changes in posture and orthostatic stress [40].

Some PPG analyses needed for an efficient mathematical modeling of the signal to increase measurement speed and get the most accurate feature extraction results. Curve fitting methods were widely used for parametric modeling of biological signals such as electroencephalographic (EEG) signals [41]. In the case of PPG signals there are also several studies that have used waveform fitting methods (which break down PPG pulse into several distinct sub-waveforms) for representation of PPG pulses. Published studies in this field contained analyzing PPG signals recorded concurrently from finger and ear using Gaussian functions [42] and Huotari's approach for representation of PPG pulses obtained from different body sites by fitting with lognormal functions [43,44]. In [42], a simple algorithm was presented by Rubins for extracting pulse parameters from PPG waveform.

Huotari's studies illustrated that parameters of the fitted models were extremely related to some cardiac system parameters.

Many properties of PPG were studied in literature, but all attributes and different aspects of PPG signals is not fully discovered yet [45]. Using of complex PPG signals with two (or more) simultaneous different PPG signals is relatively new field of researches and it is usually called dual (or multi)-wavelength PPG. In previous works, there are a few number of studies related to complex PPG signals with two or more unlike light wavelengths, the most of which are limited to application of amplitude ratios in order to pulse oximetry, analyzing vascular pressure variations at different depths of human skin [46] or analysis of skins blood circulation specifications [47,48]. Neither the mentioned studies nor any other study have considered the variations of time difference between separate PPG signals (phase shifts) with respect to physiological conditions of human. Actually, despite the fact that two-or more wavelength PPG signals have been used previously, none of the works have concentrated the time difference (TD) changes of distinct simultaneous PPG signals relative to each other in terms of individual's biological conditions.

## **1.2. The Main Applications of PPG**

The potential of photoplethysmography for evaluating vascular diseases has been recognized many decades ago. But, in more recent years, the need for small, accessible, reliable, cost effective, simple to use and non-invasive cardiovascular assessment techniques has led to greater use of PPG. This technique has been used in a wide range of clinical applications such as physiological monitoring, diseases diagnosis and cardiovascular assessments. Some important applications of PPG are described as follows:

### **1.2.1. Blood Pressure Estimation**

Estimating of blood pressure (BP) using PPG signals is one of the most interesting applications of photoplethysmographic signals. Measurement of BP is a major task to evaluate individual's biological situation and healthcare. BP can be estimated from pulse transit time (PTT). PTT can be calculated by measuring of beat-to-beat time differences

between an electrocardiographic (ECG) and a photoplethysmographic (PPG) signal. In fact PTT is the time delay between R point of ECG and peak point of PPG waveforms. Important advantage of this method is avoiding from using of cuff that it is customary in the usual methods of blood pressure measurement. Figure 1.1 shows typical PTT obtained by using concurrent ECG and PPG signals.

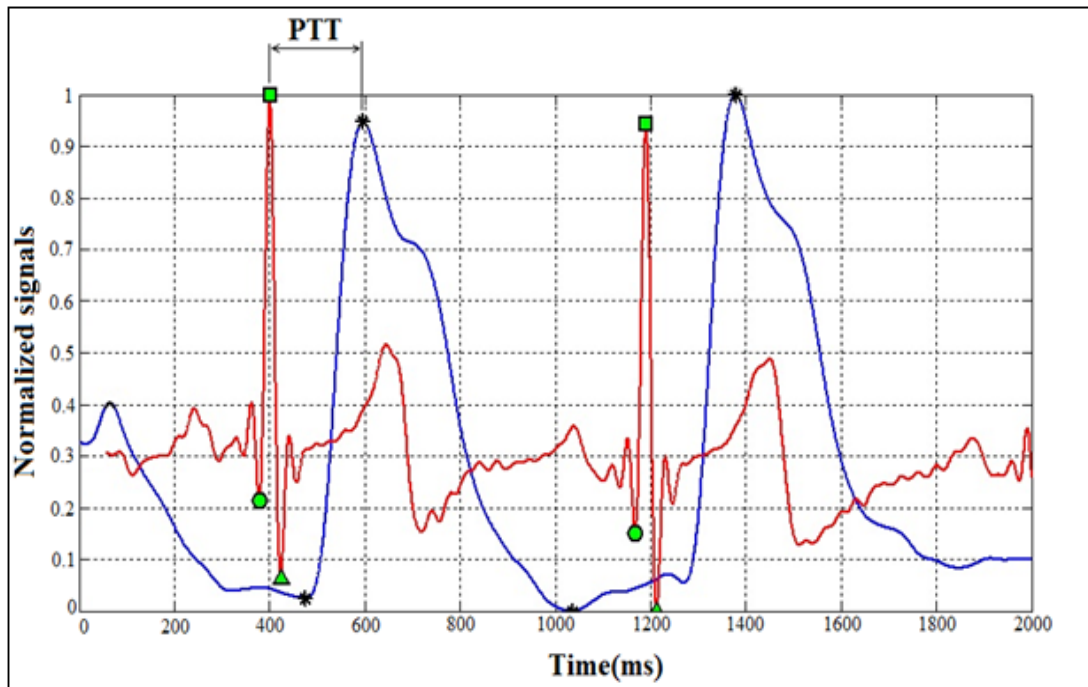


Figure 1.1. Simultaneous ECG and PPG signals and obtained PTT

### 1.2.2. Respiratory Monitoring

Monitoring of breathing is feasible using PPG. This is due to respiration causes changes in the peripheral system. Respiratory-induced intensity variations (RIIV) are well known issue and can be extracted from PPG signals [49]. RIIVs are amplitude modulated oscillations in PPG and are mainly due to the variations in venous return to the heart, caused by the alterations in intrathoracic pressure. The basics of RIIV is not fully understood, but is believed to be caused by skin blood volume fluctuations induced by the respiratory variations in intra-thoracic pressure transmitted to the measurement site by the venous system [50]. Using PPG for respiratory monitoring can be led to avoid from use of

types of gas sensors and face or nasal masks that are bothering the patient in the clinical or hospital applications.

### **1.2.3. Apnea Detection**

Central apnea is described as the incidence of a glancing pause of breathing, normally accompanied by a resting heart rate. So, each pause in respiration is named apnea. Apnea arises because of different reasons such as intermittent airway closure due to pharyngeal muscle relaxation and is a very common indication for several medical situations [51]. Another widespread reason for apnea is unripe birth [51]. Other reasons such as paroxysmal attacks, seizures, circulatory arrest, neurological disorders, head injury and drug overdose could be lead to apnea [52]. Apnea detection by PPG signals without using chemical or physical sensors is an advantageous technique in clinical uses.

### **1.2.4. Pulse Oximetry**

The oxygen carried in the blood is called the oxygen saturation level ( $SpO_2$ ). Each red blood cell contains several millions of Hemoglobin molecules. When it contains its full complement of four oxygen molecules, hemoglobin is known as Oxyhemoglobin ( $HbO_2$ ). If it contains no oxygen, it is referred to as Reduced Hemoglobin (Hb). An important and widely used application of PPG is a well-known evaluation technique called pulse oximetry and it is used to measure  $SpO_2$ . Pulse oximetry attempts to estimate the amount of oxygen contained in arterial red blood cells by non-invasively measuring the oxygen concentration at a peripheral point such as the finger. Pulse oximetry has been one of the most meaningful advances in biomedical engineering over the last few decades. Types of commercial pulse oximeters are available and used in many home or hospital applications. In pulse oximetry, a sensor probe is located on a small area of the subject's skin (often on the finger). The sensor illuminates two unlike wavelengths of light on the skin and transmitted lights are received by a photodetector. The technique calculates the absorbance difference of the wavelengths and measures the ratio of amplitude variations of the wavelengths relative to each other.  $SpO_2$  goes up or down according to how well a person

is breathing and how well blood is being pumped around the body.  $SpO_2$  is obtained by using the amplitudes ratio and can be calculated as Equation (1.1).

$$SpO_2 = \frac{100 \times C_{HbO_2}}{C_{HbO_2} + C_{Hb}} \% \quad (1.1)$$

where  $C_{HbO_2}$  and  $C_{Hb}$  refer to concentration of Oxyhemoglobin and Reduced Hemoglobin respectively. Typical reading for  $SpO_2$  value is usually between 95% and 100% in healthy humans. Variety types of pulse oximeters are commercially available. A portable instance of these devices can be seen in Figure 1.2.



Figure 1.2. A wireless commercial finger pulse oximeter

### 1.2.5. Assessment of Arterial Disease

Another field of PPG applications is assessing of peripheral arterial disease. There are several studies in the case of vascular evaluations by using PPG. Assessment of disease using PPG is feasible due to PPG pulse shape often is changed when severity of vascular disease is occurred [53-55]. PPG signal collection from multiple body sites have been used to evaluate peripheral vascular diseases in [56, 57]. Also, assessment of endothelial function and dysfunction in diabetic patients was assessed by using the PPG-extracted data

in studies [58, 59]. In another study, PPG signals recorded from healthy subjects and Raynaud's patients were analyzed [60]. The results of those study demonstrated that pulse shape was a reliable indicator of situation. In addition to above, PPG signal revealed significant capability for neurological evaluation, with the possibility to present new vision for the nervous systems [61-63].

### **1.3. The Basics of PPG Pulse**

PPG provides the necessary ground to monitor heartbeat-synchronized blood volume variations in microvascular beds. This technology has been applied in a wide range of clinical aims, by the help of commercial medical instruments. As mentioned before, instance of these devices are pulse oximeters, vascular diagnostics and digital beat-to-beat blood pressure measurement devices [64]. The amplitude of PPG signal depends on the measurement device and can change from a few millivolts to several volts. PPG signals have a small frequency band that may change in the range of 0.5-5 Hz.

PPG technique is based on the measuring of the optical response of a small region of the skin surface. Blood is driven by the heart all over the body arteries in a rhythmic mode called cardiac cycle. It was turned out that PPG pulse mainly represents the flow of blood in the arteries of the region being considered [65].

PPG pulse consists of AC and DC components [66]. The pulsatile component of the PPG is called 'AC' component. Basic frequency of AC component related to cardiac cycle is about 1 Hz (it may be changed depending on individual's heart rate) [66]. AC component is modulated onto a non-pulsating DC component relevant to the tissues and average blood volume. DC component may changes slowly due to some reasons such as respiration.

The light has a complex interplay with biological cells. It contains the optical processes such as scattering, absorption, reflection, transmission and fluorescence [2]. Beer-Lambert's law can support the concept of the light absorbance and its interaction with the vital tissue. This law expresses the debilitation of light passing through an absorbing material. When a single wavelength light with the intensity of  $I_0$  enters a matter, a portion of the light is transmitted through the matter, but another portion is absorbed. The intensity of light passing through the matter is reduced in exponential form.

Output light intensity is called  $I$  and can be defined as:

$$I = I_0 e^{-\varepsilon(\lambda)cd} \quad (1.2)$$

where  $\varepsilon(\lambda)$  is the extinction coefficient or absorptivity of the absorbing matter at the wavelength of  $\lambda$ ,  $c$  is uniform concentration of the absorbing matter, and  $d$  is the optical path length. Beer-Lambert law can be extended for multiple absorbers in the cases with two or more light wavelengths as:

$$I = I_0 e^{-(\varepsilon_1(\lambda)c_1 + \varepsilon_2(\lambda)c_2 + \dots + \varepsilon_n(\lambda)c_n) d} \quad (1.3)$$

where  $\varepsilon_i(\lambda)$  are the respective extinction coefficients and  $c_i$  are the respective concentrations. Figure 1.3 shows the concept of light absorbance in pulse oximetry.

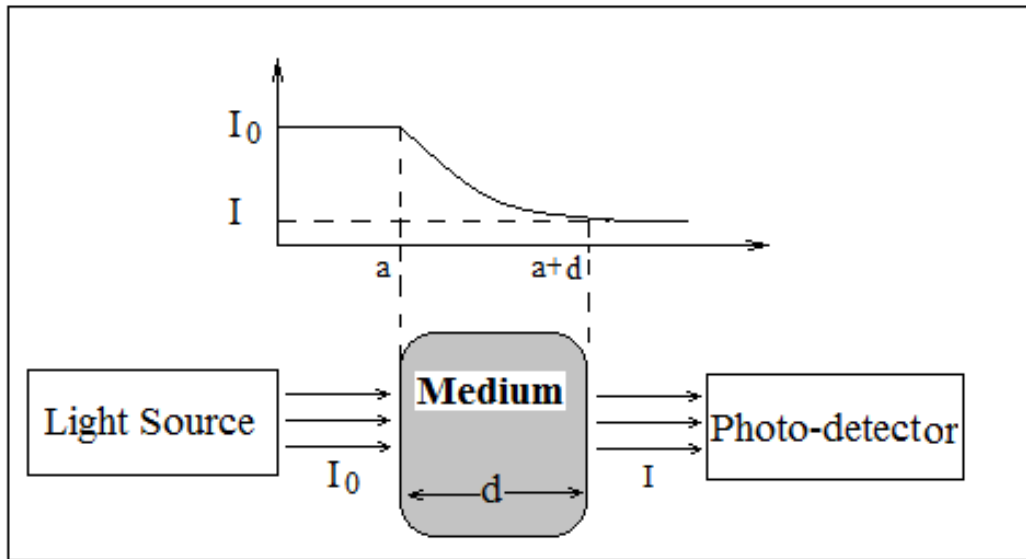


Figure 1.3. Light absorbance concept in pulse oximetry



Light absorbing components of blood are hemoglobin compounds (HbO<sub>2</sub> and Hb) and their extinction coefficients are changed with the wavelength [67-69]. Table (1.1) shows extinction coefficient variation in the wavelengths of 660nm and 940nm.

Table 1.1. Extinction coefficient with respect to wavelength

| Wavelength(nm) | Extinction Coefficient |                  |
|----------------|------------------------|------------------|
|                | Hb                     | HbO <sub>2</sub> |
| 660            | 0.81                   | 0.08             |
| 940            | 0.18                   | 0.29             |

#### 1.4. Optimum Placement of LED and Photodiode

The effect of the distance between the light source and the detector were studied in [70]. It was turned out that greater PPG amplitudes were obtained by installation the photodiode farther from the LED. However, since the optical path length was longer, higher LED driving currents were required to dominate the further absorption of light. This study also revealed that by installing more than one photodetector, a larger part of backscattered light can be detected and larger PPG amplitudes may be obtained.

In addition to above, there was a like inference about the distance between LEDs and photodetectors in [71]. It was concluded that the number of photodiodes was effective on the amount of detected light. That study revealed that 7mm was the optimal distance between the LED and photodiode to obtain the largest PPG signal.

#### 1.5. Suitable Wavelengths

In most PPG sensor systems wavelengths at which the blood volume is normally measured, are 660nm for visible light and 910 nm or 940 nm for infrared, but it is possible to apply PPG at different wavelengths and also with more than a single wavelength. The benefit to using several wavelengths is that it makes it able to measure amount of some blood dissolved gases. There are a few researches in which different light wavelengths

were used to obtain PPG signals. For example, red, green and blue PPG signals were applied for heart rate monitoring and compared with each other [72]. Also, changing the two selected wavelengths from 665/910 nm to 730/880nm to show a linear relationship for oxygen saturation rate was performed in [73]. According to conducted studies it can be said that each wavelength of light can be suitable for a particular aim.

### 1.6. Characteristic Parameters of PPG Pulses

The important characteristics of a single PPG pulse including pulse height, full width half max, peak of the pulse, rising edge and falling edge are labeled in Figure 1.4. The peak of pulse is the maximum value of PPG pulse. The Pulse Height (PH) is the difference between the maximum value of a pulse and minimum value of the same pulse. The Full Width Half Max (FWHM) is a statement of the width of a function, obtained by the difference between the two boundary values of a function at which the function is equal to half of its maximum value. In the case of PPG pulse, FWHM is the width of the pulse at half the maximum value of PPG pulse. The rising edge of the pulse is known as anacrotic phase and the falling edge as catacrotic phase [5, 6].

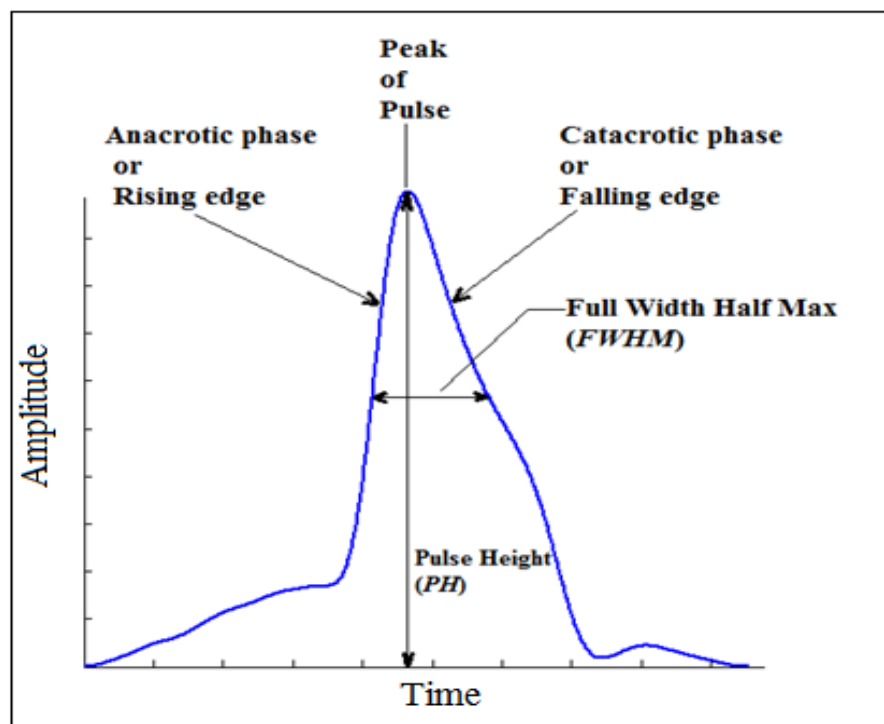


Figure 1.4. Characteristic parameters of a single PPG pulse

### 1.7. Photoplethysmographic Signals

In photoplethysmography, the light is illuminated by transmitter part of the sensor. The illuminated light may be reflected, absorbed or passed by different parts of the human skin, tissues or blood. In the receiver part of the sensor, arising light is detected as an electrical voltage that is called PPG signal. This analog signal is usually changed to a discrete signal by using different types of data acquisition devices to be able to record by digital computers. A typical short-term PPG signal in normal physiological conditions can be seen in Figure 1.5 (a). A long-term instance of PPG signal that was obtained for several minutes while the subject was in deep sleep has been shown in Figure 1.5 (b).

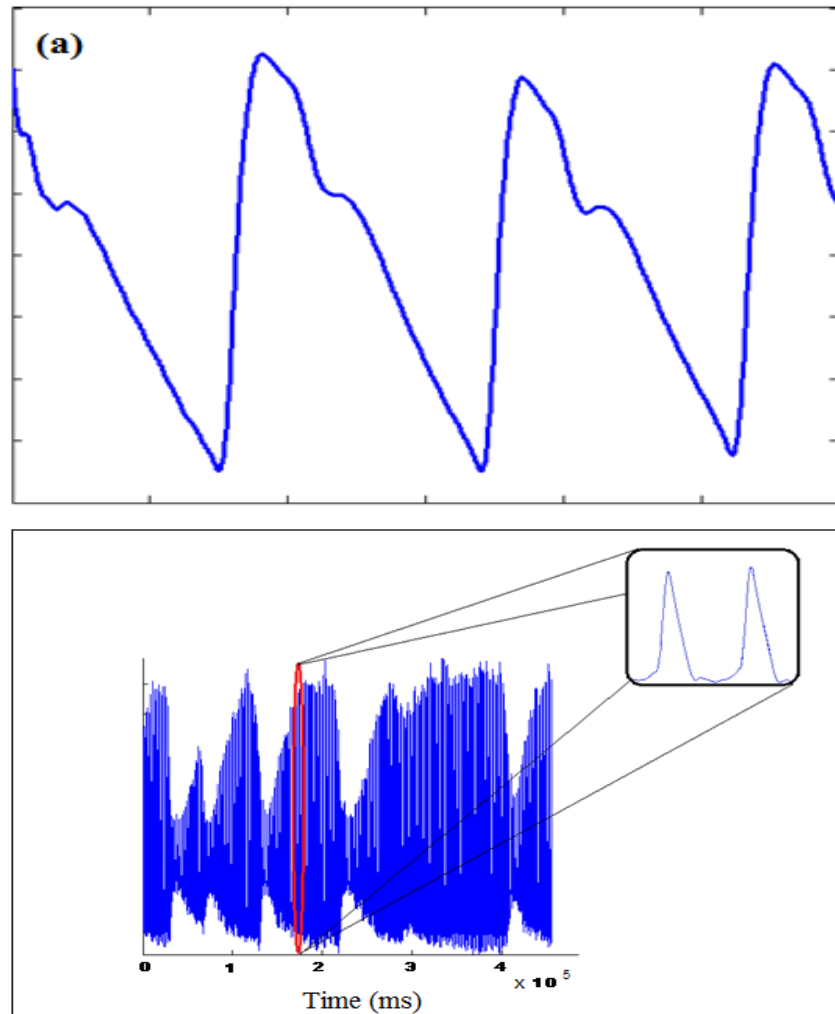


Figure 1.5. (a) A sample short-term PPG signal (b) A sample long-term PPG signal

### 1.8. Artifacts in PPG

PPG signals have a suitable structure for statistical analysis and signal processing operations. PPG has a good signal to noise ratio, but it may be affected by some unwanted factors such as noise, network initiative, environmental factors and so on. Some reasons that may be led to damage PPG signals can be mentioned as below:

- Abundance of the environmental light
- Colors and materials that are rubbed into the skin (Methylene blue, nail polish, henna)
- Adhesive bands
- Pigmentation (deep pigmentation makes a decrease in signal)
- Motion artifacts
- Low perfusion (the fall of cardiac output, hypothermia, decrease in systemic vascular resistance, shock and many others)
- Incorrect use of the sensor (optical shunt formation as a result of insufficient sensor contact)
- Network artifacts (radio waves, electrostatic artifacts and mains noise)

Variety types of methods may be used to decrease the effects of artifacts. Some of these methods are as below:

- Use accelerometer to detect the movement to decrease motion artifacts [74].
- Use DSP techniques to template match [75].
- Using of discrete saturation transforms (DST) [76].
- Many types of filtering techniques [77-79].
- Methods based on time and period domain analysis [80].

## 1.9. Methods of Light Detection

A PPG sensor system includes a transmitter part (light source) which emits visible (often a red LED with the wavelength of 660nm) or infrared (often an IR LED with the wavelength of 940nm) light onto the skin surface and illuminates a tissue bed. Some light is absorbed by blood, and the transmitted or reflected light (depending on the mode of PPG) is detected and recorded by a receiver part (a light-sensitive photodiode). Detection of light may be carried out either in transmission or reflection modes. In fact, PPG sensor systems are generally classified as transmission mode and reflectance mode [81]. Output magnitude of a transmission mode PPG is much greater than its reflection mode [64]. PPG measurement mode depends on the relative positions of the light source and photo-sensitive element. Figure 1.6 shows the placement of transmitter and receiver parts of the sensor for both of transmission mode and reflection mode PPG sensor systems.

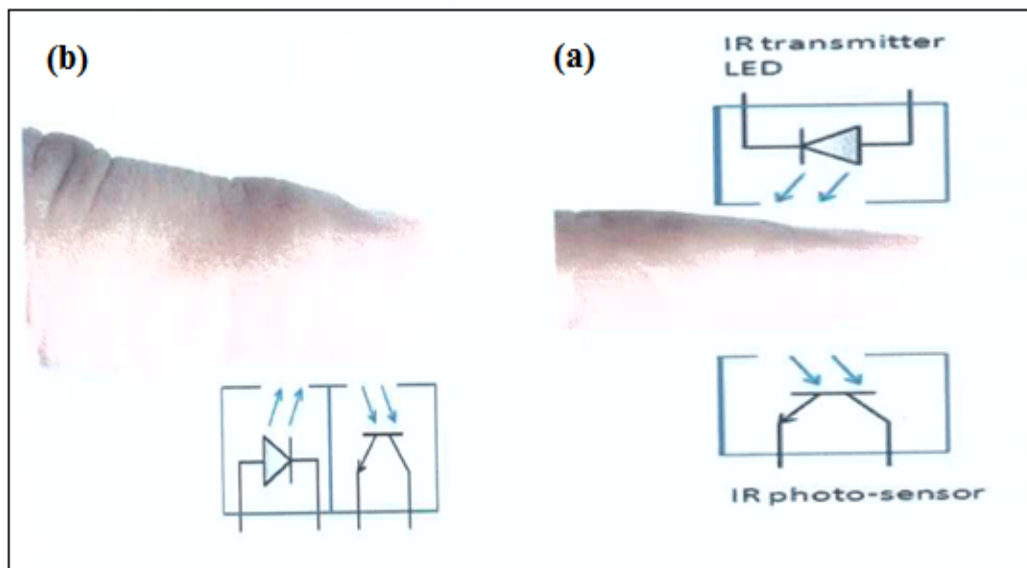


Figure 1.6. (a) Transmission and (b) reflection mode PPG types [81]

In the transmission mode PPG, skin is illuminated by the transmitter part of the sensor. Transmitted light is detected by the receiver part which is positioned on the opposite side of the transmitter in the measuring area. In different phases of a heartbeat (systolic and diastolic phases), blood volume is changed in tissues and so, the intensity of the absorbed and transmitted light is changed. Consequently, these light intensity

variations can be measured at the receiver part of the sensor. Transmission mode PPG sensors may be placed on different body sites such as finger, toe, ear or nose.

In the reflection mode PPG, both of the transmitter and receiver parts of the sensor are placed near each other on one side of the skin. Here, backscattered light (returned from different depths of the skin) is received by receiver sensor. A special opaque substance is normally placed between two parts of the sensor as a guard to avoid from direct radiation between the transmitter and the receiver without relation to the subject's body. This type of PPG sensors supports data acquisition from several body sites (such as chest, wrist, ankle and forehead).that is not available in the transmission mode PPG.

### **1.10. Simple and Complex PPG**

Apart from those already mentioned modes (transmission and reflection), PPG signal can be also classified with respect to another aspect as simple and complex signals. These concepts are described in the following subsections.

#### **1.10.1. Simple PPG**

In order to collect simple PPG data, a light source with a single wavelength of  $\lambda$ , is placed on the skin surface and a photo-detector receives the transmitted (or reflected) light. So, in this type of PPG, just one wavelength of light is used and the resulting signal is achieved with respect to transmittance/absorbance characteristics of the same wavelength of the light. Simple PPG is not applicable to assess biological parameters such as blood oxygen saturation (pulse oximetry) in which multiple factors (Hb and HbO<sub>2</sub>) need to be measured.

#### **1.10.2. Complex (Multi-Wavelength) PPG**

Some biological measurements need to two (or more) simultaneous PPG signals with different wavelengths. This complex kind of PPG is generally used for pulse oximetry and is called multi-wavelength PPG. To obtain a complex PPG data, the transmitter portion of the sensor needs to separate light sources, the wavelengths of which are  $\lambda_1, \lambda_2, \dots, \lambda_n$ . The

receiver part of the sensor, detects light intensities corresponded with each of the wavelengths separately. Time division multiplexing method is usually used for this end. This method is expressed in below.

### 1.10.3. Time Division Multiplexing (TDM)

In the existing multi-wavelength PPG biosensor devices with two or more wavelengths of emitting, a single photodetector with a wide spectral response -in the range visible and infrared light- is employed to detect all of the wavelengths. Separate light sources were driven and emitted different lights in sequence one after the other with a dark space between each of them (to prevent overlap) at a suitable repetition rate in antiparallel mode. This way, each of the different PPG waveforms with separate wavelengths was allotted a time division and their amplitudes in these time divisions were caught. In fact, PPG waveforms were multiplexed by sampling each of them at certain time divisions. This method was called time division multiplexing (TDM) approach. For instance of time multiplexing, timing diagram for driving two light sources (Red and IRLEDs) by TDM method with the emitting frequency of 1 KHz for each light source has been shown in Figure 1.7.

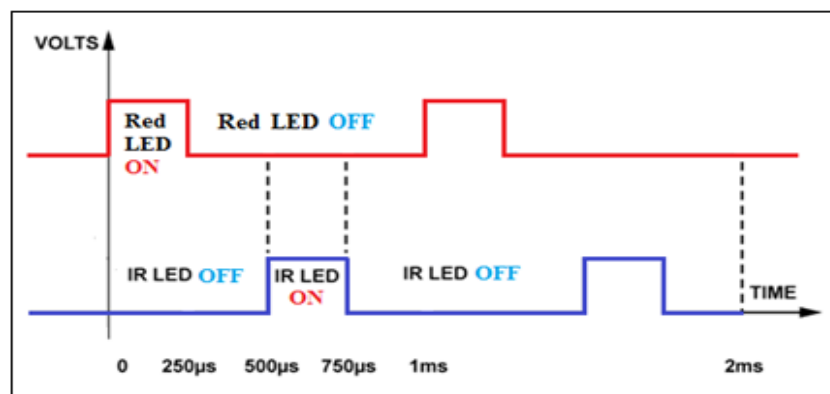


Figure 1.7. Instance timing for driving two different light sources

In the receiver portion of TDM based PPG sensor, multiplexed PPG signal is split into separate paths using sample and hold, preamplifier and pre-filtering circuits. Separated different PPG signals can be applied to a multi-channel data acquisition device to record

signals. Figure 1.8 shows a dual-wavelength PPG sensor system including Red and IR lights connected to a dual-channel audio codec as the acquisition device.

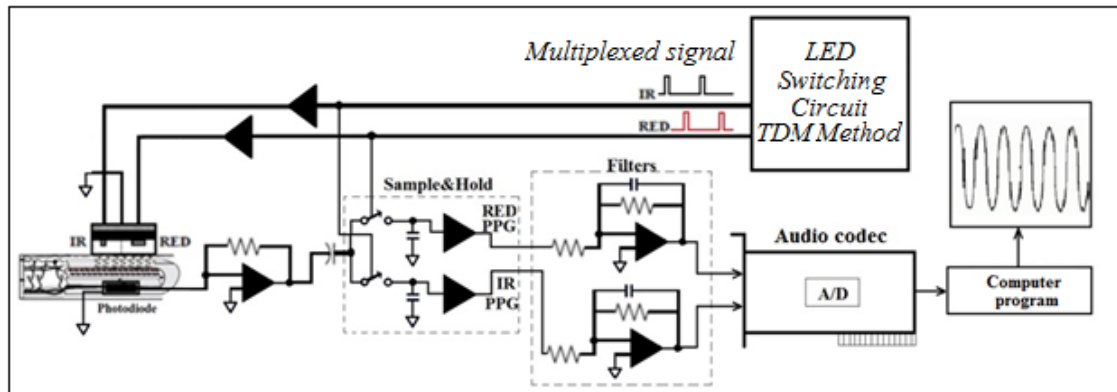


Figure 1.8. Dual-wavelength PPG sensor using TDM method

Dual-wavelength PPG system can be expanded to a system with further light wavelengths by using more emitting light sources. For example, a four wavelength PPG sensor system with the red, green, blue and IR lights has been revealed in Figure 1.9.

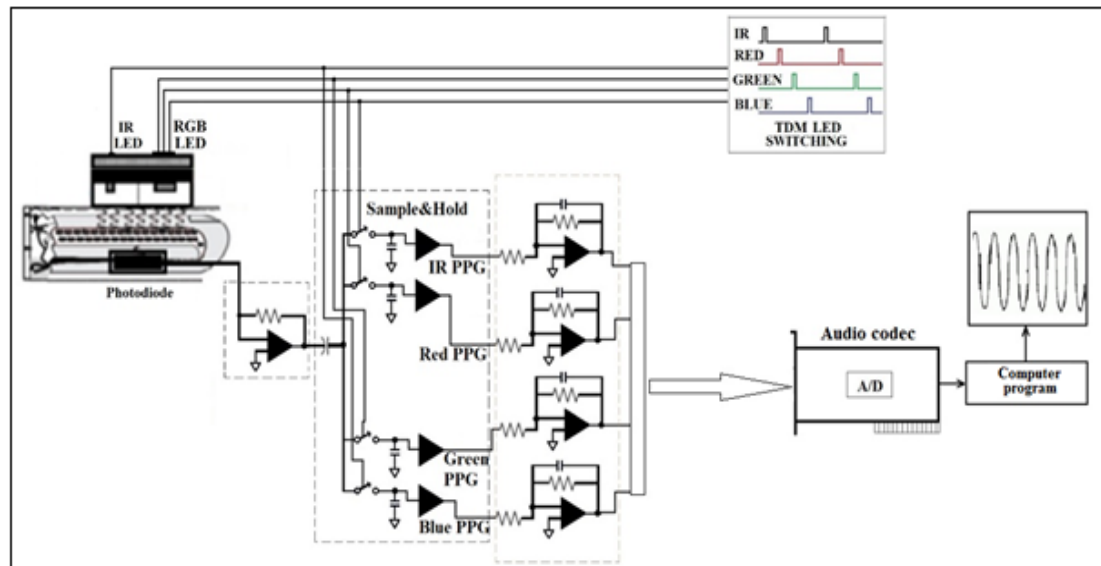


Figure 1.9. Expanding dual-wavelength PPG sensor to four separate wavelengths



#### **1.10.4. Disadvantages of TDM Method**

In TDM, light sources (LEDs) in the measurement setup are alternatively driven by impulses at a certain sampling rate. For instance, in the typical timing example presented in Figure 1.8 this rate was equal to 1000 Hz for each of LEDs. So, the IR and Red signals were not measured synchronously, but with the time delay of 0.5ms. Usually, the sampling rate is less than 1000Hz in real implementations and this makes it more inaccurate. Thus, TDM method can have serious challenges with applications in which synchronicity of PPG signals is important. In addition, there is a large switching noise in TDM method.

#### **1.11. Aims and Objectives**

The main aim of the present thesis was propose time differences (TDs) extracted from complex PPG signals as alternative physiological measure for interpretation of PPG signals. In this thesis, the possibility of using of dual-wavelength PPG signal to evaluate physiology of human was investigated with respect to the following specific objectives:

1. To introduce a new method for obtaining complex PPG signals -without disadvantages of TDM method (Study 1);
2. To analyze physiological situations by using of the introduced TD variations (Study 2);
3. To use TDs to assess respiratory system (Study 3);
4. To assess biological conditions by using of three different PPG pairs and compare between the pairs to determine the most suitable PPG pair (Study 4);
5. To Apply TDs for fast identification of apnea (Study 5);
6. To use TDs for fast and accurate wake/sleep classification (Study 6);
7. To compare PTTs obtained from an ECG signal and different PPG signals with separate wavelengths (Study 7);
8. To compare TDs and PTTs during exercise test (Study 8).

### **1.12. Thesis Overview**

The thesis is divided into five chapters. Chapter one begins by introducing research background, and includes research motivations, basic aspects of the PPG technique, understanding the principle of PPG, basic aspects of PPG technique, research aims and objectives. Chapter two presents the used tools, materials and methods to obtain dual-wavelength PPG signals, extract different TD features from them and analyze the obtained features with respect to physiological situations. The results of different studies conducted in this thesis, has been presented in Chapter Three. Chapter Four discusses about the obtained results from the presented method and compares them with the previous works. Chapter five provides concluding remarks, and addresses future works.

## **2. MATERIALS AND METHODS**

This section explains clearly that how the studies were conducted to reach the main goal of this dissertation (analysis of TD variations in terms of biological situations). In the following subsections, performed studies, used tools, materials and methods are described in detail.

### **2.1. Planning of the Studies**

In this thesis, several studies were carried out to investigate paired PPG signals with respect to their time domain differences and subject's biological situations. The conducted studies are introduced and abstracted in below subsections.

#### **2.1.1. Study (1): New method to Obtain Dual-Wavelength PPG Signals**

This study was carried out in order to design a new approach for obtaining dual-wavelength PPG signals instead of TDM method, compare the obtained results and determine the most suitable approach for extracting of TDs. Based on the obtained results, in the case of TDM method, TD variations were not statistically significant, but in the proposed method, TDs had very statistically significant variations.

#### **2.1.2. Study (2): Bio-Physiological Analysis Based on TD Variations**

In this study, TD variations between Red and IR PPG signals were extracted and proposed as a new strategy for the analysis of dual-wavelength PPG. For this aim, the new designed dual-wavelength PPG sensor system was applied to obtain simultaneous IR and Red transmission mode PPG signals. Then, TDs between the obtained PPG pulses were extracted in each heartbeat for monitoring of various physiological conditions. The proposed method was verified in three different physiological changing situations (wakefulness-sleep, rest-run, nonsmoking-smoking). Results showed that different PPG signals had significant TD variations (time shifts relative to each other) with change in a psychophysical state of investigated subjects.

### **2.1.3. Study (3): Use of TDs to Assess Respiratory System**

This study was planned to propose TDs inferred from dual-wavelength PPG signals to assess respiratory system. Two different types of respiratory challenge tests were planned and the details of TDs and their variations according to respiration changes were analyzed using the recorded signals. Statistical analysis was performed using the obtained data. The results showed that PPG signals with distinct wavelengths had respiratory-related TD variations and there was significant difference between mean and standard deviations of TDs in separate stages of the experiments ( $P < 0.05$ ).

### **2.1.4. Study (4): Biological Assessments by Using of Multi-Wavelength TDs**

The aim of this study was to obtain TDs between three different pairs of PPG signals during a breath holding experiment (as biological challenge test) in order to investigate and compare their TD variations within the tests. Based on the results, all of the three PPG pairs of Red-IR, Green-IR and Blue-IR had significant biological related TD variations, but the Red-IR pair was the most relevant case for biological applications.

### **2.1.5. Study (5): Apnea Detection Using TDs**

This study was aimed to apply TDs as time domain features for fast detecting of apnea during respiratory monitoring. The use of TDs to fast identify abnormal breathing could be an interesting research field. Four separate TD features along with a pulse height feature and  $k$ -NN classification method were used in this study. The results revealed that TDs could be good indicative for normal and abnormal respirations.

### **2.1.6. Study (6): Use of TDs for Wake/Sleep Classification**

The aim of the present study was to investigate time domain differences inferred from dual-wavelength PPG signals in order to feasibility of fast and accurate wake/sleep classification. For this purpose, the developed computer connectable dual-channel PPG sensor system (including Red and IR lights) was employed to obtain paired PPG signals from a small hole of the finger skin during wake/sleep experiments. Three separate TD

features and  $k$ -NN classification algorithm were employed in this study. The promising classification results were achieved and it turned out that TDs may have a good potential for wake/sleep detection.

#### **2.1.7. Study (7): To Compare PTTs Obtained from ECG and Different PPGs**

Complex PPG signals were recorded along with the ECG signal simultaneously. This job was carried out by the same PPG sensor system plus an additional circuit including an instrumentation amplifier to record ECG signal. Breath holding experiments were performed and the time differences between peak points of PPG signals (TDs) and also the differences between 'R' point of ECG and peak points of PPGs (PTTs) were obtained from experimental recordings separately for each heartbeat. The results showed that PTTs extracted using different PPG signals were different with each other. This outcome can be an important finding and must be considered in applications such as calculation of blood pressure.

#### **2.1.8. Study (8): To Compare Simultaneous TDs and PTTs in Exercise Test**

Similar to the study (7), dual-wavelength PPG signals were recorded along with the ECG signal simultaneously. Exercise test (rest run experiment on treadmill) was carried out instead of the breath holding experiment. Finally, TDs and PTTs were extracted from experimental recordings for further investigations.

### **2.2. Sensor Systems**

Two types of dual-wavelength PPG sensor systems (proposed and TDM methods) along with a sensor system to record ECG signals were prepared and used for data collection in corresponding studies. TDM method for dual-wavelength photoplethysmography was explained in Section 1.10.1. The proposed PPG sensor system and ECG are explained in the following subsections.

### 2.2.1. Proposed Dual-Wavelength PPG Sensor System

In the TDM method, due to the use of a wide range single output photodetector, LEDs in the measurement setup should be alternatively driven by impulses at a special rate, so the different PPG signals were not tested absolutely synchronous, but with a small time delay in the range of milliseconds. In addition, due to the switching, sampling and holding, it was conceivable that signal to noise ratio and also the phases of PPG signals were interfered by these stages. To overcome these problems, a computer connectable transmission mode multi pair dual-wavelength PPG signal recorder prototype device with a new arrangement of transmitter-receiver was developed. Angular position of transmitters and receiver sensor was empirically set to  $90^\circ$  to have the improved output magnitude of sensor and the largest PPG signals. This type of sensor arrangement not presented in previous works. Optimum placement of the sensors can be seen in Figure 2.1.

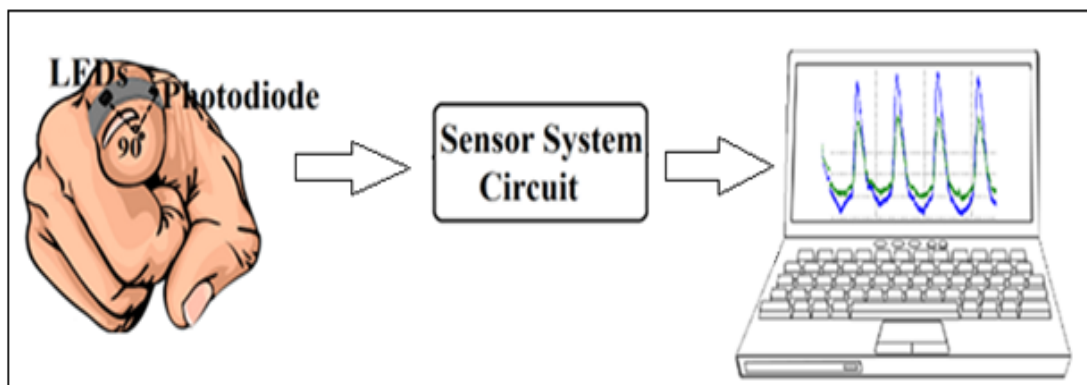


Figure 2.1. Position of sensors and connections

The main difference between TDM and the proposed methods was in their photodetectors. TDM method used a photodiode with a broad-spectrum and a single output for both of visible and infrared lights. However, in the proposed method photodiode had two separate analog outputs for visible and infrared beams. These two direct analog outputs were caused to prevent from any delay and switching noise (that there were in TDM method). A typical block diagram for PPG sensor system based on dual-output photodiode with two separate analog outputs can be seen in Figure 2.2. As seen in this figure, the periodic driving of LEDs (time multiplexing) in the transmitter section and also sample & hold part in the receiver part has been eliminated in the presented approach. Two separate

outputs of the photodiode could be directly applied to a dual-channel analog to digital converter (ADC) after an amplification stage.

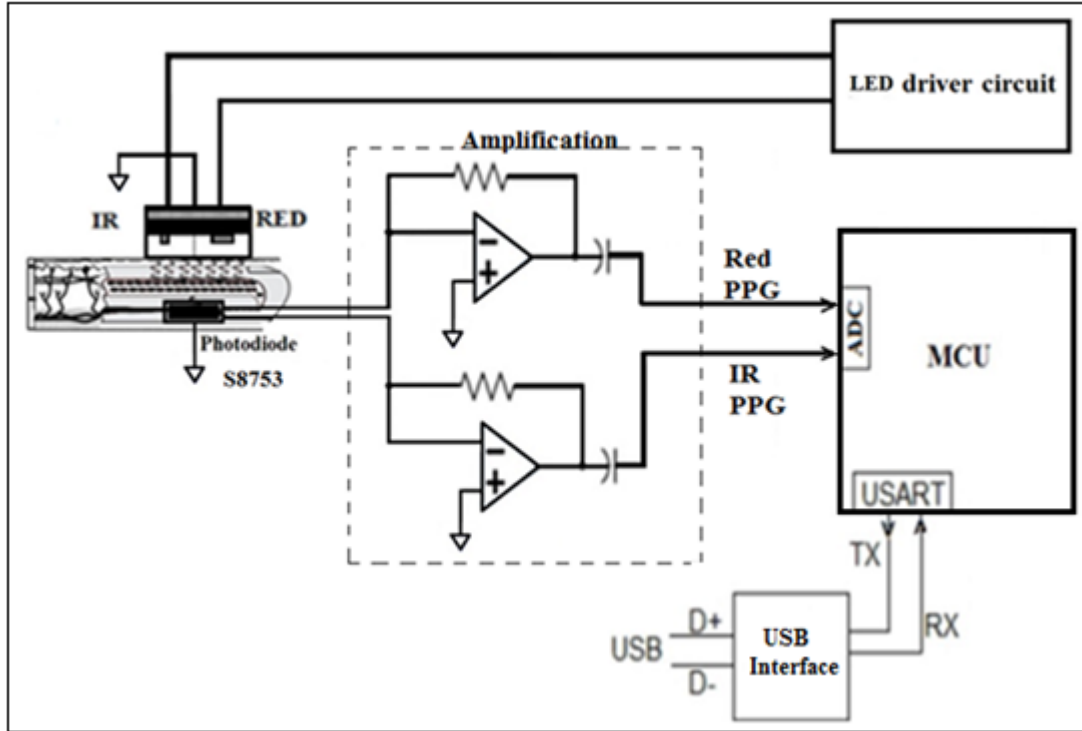


Figure 2.2. A proposed block diagram for dual-wavelength PPG sensor

One of our goals in this thesis was to determine the most suitable wavelength pair to extract TDs for using in bio-physiological analysis. Hence, we needed a multi paired dual-wavelength PPG sensor system. Multi pair means that the developed system had choice between several PPG signal pairs. Such a system was developed with PPG pairs as below:

1. Red-IR PPG pair
2. Green-IR PPG pair
3. Blue-IR PPG pair

In this system, a single Red-Green-Blue (RGB) LED with the wavelengths of 660nm (Red), 520nm (Green) and 460nm (Blue) and a near infrared LED with the wavelength of 940nm (IR) were used as transmitters. The RGB and IR LEDs were glued to each other in order to avoid gap between them. As mentioned above, three separate pairs of simultaneous PPG signals with the wavelength pairs of 660-940nm (Red-IR), 520-940nm (Green-IR) and 460-940nm (Blue-IR) could be selected by this device. In the designed

sensor system a dual-element common cathode S8753 photodiode (HAMAMATSU PHOTONICS) with two separate simultaneous analog outputs (for visible and infrared range) was used as receiver sensor. Both of the LED and photodiode were placed on a ring-shape holder. Separate outputs of the photodiode produced two concurrent analog paths of the visible and infrared PPG signals that could be connected to a data acquisition device after amplification. In the developed device, the computer connection was provided by using a dual channel USB connectable audio codec (PCM 2902). Complete circuit diagram of the developed PPG sensor system using the proposed method is shown in Figure 2.3. In this circuit, one of the Red, Green or Blue parts of RGB LED was selected and driven along with IR LED by constant DC voltages. On the other hand, distinct outputs of the photodiode provided two separate signals that one of them was corresponded with IR beam and other one was corresponded with Red, Green or Blue light. Each of obtained PPGs was amplified and applied to ADC input of USB connectable audio codec.

### **2.2.2. Dual-Element Photodiode**

It was expressed that the developed dual-wavelength PPG device used a S8753 photodiode with two separate analog outputs. S8753 is a wide range (visible-infrared) photo-detector. It uses two separate elements integrated in a single small package. It has two distinct photosensitive semiconductors with different spectral response characteristics to give high sensitivity for the covering range. Spectral response of this sensor has been revealed in Figure 2.4.

### **2.2.3. RGB and IR LEDs**

Spectrum of peak wavelengths of RGB and IR LEDs are revealed in Figure 2.5. As seen in this figure, the wavelengths for blue, green, red and IR are 460nm, 520nm, 660nm and 940nm respectively. These values have been measured at normal room temperature of 25°C.



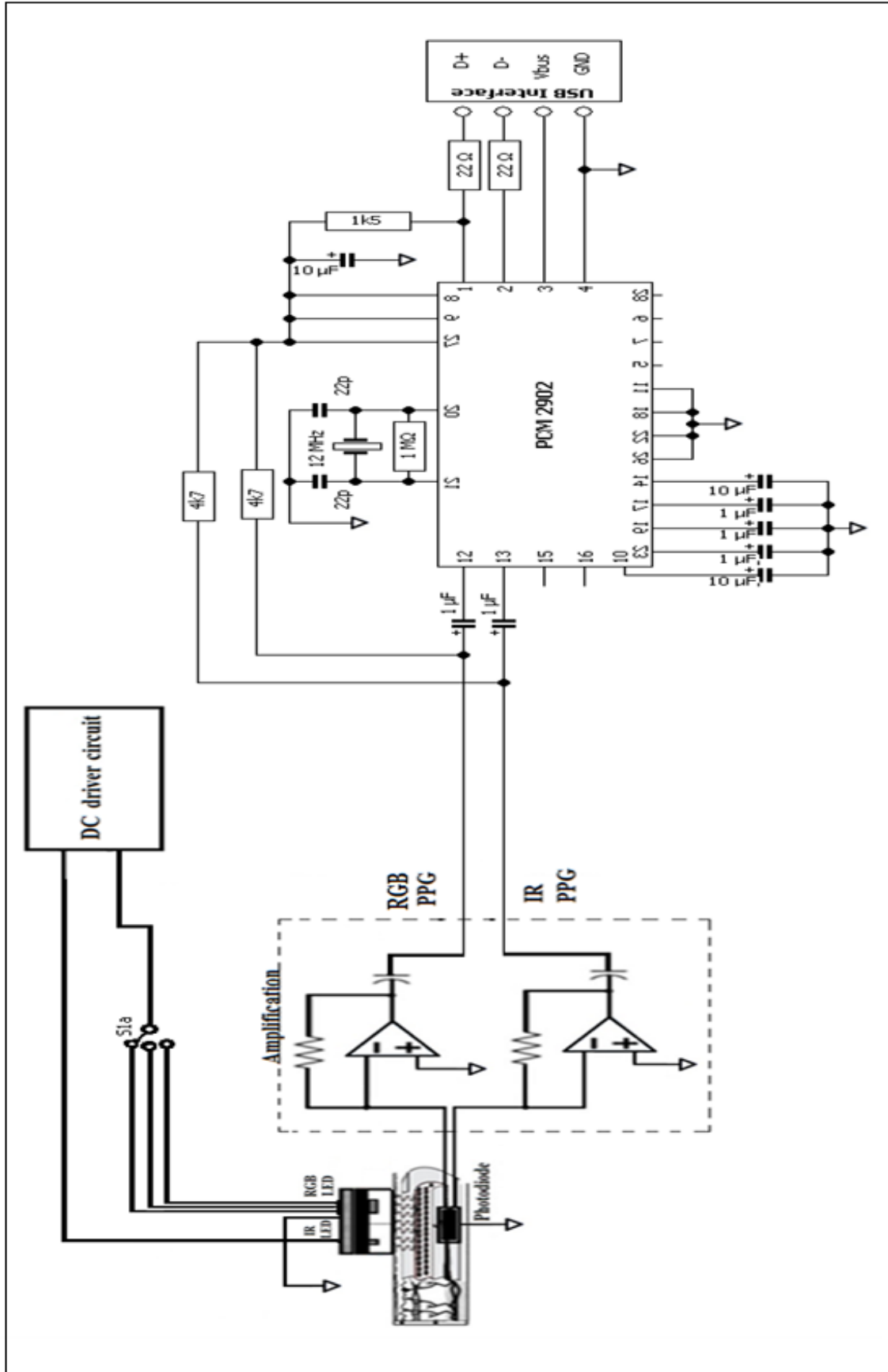


Figure 2.3. Circuit diagram of the developed sensor system

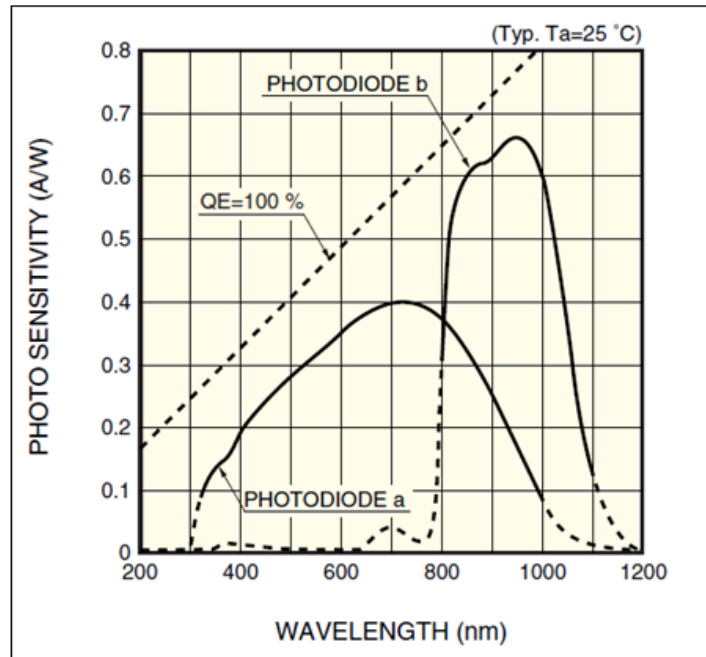


Figure 2.4. Spectral response of S8753 photodiode [82]

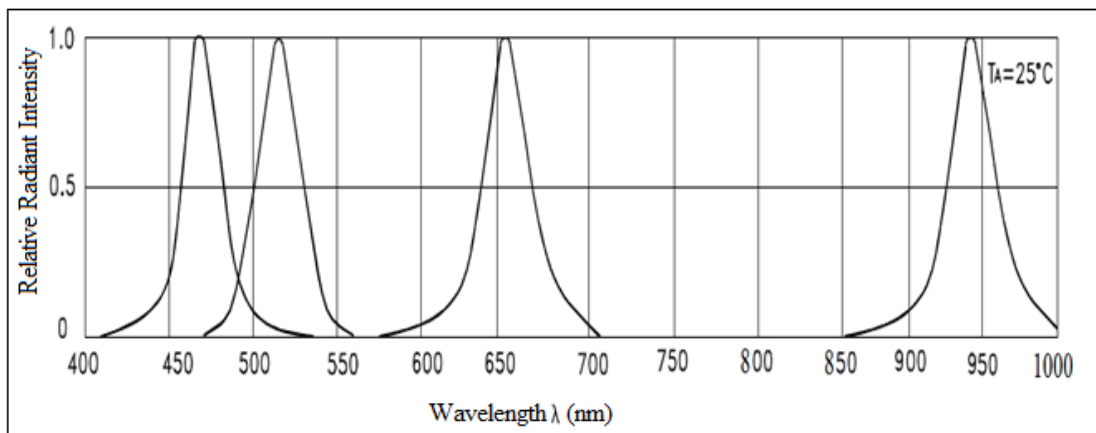


Figure 2.5. Peak wavelength spectrum of used LEDs

#### 2.2.4. ECG System

In addition to PPG sensor systems, a 3-lead ECG recorder system containing an AD 620 instrumentation amplifier (IA), an Op-Amp and filtration stages was separately prepared. Similar to PPG sensor system, the filtered output of IA was connected to audio

codec to record signals by computer. Schematic diagram of 3-lead ECG recording system is shown in Figure 2.6.

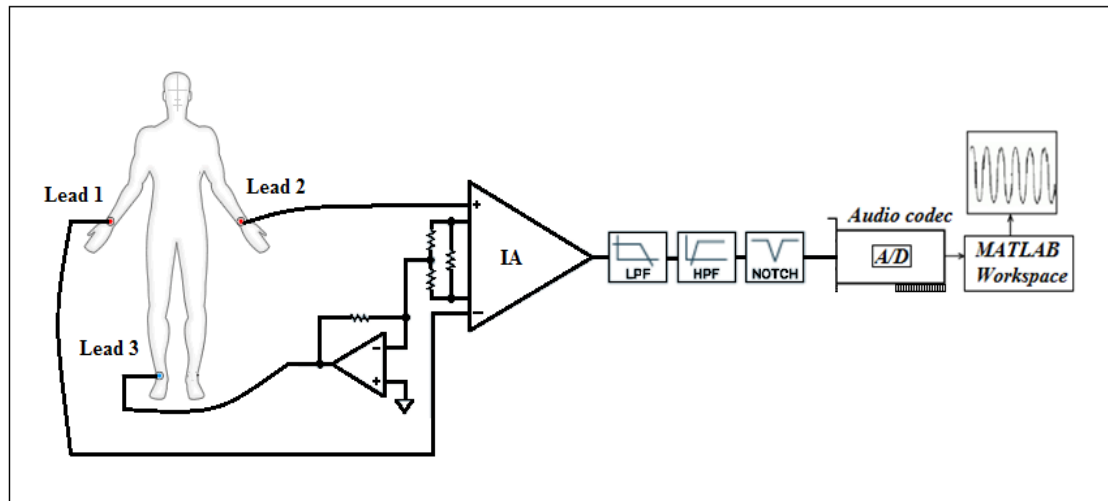


Figure 2.6. Schematic diagram of 3-lead ECG recording system

### 2.2.5. Acquiring Data Using Audio Codec

When needed to use the computer for data acquisition, audio codec and sound cards can be used instead of expensive data acquisition cards or analog to digital converters. Specially, in the case of low frequency signals such as PPG and ECG, audio codec could be a suitable selection for data acquisition due to the appropriate resolution (16-24 bit) of their internal analog to digital converters, ability of setting of sampling rate from a lowest value up to 44100 Hz and low price. On the other hand, MATLAB<sup>®</sup> supports Windows<sup>®</sup> compatible audio codecs and sound cards that use the DirectSound driver by Data Acquisition Toolbox<sup>™</sup>. The following tasks can be carried out by Data Acquisition Toolbox<sup>™</sup> MATLAB<sup>®</sup>:

- Obtaining of multi-channel data
- Setting of sampling frequency
- Setting of recording duration
- Analyze data as it is being recorded
- Real time data analysis

- Triggering the start of recording
- Working with minimal MATLAB<sup>®</sup> code

A range of commercially available audio codecs could be used for acquire low frequency bio-signals such as PPG or ECG. CM6300 from C-Media Electronics and PCM2902 from Texas Instruments are two types of double channel audio codecs with two 16-bit analog inputs. Both of mentioned codecs were suitable for acquiring the dual-wavelength PPG and also ECG data involved in this thesis. These audio codecs are USB compliant full-speed protocol controller. The USB protocol controller works with no software code.

### **2.3. Host Computer Installed Program**

Because of the high ability for processing of signals and data analysis, use of MATLAB<sup>®</sup> as a software environment can be an appropriate choice to develop automated applications. In This thesis, in addition to the hardware, MATLAB<sup>®</sup> programs were developed to record PPG signals using the prepared sensor circuit, filtering, peak detection, signal processing, statistical analysis, feature extraction, classification and others. The developed software for signal recording was able to set time duration of data collection and also sampling frequency.

### **2.4. Experimental Setup to Collect PPG Data**

This section introduces the setup to collect PPG data. Important characteristics of the prepared setup were the simplicity and portability of it. Internal circuits and the external view of the prepared prototype device can be seen in Figure 2.7 (a) and (b) respectively. Experimental setup containing sensor system, a laptop and embedded MATLAB<sup>®</sup> program, is revealed in Figure 2.7 (c). As it turns out, this setup could be easily positioned on a small table and connected to subject's finger. This setup was used for all of the studies conducted in this thesis.

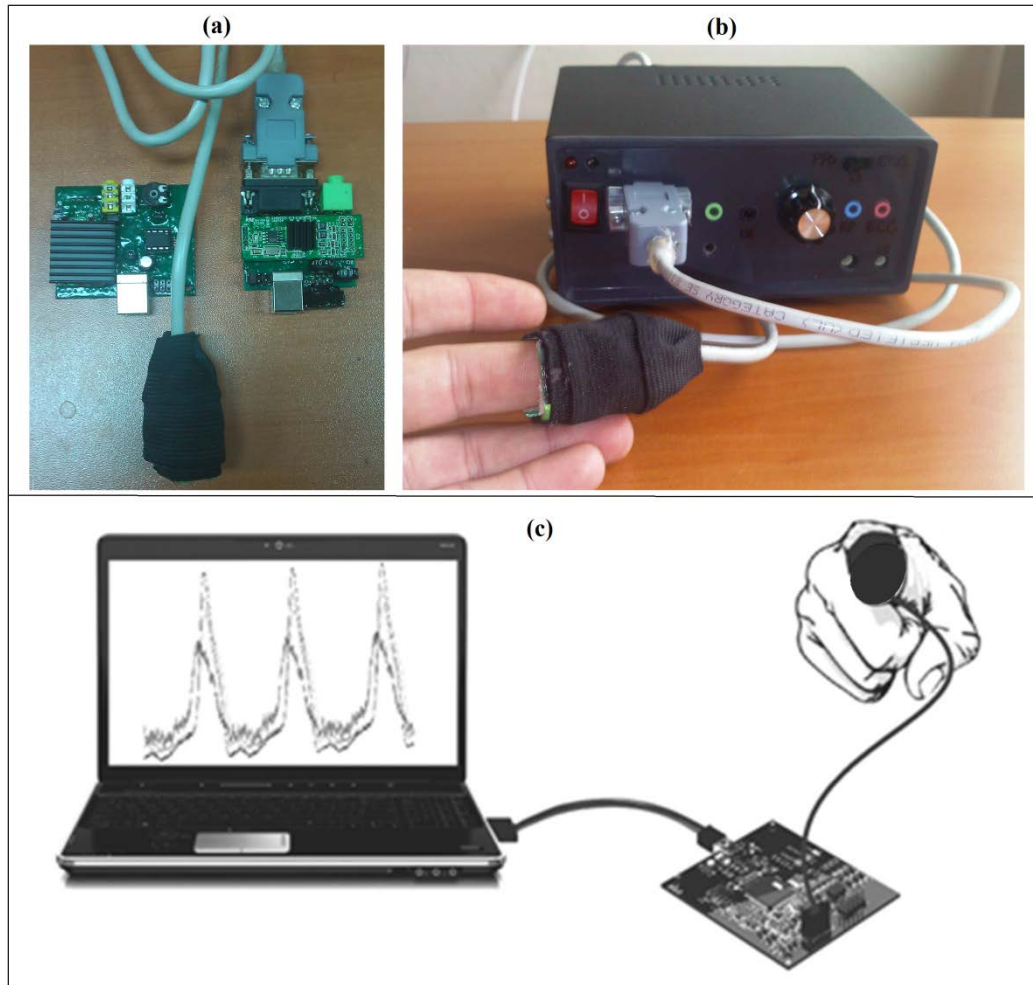


Figure 2.7. (a) Circuits (b) external view of device and (c) experimental setup

## 2.5. Experimental Protocols

In this dissertation, several studies were planned in which paired PPG signals were recorded from the number of volunteers and analyzed with respect to their biophysiological conditions. The nature of the researches was defined to the volunteers before the starting to experiments, and their informed consent was obtained. The protocols of the studies are described as below subsections.

### 2.5.1. Experimental Protocol for the Study (1)

Study (1) was aimed to compare the new designed dual-wavelength PPG sensor system with TDM based system. This comparison was performed by investigating TD

variations corresponding with bio-physiological conditions. One of the sensors (proposed sensor) was positioned on the forefinger of the left hand and the other sensor (TDM based one) was placed on the forefinger of the right hand. In this way, two separate dual-wavelength PPG data could be recorded in parallel by using both of the sensor systems. Breath holding experiments was carried out as biological challenge test. The breath holding experiments contained three steps of 30s normal breathing, holding the breath as much as possible and breathing again. Experimental recordings were obtained with the participation of fifteen healthy subjects [age=29.35±4.5 years (mean ± SD), range 24 to 38 years, male/female=11/4].

### **2.5.2. Experimental Protocol for the Study (2)**

In some situations, the physiological state of the human is changed. For example, in bedtime when human is transmitted from wakefulness to sleep some physiological changes occur. In this study, three different experiments were planned for instance of physiological changes occurring situations, and long-term PPG signals were recorded during the experiments. The separate experiments are as follows:

1. Individual's transition from wakefulness to sleep (first experiment)
2. Running on a treadmill (second experiment)
3. Smoking (third experiment)

PPG data acquisition was performed by fixed and motionless placement of the sensor on the forefinger of left hand. Signal recording in each experiment was started from a rest condition and continued until the changing physiological situation. For example, in the first experiment before beginning to signal recording, subjects were asked to lie and relax on a bed. Then signal recording was started and continued until the subject goes into deep sleep. In second experiment, PPG signals were acquired starting from standing rest and continuing with running on a treadmill. In third experiment, signals were recorded starting from non-smoking and continuing with smoking. The signals were acquired from ten healthy subjects (three females) in age groups between 24 and 39 years old [age=31.54±7.5 years (mean ± SD), range 24 to 39 years, male/female=7/3] all gave written informed consent. All the experiments were repeated twice. Each of the iterations of the experiments was done on separate day to confirm that steady state was regained before the next experiment. Time duration of signal recording was different for each case

according to physiological conditions. Sampling frequency was 1000 Hz for all recordings. The total number of obtained experimental recordings was 60 separate dual-channel PPG signals.

### **2.5.3. Experimental Protocol for the Study (3)**

In this study, TD variations were investigated with respect to respiratory changes. It has been proved that respiratory rhythm of human was different in sleep and wake situations [83, 84]. In addition, breath holding is a major respiratory challenge test [85-87]. Hence, in this study, two different types of experiments were planned for instance of respiratory changes occurring situations. These separate experiments were as follows:

Wake-sleep test as the first experiment and breathe holding test as the second experiment.

PPG data were acquired by fixed and motionless placement of the ring-shaped sensor on the forefinger of left hand. In the first experiment before beginning to record signal, subjects were asked to lie and relax on a bed. In this experiment, the signal recordings were performed at two separate stages, before falling asleep and when the subject was in deep sleep. Duration of signal recording was three minutes in each stage of this experiment. In the second experiment, volunteers comfortably positioned on a chair, and then the signals were recorded. This experiment contained three unceasing and consecutive stages of 60 seconds normal breathing (first stage), holding the breath as much as possible (second stage) and at last, breathing again (third stage). In the third stage of this experiment when the subjects started to breathe again, the first breath naturally was a deep inhalation. Timing of the steps of the experiments was carried out by a digital stopwatch. The data were collected from twenty five healthy volunteers [age=26.4±12.3 years (mean±SD), range 20 to 39 years, male/female=22/3] with one day interval between the first and second experiments to confirm that steady state was regained before experiment 2. Sampling frequency was 1000 Hz for all recordings like the previous studies.

### **2.5.4. Experimental Protocol for the Study (4)**

Experimental protocol to assess the multi-wavelength TD variations with respect to biological situations conducted in this study is expressed. Similar to previous study, breath

holding experiment was performed as an important instance of biological changes occurring conditions. The experiment was contained the same steps of one minute normal breathing, holding the breath as much as possible and normal breathing again. Timing of the experiments was performed by a digital stopwatch.

Experimental recordings were obtained with the participation of twenty-five healthy volunteers [age=26.4±12.3 years (mean±SD), range 20 to 39 years, male/female=22/3]. Before beginning to record signals, subjects were seated and relaxed on a chair, ring-shaped sensor was placed in a motionless form on their left hand forefinger and then, recording was began and the subjects were asked to execute the mentioned steps of the current experiment. All of the signals were recorded at the room temperature approximately 24 °C. Sampling frequency of signal recording was 1 KHz.

#### **2.5.5. Experimental Protocol for the Study (5)**

This study was aimed to classify normal and apneatic conditions in a fast and accurate way. The recordings of the breath holding experiment obtained from study (3) were used as the database of this study. The difference was that each of the recordings was split in separate epochs each one having duration of 5s. The first and second stages of the breath holding experiment were considered as normal situation and apneatic situations respectively. Then, TD features were extracted using the obtained epochs.

#### **2.5.6. Experimental Protocol for the Study (6)**

In this study, the recorded PPG signals in the first experiment of the study (2) were used as the database. As mentioned in Section 2.5.2, in that experiment before beginning to signal recording, subjects were asked to lie and relax on a bed. Then signal recording was started and continued until the subject goes into deep sleep. Selected data from wake and sleep situations was used as different biological states of the present study. The difference between this study and study (2) is that in the present study, was tried to detect wake/sleep situations in each heartbeat instead of time epochs with several seconds duration.



### **2.5.7. Experimental Protocol for the Study (7)**

This study was aimed to compare PTTs obtained from an ECG signal and different PPG signals. ECG signal was recorded along with simultaneous different PPG signal pairs. PPG sensor was placed on the forefinger of the left hand of the subjects. Three ECG electrodes of lead I, II and III were positioned on the right wrist, left wrist and right leg respectively. Breath holding experiment was carried out (similar to study 3) and concurrent ECG and Red-IR PPG signal pair was recorded. This job was repeated once again by Green-IR PPG signal pair with two hours interval with the first iteration to confirm that steady state was regained before second iteration. Experimental recordings were obtained with the participation of ten healthy volunteers [age=34.3±5.4 years (mean ± SD), range 21 to 39 years, male/female=9/1].

### **2.5.8. Experimental Protocol for the Study (8)**

This study was aimed to compare reliability of TDs and PTTs in cases where motion artifacts are high. Exercise test was carried out and similar to previous study, simultaneous ECG and dual-wavelength PPG signals (separately with Red-IR and Green-IR pairs) were recorded. ECG and PPG signals were acquired starting from three minutes standing rest, continuing with five minutes running on a treadmill and consequently three minutes rest again.

The basic information of the subjects and experimental protocols are summarized in Table 2.1.

## **2.6. Preprocessing**

Some preprocessing operations were need prior to extraction of TD series from experimentally recorded PPG signals. These operations are described in detail in the following subsections.

## **2.6.1. Filtering and Noise Cancellation**

The first step of the preprocessing involves filtering the signal to remove types of noises. In spite of the fact that PPG signals have a good structure for mathematical and statistical analysis, these signals may be affected and destroyed by several types of noises such as high-frequency noises, mains noise, ambient optical noise and small drifts. Furthermore, in TDM based PPG sensors, time multiplexing process leads to a strong switching noise and so simple filtering methods such as smoothing by moving average or detrending were not enough for obtaining clear IR and visible PPG signals from the time multiplexed PPGs. Hence, for removing the mentioned noises from the recorded PPG signals, appropriate filtering processes were needed in this thesis. These filters are described in the next subsections.

### **2.6.1.1. Band Pass Filtering**

Since the filtration of a signal depends on its frequency characteristics, frequency analysis of signals is very important. There are few studies on the frequency features of PPG signals. However, considering that PPG signals are a major component of arterial system [88], the basic frequency of PPG has been turned out to be 1 Hz and low frequency component of this signal is less than 0.5 Hz [89]. On the other hand, frequency range of important PPG noises is as follows:

Frequencies of mains noise, respiratory-related artifacts, baseline deflection, motion artifacts, and high-frequency noises (containing EMG artifacts) are 50 or 60 Hz, between 0.15–0.4 Hz [90], less than 0.5 Hz [91], under 0.1 Hz, and more than 170 Hz [92], respectively. Considering the frequency characteristics of PPG signals and the mentioned noises, it is easily understood that a band pass filter in the range of 0.05–5 Hz would be suitable for PPG signal filtering. In the some studies of this thesis in which TDM method has been used, noise canceling process from the recorded PPG signals was performed using well known IIR filter. Main difference equation of this type of filters can be written as Equation (2.1) [93].

Table 2.1. The basic information of experimental protocols

| Item                 | Study<br>(1)      | Study<br>(2)                   | Study<br>(3)   | Stud<br>(4)                       | Study<br>(5)   | Study<br>(6) | Studies<br>(7 & 8)        |
|----------------------|-------------------|--------------------------------|----------------|-----------------------------------|----------------|--------------|---------------------------|
| <b>Subjects</b>      | 15                | 10                             | 25             | 25                                | 25             | 10           | 10                        |
| <b>Male</b>          | 11                | 7                              | 22             | 22                                | 22             | 7            | 9                         |
| <b>Female</b>        | 4                 | 3                              | 3              | 3                                 | 3              | 3            | 1                         |
| <b>Age</b>           | 29.3±<br>4.5      | 31.5±<br>7.5                   | 26.4±<br>12.3  | 26.4±<br>12.3                     | 26.4±<br>12.3  | 31.5±<br>7.5 | 34.3±<br>5.4              |
| <b>Sensor System</b> | Proposed &TDM PPG | Proposed PPG                   | Proposed PPG   | Proposed PPG                      | Proposed PPG   | Proposed PPG | Proposed PPG &ECG         |
| <b>PPG Pair</b>      | Red-IR            | Red-IR                         | Red-IR         | Red-IR &<br>Green-IR &<br>Blue-IR | Red-IR         | Red-IR       | Red-IR &<br>Green-IR      |
| <b>Experiment</b>    | Breath holding    | Wake /Sleep & Rest/Run & Smoke | Breath holding | Wake /Sleep & Breath holding      | Breath holding | Wake /Sleep  | Breath holding & Exercise |

$$y[n] = -\sum_{k=1}^{N-1} a_k y[n-k] + \sum_{k=0}^{M-1} b_k x[n-k] \quad (2.1)$$

where  $b_k$  and  $a_k$ ,  $y_{n-k}$ ,  $x_{n-k}$  and  $M$  represent the tunable coefficients of the filter, output signal of the IIR filter, delayed version of the output signal of the filter, delayed version of the input signal to the filter and order of the filter, respectively, and  $n$  is the time index. Transfer function of the filter can be obtained taking the z-transform of (2.1) as (2.2).

$$H(z) = \frac{Y(z)}{X(z)} = \frac{B(z)}{A(z)} = \frac{\sum_{k=0}^{M-1} b_k z^{-k}}{1 + \sum_{k=1}^{N-1} a_k z^{-k}} \quad (2.2)$$

where  $H(z)$  is the filter's transfer function and  $B(z)$  and  $A(z)$  are numerator and denominator polynomials. The 4th-order IIR filter (pass band = 0.5–5 Hz and sampling frequency=1 kHz) that was designed respecting to Equation (2.2), is expressed by Equation (2.3).

$$H(z) = \frac{B(z)}{A(z)} = \frac{1.9592 + 3.9185z^{-2} + 1.9592z^{-4}}{1 - 3.9598z^{-1} + 5.88044z^{-2} - 3.8814z^{-3} + 0.9608z^{-4}} \quad (2.3)$$

PPG data obtained from TDM method in study (1) were filtered applying Equation (2.3) and prepared for next stages of signal processing. A part of the recorded time multiplexed PPG data and its filtered form is revealed in Figure 2.8 (a) and (b). This figure contains simultaneous Red and IR PPG pulses obtained from a unique heartbeat.

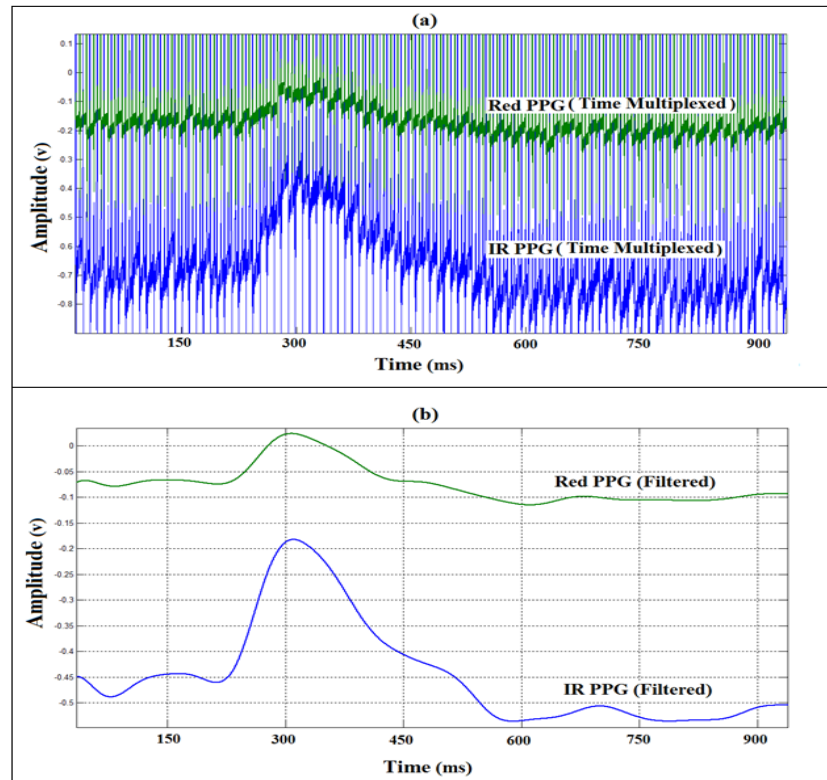


Figure 2.8. (a) Time multiplexed and (b) Filtered PPG signals

### 2.6.1.2. Smoothing and Detrending

Despite TDM method, in the proposed PPG sensor system there was no modulation and so there was no complicate signals. Therefore, it was possible to filter signals without the need for complex filtering. Two simple filters were applied for signal cleaning in these types of signals. The first one was a detrending filter based on smoothness prior approach [94]. This filter was used to remove slow-varying baseline drift from the infrared and red signals, which may also disturb the proper assessment of their maxima. In the smoothness prior approach, bio-signals could be presented by two general components of the stationary and the non-stationary. Then PPG signal could be expressed by (2.4).

$$P = P_{stat} + P_{trend} \quad (2.4)$$

where  $P$  is recorded PPG signal,  $P_{stat}$  is the approximately desired stationary PPG signal and  $P_{trend}$  is the slow trend component. An estimation of trend component can be defined as [94]:

$$P_{trend} = H\Theta \quad (2.5)$$

where  $H$  is the observation matrix and  $\Theta$  is the estimate of the regression parameters by the regularized least squares method. With respect to (2.4) and (2.5), an estimation of  $P_{stat}$ , can be represented as:

$$P_{stat} = P - H\Theta \quad (2.6)$$

More detailed explanations in the case of smoothness prior approach could be studied in [95].

The next applied filter was a moving-average filter to smooth and remove random noises. Mathematic description of this type of filters can be shown as (2.7).

$$y(n) = \frac{1}{N} \sum_{i=0}^{N-1} P_{stat}(n-i) \quad (2.7)$$

where  $y(n)$  and  $N$  represent the filtered signal and order of the filter, respectively, and  $n$  is the time index. All of the recordings obtained from the proposed method were filtered using these filters and prepared for next stages of signal processing. A sample PPG signal obtained directly from one of the outputs of photodiode (proposed method) and its filtered form is shown in Figure 2.9 (a) and (b).

### 2.6.2. Removal of DC Component

It was expressed that AC component of PPG, illustrates pulsations of blood vessels and DC component indicates the light scattered from constant blood volume in tissues. Therefore, temporal characteristics of PPG signals only depend on the AC component and there is no requirement for time difference calculation of DC components; especially to eliminate DC offset, it is essential to reduce or remove the DC component. In this study, a DC offset removal preprocess was carried out, as (2.8).

$$P_{AC} = y - E(y) \quad (2.8)$$

Here,  $P_{AC}$ ,  $y$  and  $E(y)$  denote DC component removed PPG signal, PPG signal obtained from filtration stage and mean of  $y$ , respectively. Figure 2.10 shows a part of recorded dual-wavelength PPG signals without DC component cancelling (obtained the proposed method). The same signals after cancelling DC component can be seen in Figure 2.11.

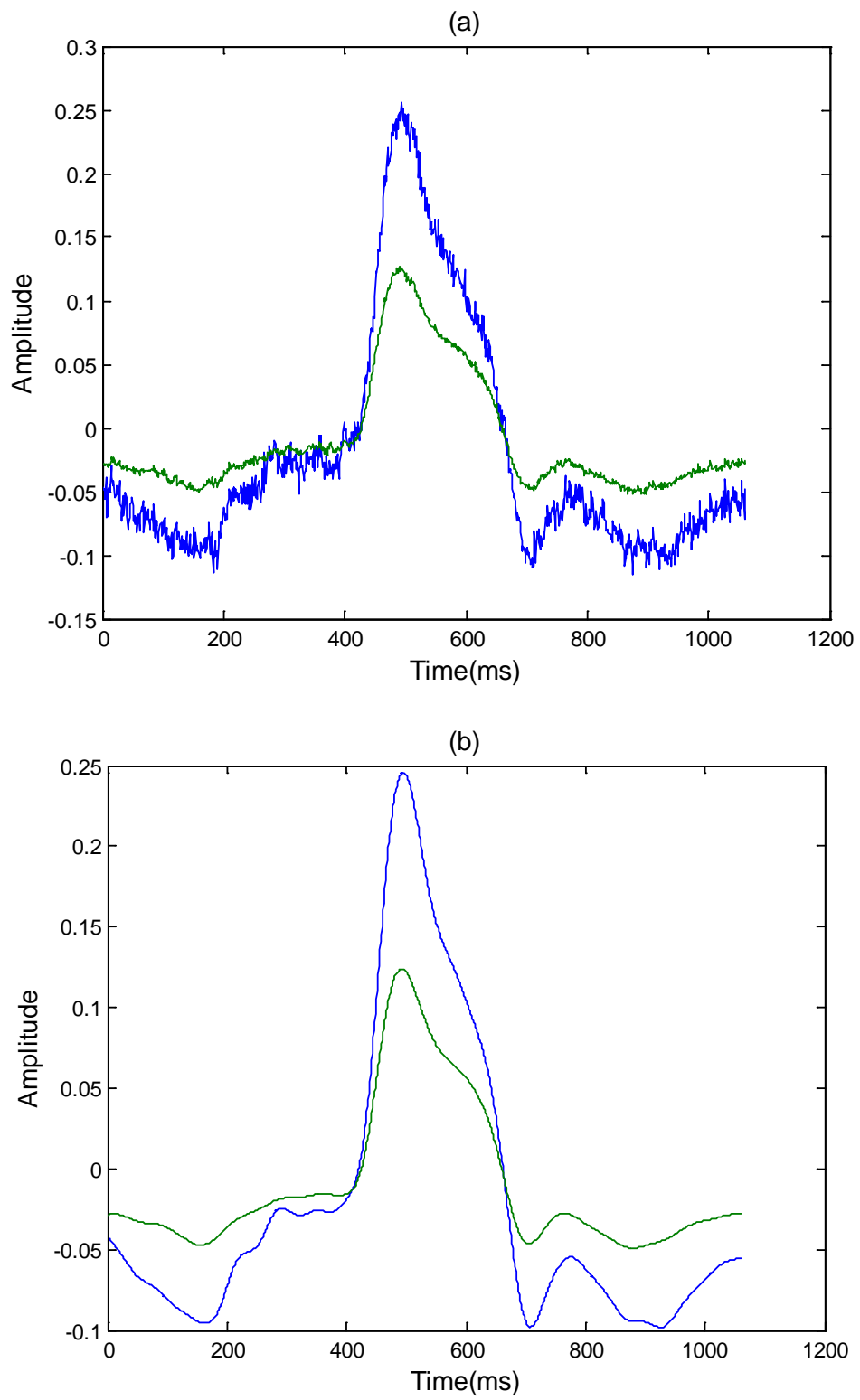


Figure 2.9. (a) Recorded PPG and (b) filtered PPG signals

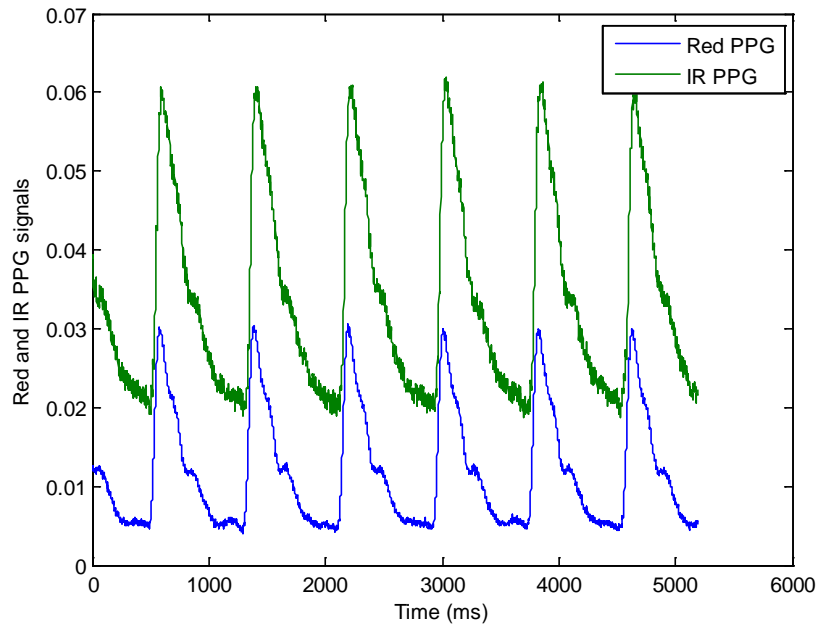


Figure 2.10. PPG signals without DC component cancelling

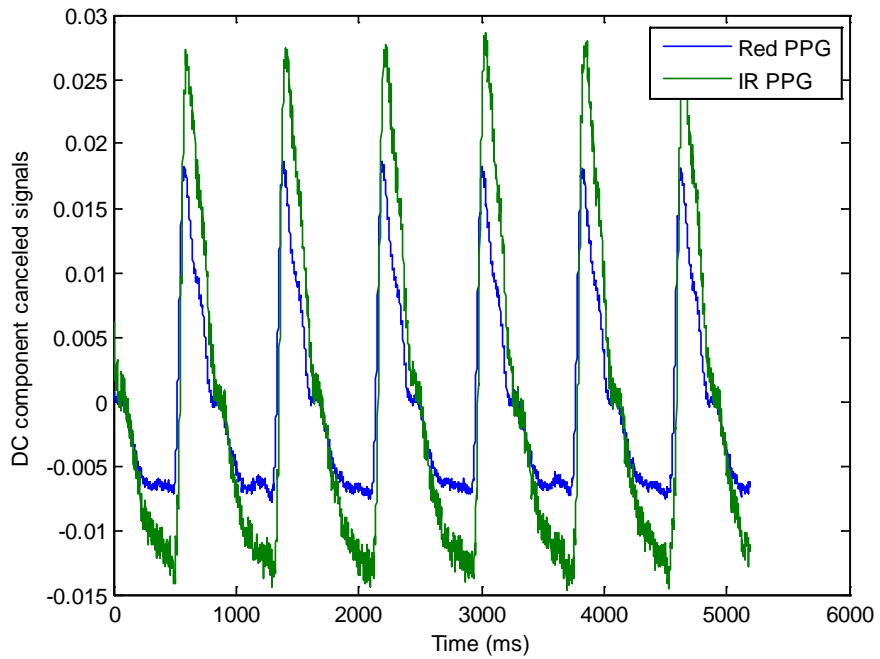


Figure 2.11. PPG signals after cancelling DC component



### 2.6.3. Normalization

After the DC component removal, a normalization operation was employed to cancel amplitude differences between the PPG signals at separate wavelengths that may be occurred due to the different light absorbance [96]. To do this, 0-1 normalization process [97] was accomplished on all the trials, as demonstrated in (2.9).

$$Normalized(P) = \frac{P_{AC} - E_{min}}{E_{max} + E_{min}} \quad (2.9)$$

where  $E_{max}$  and  $E_{min}$  denote maximum and minimum values for  $P_{AC}$ , respectively. Figure 2.12 shows the normalized PPGs.

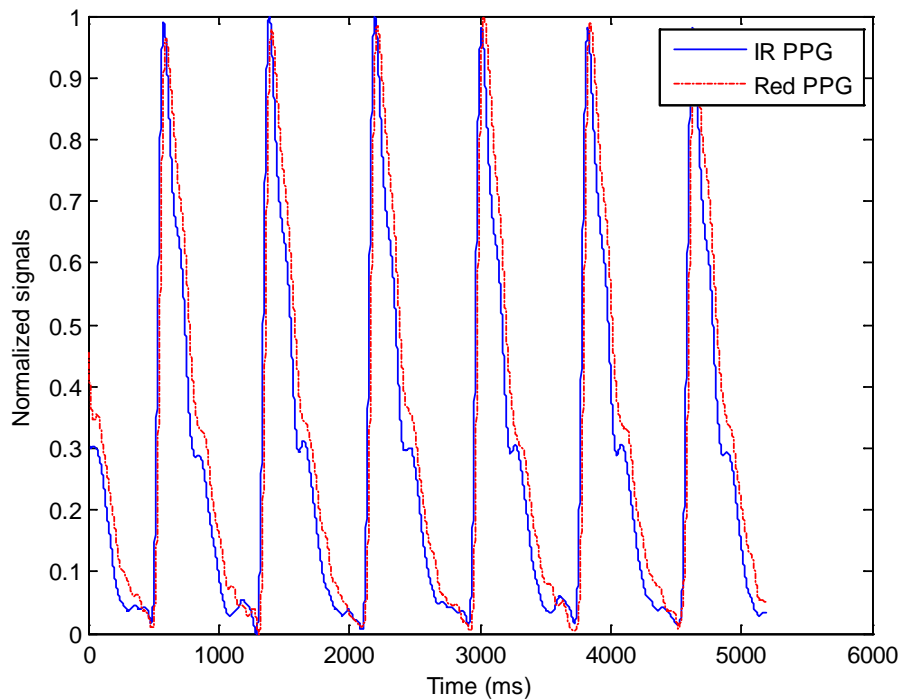


Figure 2.12. Normalized PPG signals

#### 2.6.4. Peak Detection

Finding of peak points is a major task in various signal analyzing processes including the time difference extraction involved in this study. PPG signal has a relatively simple shape and it seems that isn't hard to peak detection. Nevertheless, major baseline wander and respiration effect may be superimposed on PPG signal. This signal also can be quickly affected by frequently happened physiological oscillations or motions. The conventional methods for peak detection are difficult to exert for quick variations of PPG waveform in various heart rates, and they also may have time lag [98, 99] which can interfere with the time difference computing operations involved in this thesis and led to inaccurate measurements. Thus, for PPG signal conditioning and peak calculation, adaptive threshold peak detection algorithm [98] was employed. This algorithm was specially introduced and applied as a promising method to overcome respiration and other damaging effects for the peak detection of photoplethysmographic signals.

In the adaptive threshold peak detection, an amplitude controlled virtual threshold was considered. Virtual threshold was reduced or increased by a permanent slope parameter. In peak point detection, the value of threshold was decreased as long as amount of the main signal was less than the threshold. When the threshold was equal to the signal, its value would be equal to the magnitude of signal until reaching the peak. After peak finding, the threshold was reduced again by a modified slope parameter. These operations were repeated until all the peaks were found. Permanent slope parameter and modified slope parameter can be resolved by (2.10) and (2.11) respectively.

$$S_p = 0.2 \operatorname{argmax}_{(PPG)} \quad (2.10)$$

$$S_k = S_{k-1} + R_s \frac{(P_{n-1} + PPG_{std})}{F_s} \quad (2.11)$$

In (2.10),  $S_p$  indicate the permanent slope parameter and  $\operatorname{argmax}_{(PPG)}$  is argument of the peak points of the PPG signal. In (2.11),  $S_k$ ,  $R_s$ ,  $P_{n-1}$ ,  $PPG_{std}$ , and  $F_s$  denote the  $k$ -th slope amplitude, changing rate of slope, value of previous peak, standard deviation of original PPG signal, and sampling frequency, respectively. Changing rate of slope is empirically

given as -0.6 for peak points. Detected peak points for sample pulses are revealed in Figure 2.13.

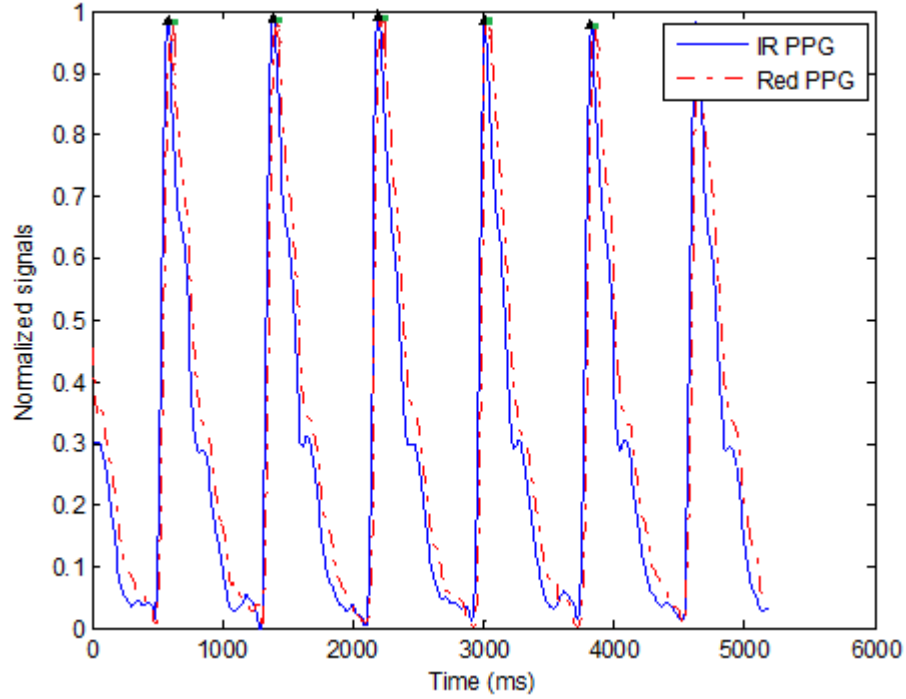


Figure 2.13. Peak points of PPG pulses and their time difference

## 2.7. Calculation of TDs

Beat-to-beat time differences between the PPG pairs could be obtained after the peak detection process. For example, TDs between peak points of Red and IR PPG signals could be calculated by subtracting the detected peak point time of the PPG pulses in each heartbeat. Equation (2.12) shows this operation. TD series correspond to the peak points could be formed by using the achieved TD values as (2.13).

$$\Delta t_{p_i} = t_{Peak2} - t_{Peak1} \quad (2.12)$$

$$TDs = (\Delta t_{p1}, \Delta t_{p2}, \dots, \Delta t_{p_i}) \quad (2.13)$$

In (2.12),  $\Delta t_{pi}$ ,  $t_{Peak1}$ , and  $t_{Peak2}$  denote the time difference between peak points of PPG pulses in  $i^{\text{th}}$  heartbeat and peak point times of PPG pulses respectively and  $i$  is the heartbeat number index. In (2.13)  $TDs$  denote the TD series obtained by using peak point time.

In addition to time differences between peak points, in this thesis, we needed to calculate some other time domain difference features in which TDs between important characteristic parameters of PPG pulses (introduced in Section 1.6) should be measured. These time domain differences were as follows:

- The difference between rising edges of PPG pair (Anacrotic phase difference)
- The difference between falling edges of PPG pair (Catacrotic phase difference)
- The difference between pulse heights of PPG pair
- The Full Width Half Max (FWHM) of each of the pulses (this feature was obtained by calculation the difference between the rising edge and falling edge of each unique pulse separately for Red and IR signals)

Figure 2.14 shows the time domain differences as, (a) difference between peak points, (b) difference between falling edges, (c) difference between rising edges, (d) FWHM of Red PPG and (e) FWHM of IR PPG.

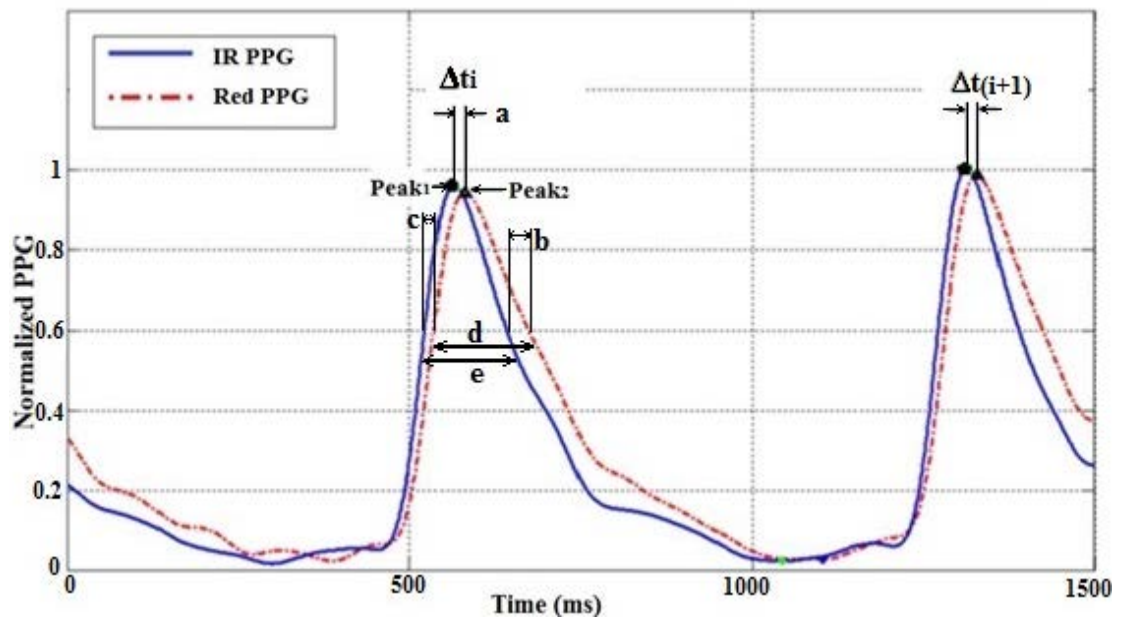


Figure 2.14. TDs between unlike PPG signals

Above mentioned TDs could be obtained after peak detection. To this end, a MATLAB<sup>®</sup> program was developed based on an algorithm. The algorithm to obtain all of TD features is expressed as below:

- 1- Detect the minimum and maximum (peak) points separately for the both of Red and IR PPG signals.
- 2- Get the interval between a minimum point and the next minimum as a unique PPG pulse obtained from a beat of the heart.
- 3- Calculate the difference between pulse heights as below:

$$IR_{PH} = IR_{Max} - IR_{Min} \quad (2.14)$$

$$Red_{PH} = Red_{Max} - Red_{Min} \quad (2.15)$$

$$D_{PH} = IR_{PH} - Red_{PH} \quad (2.16)$$

where  $IR_{Max}$ ,  $IR_{Min}$ ,  $IR_{PH}$ ,  $Red_{Max}$ ,  $Red_{Min}$ ,  $Red_{PH}$  and  $D_{PH}$  denote the maximum point of IR pulse, the minimum point of IR pulse, pulse height of IR PPG, maximum point of Red pulse, the minimum point of Red pulse, pulse height of Red PPG and the difference between pulse heights respectively.

- 4- Calculate Half Max (HM) of the peak for each pulse as Equation (2.17)

$$HM = \frac{Max}{2} \quad (2.17)$$

where  $HM$  and  $Max$  are Half Max of peak and the maximum point of the pulse respectively.

- 5- Find the times of calculated  $HM$  points. In this step, two time values are achieved for each  $HM$  point, one of them is related to a  $HM$  point on the rising edge and the other one is related to the same  $HM$  point on the falling edge.
- 6- Call the obtained  $HM$  points as:
  - $IR_{HM1}$ : the time of HM point on the rising edge of IR PPG pulse
  - $IR_{HM2}$ : the time of HM point on the falling edge of IR PPG pulse

- $V_{HM1}$ : the time of HM point on the rising edge of visible (Red, Green or Blue) PPG pulse
- $V_{HM2}$ : the time of HM point on the falling edge of IR PPG pulse

7- Calculate FWHM for each of PPG pulses as Equations (2.18) and (2.19):

$$IR_{FWHM} = IR_{HM2} - IR_{HM1} \quad (2.18)$$

$$V_{FWHM} = V_{HM2} - V_{HM1} \quad (2.19)$$

where  $IR_{FWHM}$  and  $V_{FWHM}$  denote *FWHM* of IR and visible signals respectively.

8- Calculate the difference between the rising edges of two simultaneous PPG pulses as Equation (2.20):

$$\Delta tr = IR_{HM1} - V_{HM1} \quad (2.20)$$

where  $\Delta tr$  is the difference between rising edges.

9- Calculate the difference between the falling edges of two simultaneous PPG pulses as Equation (2.21):

$$\Delta tf = IR_{HM2} - V_{HM2} \quad (2.21)$$

where  $\Delta tf$  is the difference between falling edges. This algorithm can be summarized as Figure 2.15.

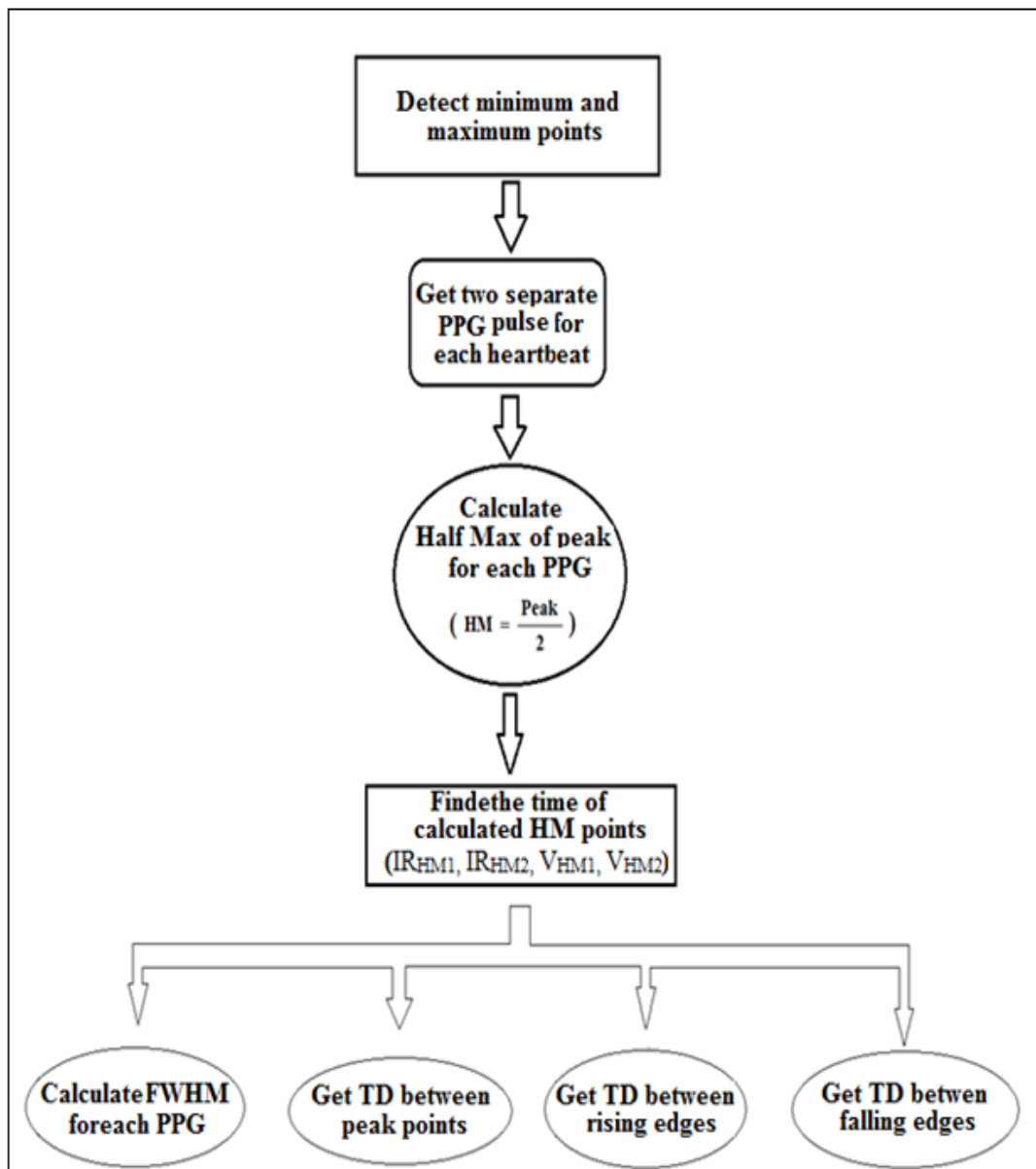


Figure 2.15. The algorithm to extract TDs

## 2.8. Features and Specifications Used in Each Study

Different features and specifications were used in separate studies that are described in the following subsections.

### 2.8.1. Features Used in the Study (1)

In study (1), two types of dual-wavelength PPG signals (obtained by TDM and proposed systems) were compared in terms of their TD variations. To make a quantitative analysis, some features were needed to compare TDs in different physiological conditions and study whether significant variations were observed between groups or not. In analyzing biomedical signals, the mean, standard deviation (SD) and standard errors (SE) are important parameters. In this study, the mean ( $\mu$ ) and standard errors (SE) of the mean of TDs were used as specifications. Recorded signals in different phases of the experiments were separated and arithmetic mean and SE of TDs correspond with these separate stages were obtained as below Equations (2.22) and (2.23) respectively.

$$u = \frac{1}{N} \sum_{i=0}^{N-1} \Delta tp(i) \quad (2.22)$$

where  $\Delta tp(i)$  denote the time difference between peak points of Red and IR PPG pulses in the  $i^{\text{th}}$  heartbeat,  $i$  is the heartbeat number index,  $N$  is the number of TDs ( it is equal to the number of heartbeats in the related phase of the experiment) and  $\mu$  is the mean of TDs.

$$SE = \frac{SD}{\sqrt{N}} \quad (2.23)$$

where, standard deviation of the time difference series ( $SD$ ) is obtained by Equation (2.24).

$$SD = \sqrt{\frac{1}{N} [(\Delta tp1 - u)^2 + (\Delta tp2 - u)^2 + \dots + (\Delta tpN - u)^2]} \quad (2.24)$$

### 2.8.2. Features Used in the Study (2)

Red-IR PPG pair and TDs of peak points were investigated in this study. TD analyses in this study were performed by using  $u$  and  $SD$  related to separate phases of each experiment. Equations (2.22) and (2.24) were employed to obtain  $\mu$  and  $SD$  of TDs.



For graphical illustrating an instance of TDs in different biological conditions, the obtained TDs in wake and deep sleep situations are shown in Figure 2.16 (a) and (b) respectively.

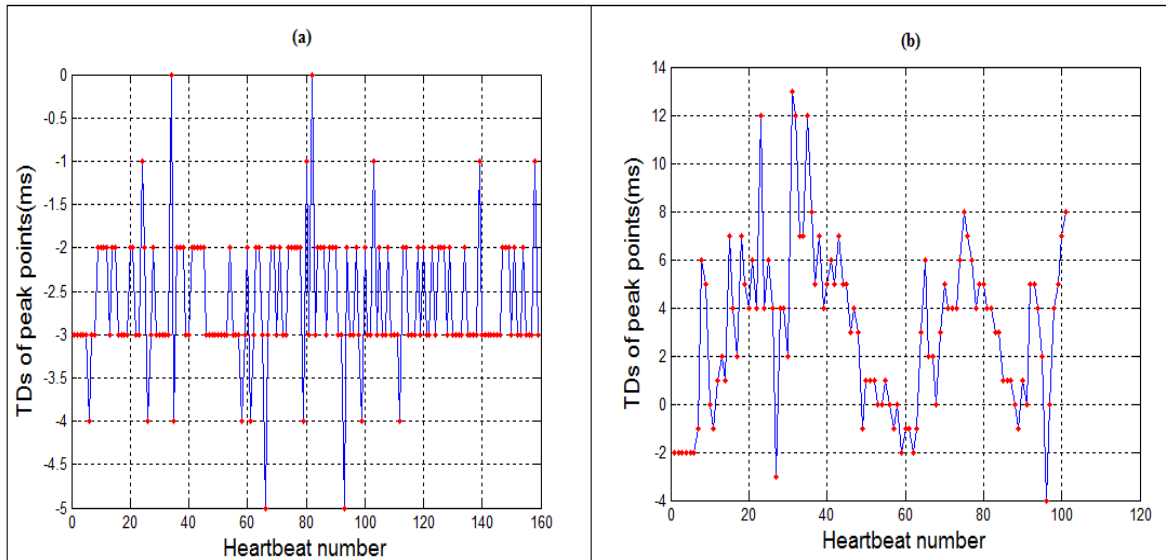


Figure 2.16. TDs obtained in (a) wake and (b) deep sleep situations

### 2.8.3. Features Used in the Study (3)

Similar to previous study, the mean and SD of TDs were calculated and used to analyze Red-IR PPG data with respect to conditions of respiratory system. Figure 2.17 (a) and (b) show the scatter plot separately for mean and SD features obtained in different phases of corresponding breath holding experiments. In this figure, the horizontal axis is the index of trial numbers, and the vertical axis is the value of mean or SD. As seen from the figure, values of mean and SD were generally different and based on these clues, these values could be selected as features to separate groups. Figure 2.18 shows the obtained features in a common space. Horizontal and vertical axes of this feature space are mean and SD of TDs, respectively. This figure explain that the pair of mean and SD reflects the variations of TDs associated with normal and abnormal breathing and can be indicative of significant differences between two groups.

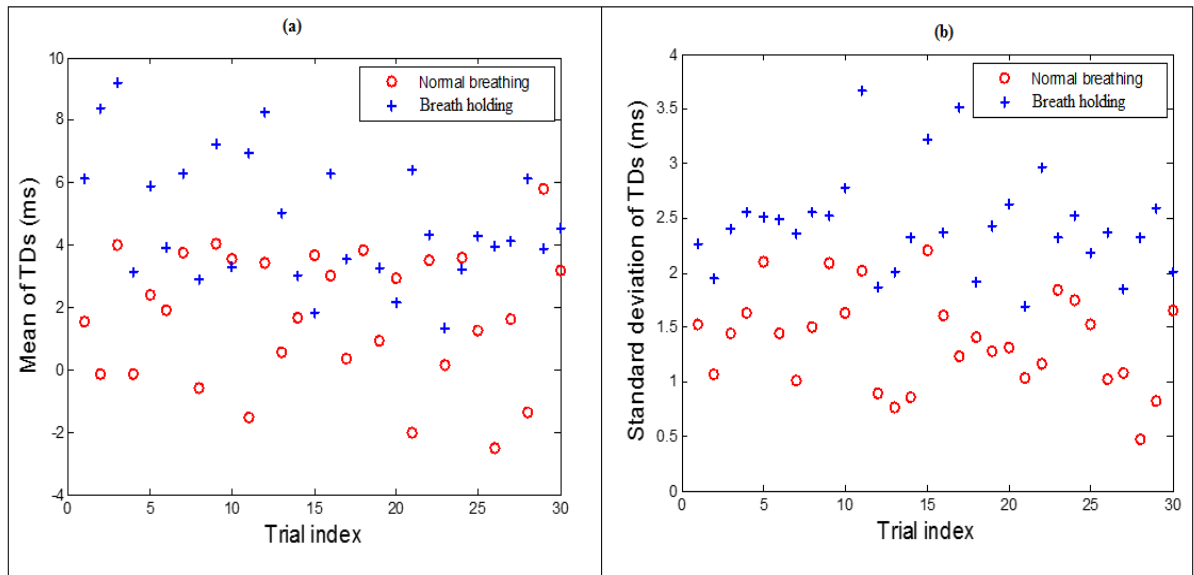


Figure 2.17. Scatter plot for (a) mean and (b) SD of TDs

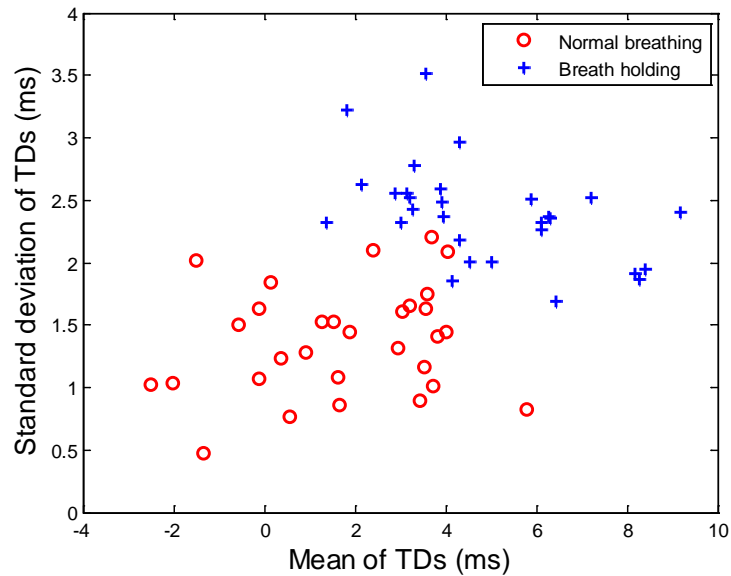


Figure 2.18. Feature space formed by mean and SD of TDs

#### 2.8.4. Features Used in the Study (4)

Like the study (1), mean and SE were used as specifications to analyze TDs. This time, TD variations were investigated and compared for three different pairs of the PPG signals with different wavelength pairs.

### 2.8.5. Features Used in the Study (5)

This study was aimed to fast detection of breathing disorders such as apnea. For rapid identification of apnea, the selected features should be able to recognize abnormal respiration in a fast way. To achieve this aim, the experimental recordings were segmented into classifiable intervals called epochs. Time duration of the epochs was 5s. Four time domain difference features that introduced in Section 2.7 ( $FWHM$ ,  $\Delta tr$ ,  $\Delta tf$  and  $\Delta tp$ ) plus the difference between pulses heights ( $D_{PH}$ ) were extracted from each PPG pulse. The averaged values for each data segment formed a  $1 \times 5$  feature vector. One hundred set of these feature vectors were prepared from normal breathing recordings and other one hundred set were obtained from apneatic recordings. All of these two hundred points formed the data set of this study.

### 2.8.6. Features Used in the Study (6)

This study was aimed for fast wake/sleep detection using TDs. For the fast and accurate wake/sleep identification, the selected features should be able to recognize wake or sleep conditions in minimum time. To reach this, a three dimensional feature vector was tested to detect wake/sleep situations in a unique heartbeat. Three separate time domain differences were used to formation a three dimensional feature vector. These features were as follows:

1. A feature obtained by using both FWHMs (Equations 2.18 and 2.19) named average FWHM ( $A_{FWHM}$ ):

$$A_{FWHM} = \frac{I_{FWHM} + V_{FWHM}}{2} \quad (2.25)$$

2. The difference between rising edges ( $\Delta tr$ ) that was defined as Equation (2.20)
3. The difference between falling edges ( $\Delta tf$ ) that was expressed in Equation (2.21)

All of the mentioned features were extracted for each heartbeat and were considered as separate coordinates of a three dimensional feature space. Each set of  $A_{FWHM}$ - $\Delta tr$ - $\Delta tf$

was determined a point on the given space. One hundred points (features) were prepared from recordings in wake conditions and other one hundred points were obtained from the sleep recording. All two hundred points formed data set. Scatter plot of the obtained three dimensional feature spaces has been shown in Figure 2.19. As seen in this figure, use of this features could led to a good wake/sleep classification results. The time and shape differences between Red and IR PPG pulses in two different physiological conditions (wake and sleep) of a unique subject can be observed in Figure 2.20 (a) and (b). As seen in these figures, the time domain differences were considerably changed in the sleep relative to wake situation.

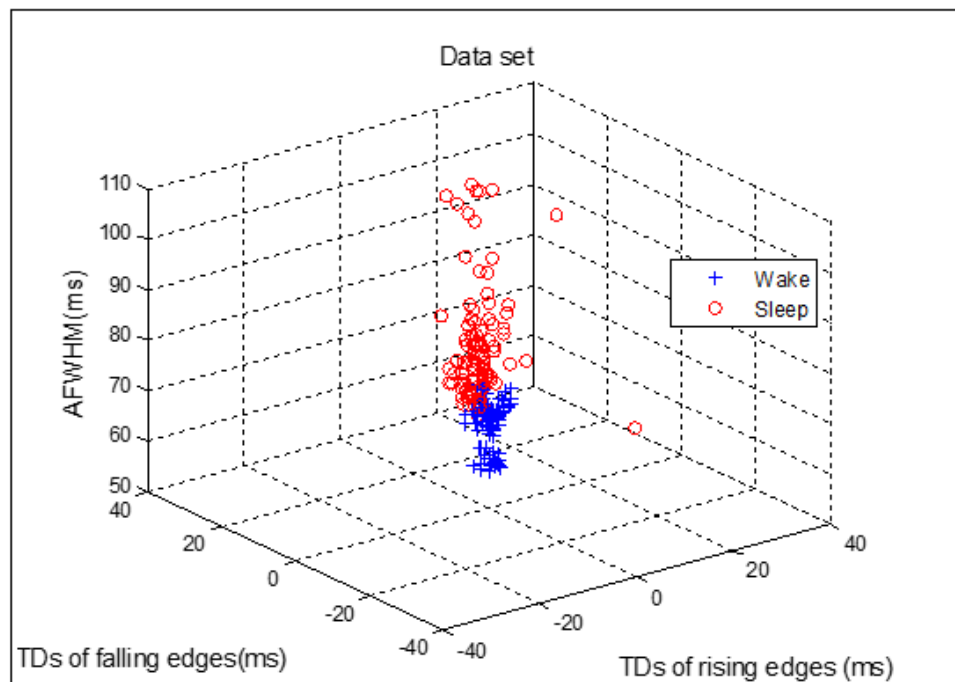


Figure 2.19. Feature space formed by  $A_{FWHM}-\Delta t_r-\Delta t_f$

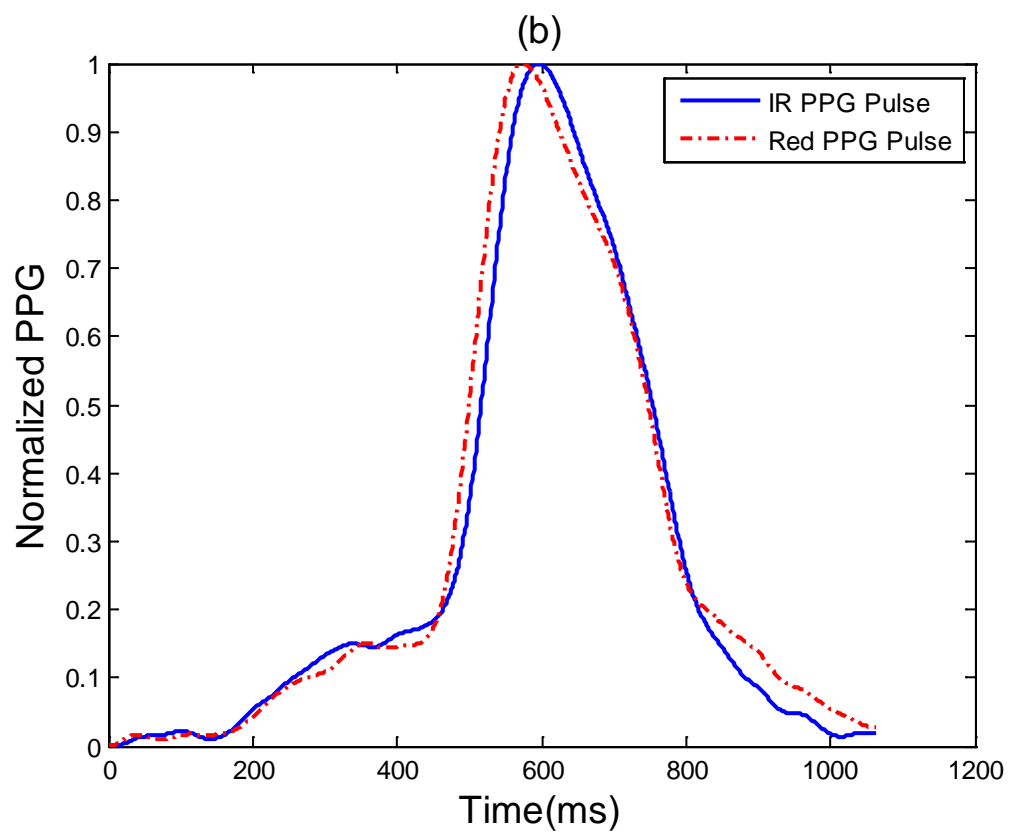
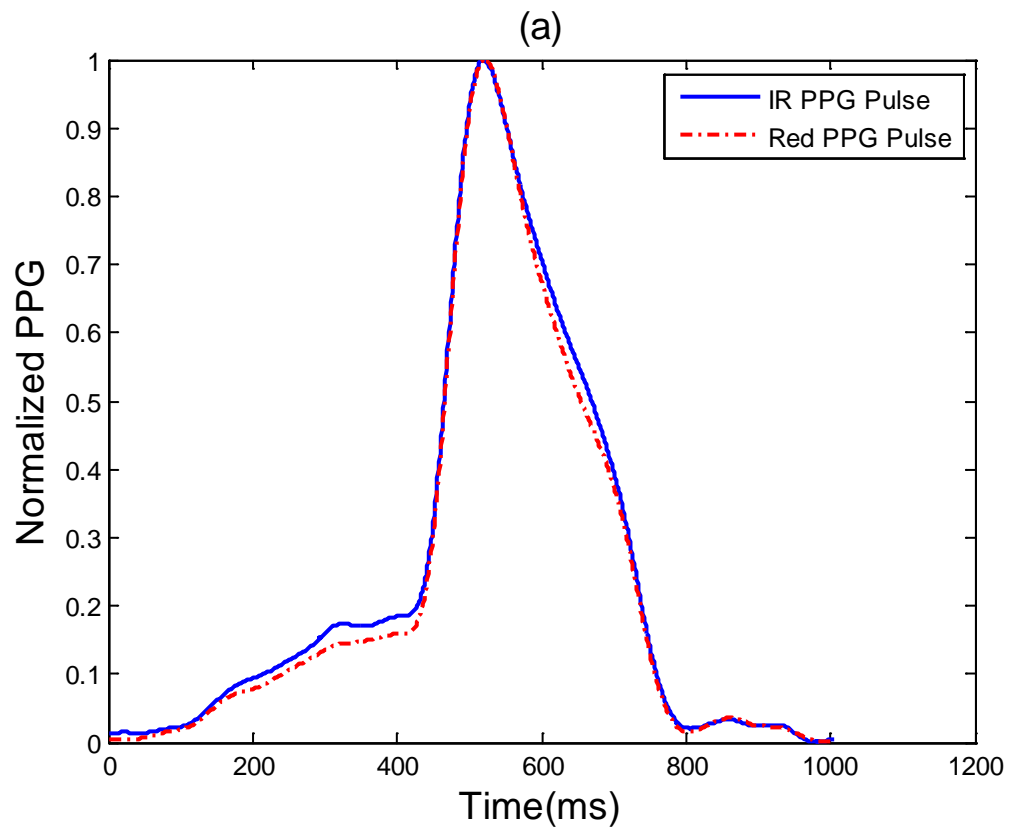


Figure 2.20. Red-IR PPG pulse pairs in (a) wake and (b) sleep conditions

### 2.8.7. Features Used in the Studies (7 and 8)

In these two studies,  $\Delta tp$  (the time difference between peak points of unlike PPG pulses) and PTT (the time difference between peak points of concurrent PPG and ECG signals) were used as the features. To obtain PTT, 'R' points of ECG signal were detected by using peak detection algorithm. Then PTTs were achieved in each heartbeat by subtracting 'R' point time from the peak point time of corresponding PPG pulse as below Equation (refer to Figure 1.1).

$$PPT_i = t_{peak_i} - R_i \quad (2.26)$$

where  $PPT_i$ ,  $t_{peak_i}$  and  $R_i$  denote pulse transit time, the peak point time of corresponding PPG pulse and 'R' point time in the  $i^{\text{th}}$  heartbeat. A sample concurrent ECG and dual-wavelength PPG and their peak points obtained from two heartbeats can be seen in Figure 2.21.

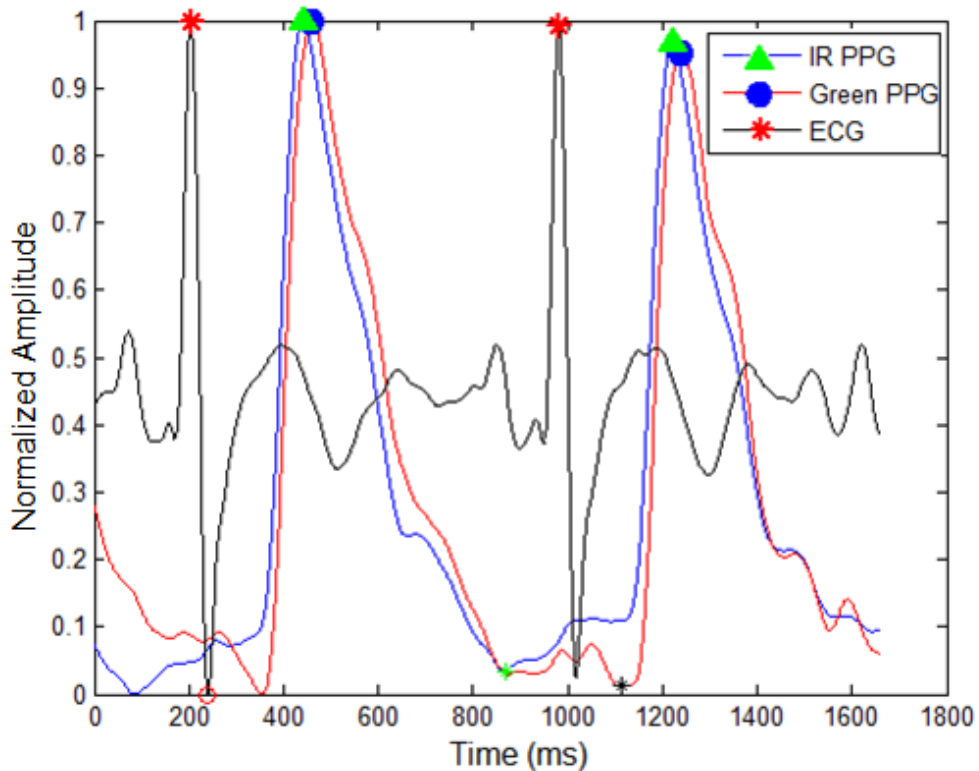


Figure 2.21. Sample EEG and dual-wavelength PPG signals obtained from two consequent heartbeats

## **2.9. Analysis and Classification Methods**

Depending on the selected specifications or features, separate analysis or classification methods were employed in different studies of this thesis. In some studies, the calculated TD features were compared using statistical analysis, indicating that all measured TDs in the separate phases of each experiment were statistically significant. In some other studies, classification methods were applied to fast identification aims by using calculated TD features. Statistical analysis and classification methods are expressed in the following subsections.

### **2.9.1. Statistical Analysis**

Statistical analysis is an important analytical part of data processing. In the case of bio-signals, statistical analysis refers to collect and investigate some samples in a data set. It is basic to some experiments that apply statistics as a research methodology. Many researches in bio-sciences and engineering are carried on by using statistical analysis. This methodology is also very helpful to find approximate solutions when the real process is complex. Statistical analysis has several hypothesis test methods. A statistical hypothesis test is an approach to test a hypothesis statistically. Some of the test methods include one-sample t-test, two sample t-test, one-way ANOVA, chi-square or binomial test and so many others. T-test is one of the most applicable analysis methods in the case of paired subjects and is described as below section.

#### **2.9.1.1. T-test**

A statistical tool to assess hypotheses about group-level differences in results is the t-test. The t-test is normally used for related means. There are two separate usages of the t-test in assessing two types of hypotheses. The first one is the one-sample t-test, in which the level of result for a group is compared to a determined standard. Another one is the two-sample t-test, where the result levels of two groups are compared with each other.

The main application of the two-sample t-test is to compare the means or standard deviations of two data sets. In fact, it usually is used to know whether the means of two

populations on some outcome differ. For instance, it may be employed to test whether subjects' respiratory system responses are different in two distinct situations. In the other words, the t-test compares the real difference between two means with respect to the variation in the data.

To determine statistical significance in a hypothesis test,  $P$  values is used.  $P$  value often determines what studies get published and what projects get funding. In order to understand the concept of  $P$  value, it must be first understood the null hypothesis. In every experiment, there is an effect or difference between groups that the researchers are testing. In the event that there is no difference between the groups, this absence of a difference is named the null hypothesis. The null hypothesis is true, means that there is no difference between the experimental groups at the population level.

The  $P$  value or calculated probability is one of the introduced criteria for hypothesis testing. A high  $P$  value indicates that the data are likely with a true null. A low  $P$  value means that the data are unlikely with a true null. In fact, the null hypothesis is rejected while  $P$  is small.

To obtain  $P$  value, first, the t-statistic must be calculated. Calculation of this test statistic requires three components of the average of both sample (observed averages), the variances of both averages and the number of observations in both populations. Having these values the t value can be calculated as:

$$t = \frac{\bar{x}_1 - \bar{x}_2}{\sqrt{\frac{S_1^2}{n_1} + \frac{S_2^2}{n_2}}} \quad (2.27)$$

where  $\bar{x}_1$  and  $\bar{x}_2$  are the sample means,  $S_1^2$  and  $S_2^2$  are the sample variances,  $n_1$  and  $n_2$  are the sample sizes,  $t$  is the test statistic with  $df$  freedom. Having the calculated t-statistic and using this value to determine  $P$  value by comparing the obtained t-value with a standard table of t-value (with degree of freedom) can determine whether the t-statistic reaches the threshold of statistical significance. Degree of freedom ( $df$ ) could be calculated as:



$$df = \frac{\left( \frac{S^2_1}{n_1} + \frac{S^2_2}{n_2} \right)^2}{\frac{1}{n_1-1} \left( \frac{S^2_1}{n_1} \right)^2 + \frac{1}{n_2-1} \left( \frac{S^2_2}{n_2} \right)^2} \quad (2.28)$$

### 2.9.2. Classification methods

In the studies 5 and 6, TD features were used along with the classification algorithms to fast identification of abnormal respiration and wake/sleep conditions respectively. The used classifiers are described in the following sub-headings.

#### 2.9.2.1. k-Nearest Neighbor (k-NN) classifier

For low dimensional feature vectors in a classification process, more accurate results may be obtained by naive classification algorithms. In pattern recognition, the k-nearest neighbor (*k*-NN) is a simple approach for classification aims. This algorithm considers all accessible subjects and classifies cases based on a likeness value. This classifier is usually applied for statistical estimation and pattern recognition. *k*-NN includes two feature groups of training data set and test data set (also called sample data set). Each of the features of the training data set is allocated to a distinct dimension of a supposed space, and the coordinates of the space are formed by them. So a set of points are distributed in the given space. Then, the similarity of the points is measured by using distance between them. A simple instance of this situation is shown in Figure 2.22. Here, there is two-dimensional feature vector for two classes of data. In this example, *k* has been selected as 3. Unlabeled test sample, is compared with three nearest labeled training data. If at last two of the nearest samples be labeled as class 2, the test sample is also classified as class 2.

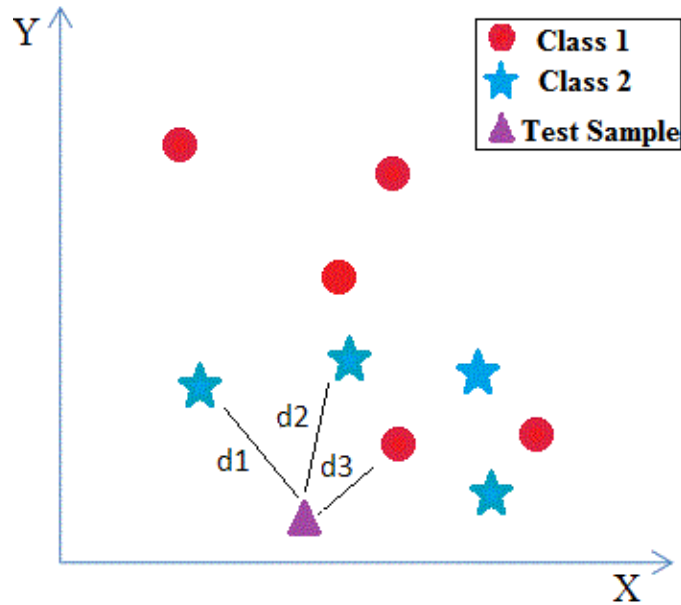


Figure 2.22. A simple example for  $k$ -NN method

### 2.9.2.2. Classifier Training Methods

Optimal parameters of the classifier to be used, is calculated using the training data set. This process is called training the classifier. The variety of approaches is available to determine the best  $k$  parameter using the training features. There are three training approaches frequently used in the literature. The first of them is K-fold cross-validation method. In this method, training data set is divided to a certain number ( $K$ ) equally subsets.  $K-1$  subsets are used as training set and one subset is used for test (also called confirmation or validation). The most suitable  $k$  parameter of the classifier is searched in this distribution. This process is repeated until each subset is to be used as a set of validation at least once. A number of problems may be occurred in this method due to random distribution.

The second training method is the random subsampling cross-validation method. In this approach, training set is randomly divided into two equal subsets (training and validation) and searched for optimum classifier parameter.

The third training method is leave one-out cross-validation. This method is a special case of the K-fold cross-validation. Here,  $K$  is chosen as the total number of examples. The algorithm of this method can be summarized as below:

- For a dataset with  $N$  examples, perform  $N$  tests.
- Use  $N-1$  examples to train and the remaining example to test.

Figure 2.23 shows the concept of leave one-out approach.

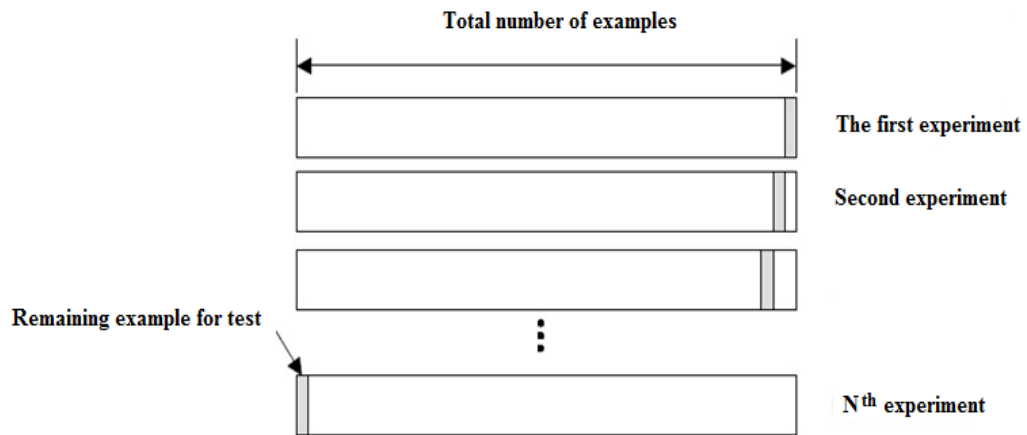


Figure 2.23. Leave one-out cross-validation with  $N$  samples

## 2.10. Analysis/Classification Method Used in Each Study

Analysis or classification method used in each study is described in below subsections.

### 2.10.1. Study (1); Statistical Analysis

Statistical analysis was performed in this study. The two-sample t-test was applied separately to mean of TDs in each phase of the breath holding experiments separately for both TDM and proposed methods. A  $P$  value less than 0.05 was considered to be statistically significant. Statistics and Machine Learning Toolbox™ of MATLAB® was used to perform statistical analysis.

### 2.10.2. Study (2); Statistical Analysis

In this study to have quantitative analysis, similar to study (2), the calculated TD values were compared with two-sample t-test, indicating that all measured TDs in the

separate phases of all of three different physiological changing experiments (wakefulness-sleep, rest-run, nonsmoking-smoking) were statistically significant. A  $P$  value less than 0.05 was considered to be statistically significant. The t-test was applied separately to mean and standard deviation of TDs in each experiment.

### **2.10.3. Study (3); Statistical Analysis**

To be sure that TD variation was significant ( $P < 0.05$ ) the obtained TD features in different respiratory conditions were compared with each other. To this end, the mean and standard deviations of TD series were achieved in the separate phases of each experiment. Differences between groups were investigated by two-sample t-tests.

### **2.10.4. Study (4); Statistical Analysis**

Time domain parameters as mean and standard error of means of measured TDs were calculated for each data segment obtained from separate steps of the experimental recordings. Differences between breathing spontaneously and breath holding were investigated separately for three PPG pairs (Red-IR, Green-IR, and Blue-IR) by two-sample t-test. A value of  $P < 0.05$  was considered as statistically significant.

### **2.10.5. Study (5); $k$ -NN and SVM Classifiers**

In this study there were two groups of feature vectors. The total number of samples was two hundred, one group (hundred fold) belonged to normal breathing and other group (hundred fold) belonged to apneatic situations.  $k$ -NN algorithm was employed to classify two groups. In order to determine the more accurate method for optimal usage of all available training data, three training procedures of  $k$ -NN (K-fold, random subsampling and leave one-out cross-validation) were examined. At last, the obtained data set was classified by SVM classifier once again to compare with the results of  $k$ -NN.

### 2.10.6. Study (6); *k*-NN and SVM Classifiers

Three dimensional feature vectors were used in this study. The total number of samples was two hundred, one group (hundred fold) was belonged to wake and other group (hundred fold) was belonged to sleep situations. Like the study (5), *k*-NN and its three training methods were used and compared as classifiers. Also, SVM classifier was considered in order to comparing with *k*-NN method.

### 2.10.7. Studies (7 and 8); Statistical Analysis

In these two studies, differences between groups were investigated by two samples t-tests. The mean and standard deviations of TD series were achieved in the separate phases of each experiment. To be sure that TD variation was significant ( $P < 0.05$ ) the obtained TD features in conditions were compared with each other.

The analysis/classification methods and features used in each of the studies are summarized in Table 2.2.

Table2.2. Used features and analysis/classification methods in each study

| Item                    | Study (1)                           | Study (2)                           | Study (3)                           | Study (4)                           | Study (5)  | Study (6)                                 | Studies (7 & 8)                              |
|-------------------------|-------------------------------------|-------------------------------------|-------------------------------------|-------------------------------------|--|---|--|
| <b>Applied Features</b> | $\mu$ & <i>SE</i><br>of $\Delta tp$ | $\mu$ & <i>SD</i><br>of $\Delta tp$ | $\mu$ & <i>SD</i><br>of $\Delta tp$ | $\mu$ & <i>SE</i><br>of $\Delta tp$ | $A_{FWHM}$ &<br>$\Delta tr$ & $\Delta tf$<br>& $\Delta tp$ &<br>$D_{PH}$ | $A_{FWHM}$ &<br>$\Delta tr$ & $\Delta tf$ | $\mu$ & <i>SE</i><br>of $\Delta tp$ &<br>PTT |
| <b>Method</b>           | t-test                              | t-test                              | t-test                              | t-test                              | <i>k</i> -NN<br>& SVM  | <i>k</i> -NN<br>& SVM                     | t-test                                       |

### 3. RESULTS

Different studies, materials and methods were described in the previous section. The outcomes of each study are presented in this section.

#### 3.1. The Results of the Study (1)

TDs obtained by both of TDM and proposed sensor systems are compared in breathing spontaneously and breathe holding situations. Figure 3.1 show the bar graph for the means of TDs and SE of means. As seen in this figure, there is a meaningful difference between TDs obtained from breathing spontaneously and breath holing conditions in the proposed method; however, in TDM method there are no considerable differences between groups. Table 3.1 reveals the t-test's results separately for both of the methods. In this Table, mean is the average difference between the two variables, SD is the standard deviation of the difference scores,  $t$  is the test statistic (denoted  $t$ ),  $df$  is the degrees of freedom for this test, confidence interval of the difference (CI) is the part of the t-test output that complements the significance test results and  $P$  is the value corresponding to the given test statistic  $t$ .

In the case of TDM method, the  $P$  value equaled 0.8024. By conventional criteria, this difference is considered to be not statistically significant. The mean of group one (breathing spontaneously) minus group two (breath holding) equaled 0.430000. Typically, if the CI for the mean difference contains 0, the results are not significant at the chosen significance level. The results of TDM method showed CI between -3.024461 to 3.884461, which did contain zero; this agrees with the big  $P$ -value of the not significance.  $P$  value for the proposed method equaled 0.0061. This difference is considered to be very statistically significant. The mean of group one minus group two equaled -5.9608. CI was in the interval between -10.113558-1.808042, which did not contain zero; this agrees with the small  $p$ -value of the significance test.

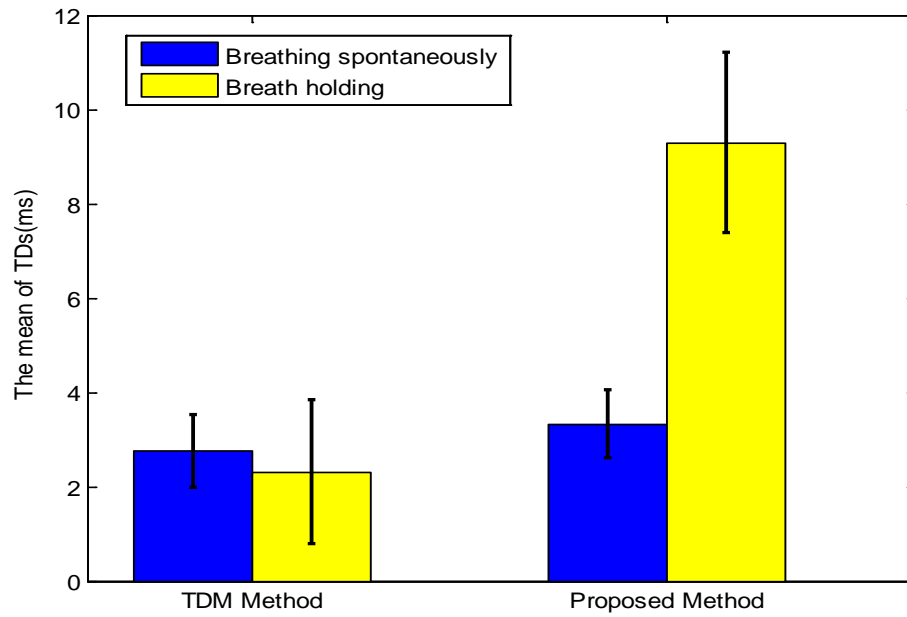


Figure 3.1. Bar plot for the mean and SE of TDs for both of the methods

Table 3.1. Results of t-test to compare proposed and TDM methods

| Method   | Differences |       |   |           | <i>t</i> | <i>df</i> | <i>P</i> Value |
|----------|-------------|-------|---|-----------|----------|-----------|----------------|
|          | Mean        | SD    | 95% Confidence Interval of the Difference |           |          |           |                |
|          |             |       | Lower                                     | Upper     |          |           |                |
| TDM      | 0.4300      | 1.706 | -3.024461                                 | 3.884461  | 0.2520   | 38        | 0.8024         |
| Proposed | -5.960      | 2.051 | -10.113558                                | -1.808042 | 2.4183   | 38        | 0.0061         |

### 3.2. The Results of the Study (2)

In this study TDs between peak points of Red-IR PPG pulses were tested to analyze biological conditions. For calculating the time difference variations of PPG signals (main

focus of the thesis), the time differences between the peak points of IR and Red PPG pulses were obtained in each heartbeat. These subtracting results were achieved from the beginning to the end of each experimental recordings and a vector was formed from these values to reach the dual-wavelength PPG time difference pseudo-signal or TD series. The obtained TD values for the first and last 80 sec epochs of each experiment that was described in Section 2.5.2 are given in Tables 3.2 and 3.3. As expressed before, data recording time duration was different for each experiment. For example, total duration of smoking was 480 sec, total duration of rest-run experiment was 700 sec, and that of wake-sleep time was in the range of 5-30 min depending on the subject. In Tables 3.2 and 3.3, the time differences of recording signals were obtained just for 80 sec epoch of starting and 80 sec epoch of the ending of each experiment. In order to brief presentation of the tables, time difference variations between these two epochs were not included in the tables. Positive or negative sign of time difference value depended on the leading or lagging phase of IR PPG with respect to Red PPG. As seen in the tables, in some experiments, the leading or lagging phase was reversed due to more changes of time difference between the two PPG signals.

For illustrating full-time TD examples, the time difference series for nonsmoking-smoking, wakefulness-sleep, and rest-run experiments obtained from subject one, are shown in Figures 3.2, 3.3 and 3.4, respectively. In these figures, the horizontal axis shows the number of heartbeats (because TDs were obtained for each heartbeat) and the vertical axis shows the amount of TDs in milliseconds. As seen in Figure 3.2, the time differences between IR and RED PPG were about 4 ms in the start of the smoking process. Over time, with continuing to smoke for 400 sec, the value of time differences reduced and reached about 10 ms and the phase angle was reversed. In Figure 3.2, a third-order polynomial curve was fitted to the obtained time difference pseudo-signal to have a more meaningful figure and higher understanding. Polynomial fitting process may be helpful for feature extraction and data classification processes in feature works. Figure 3.3 shows the obtained time difference pseudo-signal for wakefulness-sleep experiment of the object one. As seen in this figure, at the start of the test in wakefulness situation, time differences were about 3-4 ms. After approximately 14 min (1050 heart beats) when the individual slept, time differences decreased to about -15 to -5 ms. There were significant time difference oscillations in the sleep situation unlike the waking state. Time differences obtained from the object one in rest-run test are seen in Figure 3.4. In this case, time difference increased



from about 4-5 ms in the standing motionless situation to about 10 ms after 4 min of running on the treadmill. In this test, significant oscillations of time differences were appeared like the sleep state.

The results of the two-sample t-test for the mean of the TDs and standard deviation of the means in each of the experiments are shown in Table 3.4. As seen in this table,  $P$  value was less than 5%. These results confirm statistical significance both for means and for the standard deviations between different stages of the experiments. Error plot obtained using mean and standard deviations of TDs related to the each experiment is illustrated in Figure 3.5. This figure also indicates that the extracted features were significantly different for normal conditions and physiological challenging conditions.

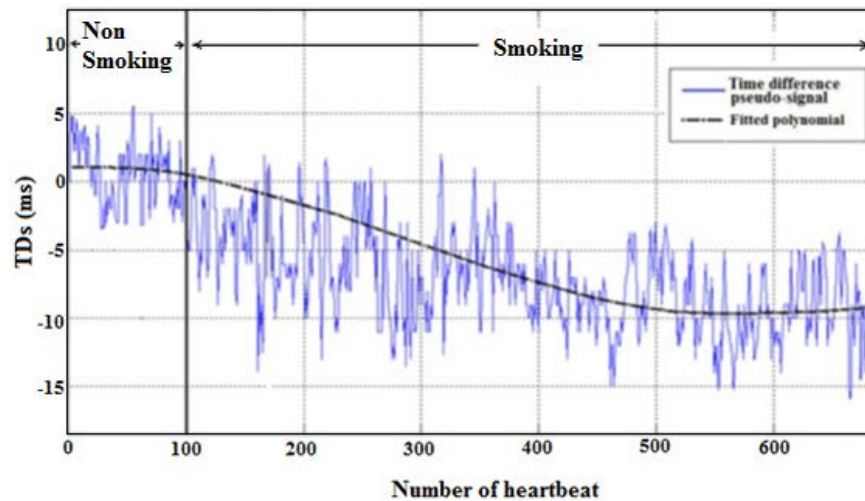


Figure 3.2. TDs obtained from nonsmoking-smoking experiment

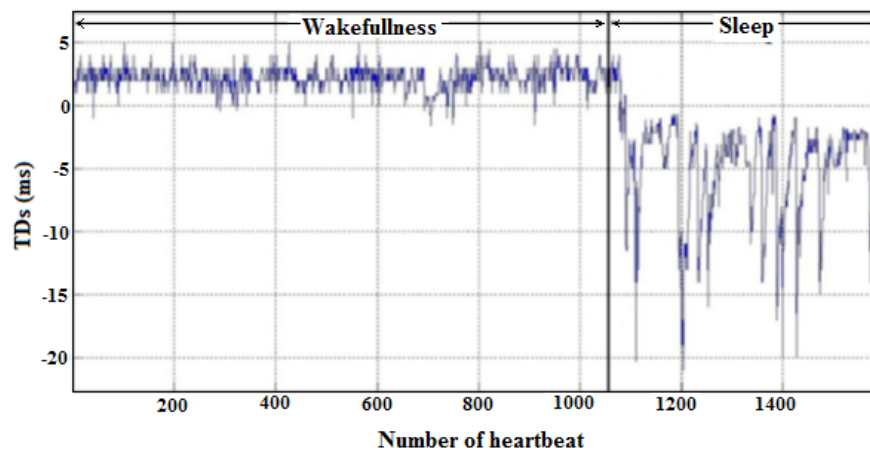


Figure 3.3. TDs obtained from wakefulness-sleep experiment

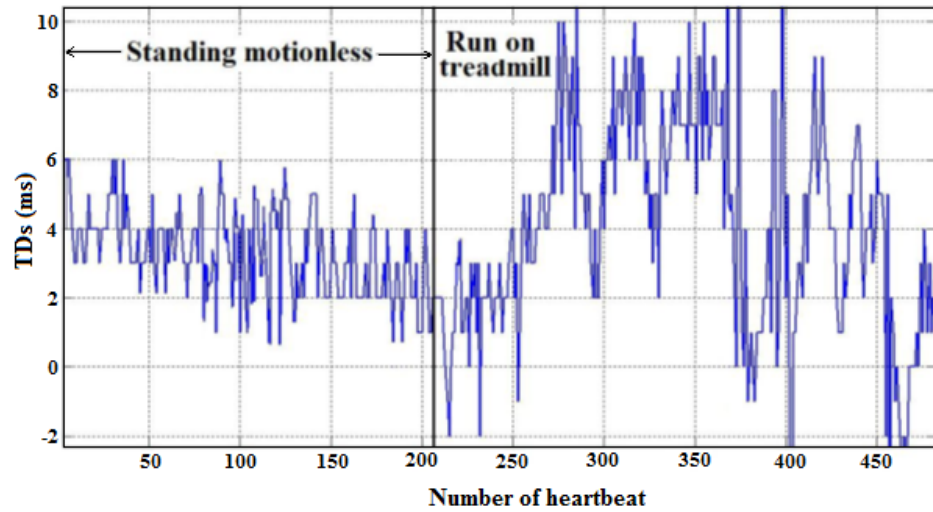


Figure 3.4. TD series obtained from rest-run experiment

Table 3.2. Obtained TDs in various conditions (first iteration of the experiments)

|                   | TDs (ms); Mean $\pm$ SD |                 |                |                  |                |                 |
|-------------------|-------------------------|-----------------|----------------|------------------|----------------|-----------------|
|                   | Non-Smoking             | Smoking         | Wakefulness    | Sleep            | Rest           | Run             |
| <i>Subject 1</i>  | 4 $\pm$ 2.25            | -10 $\pm$ 2.45  | 3 $\pm$ 1.50   | -13 $\pm$ 7.01   | 4 $\pm$ 2.52   | 8 $\pm$ 5.19    |
| <i>Subject 2</i>  | 8 $\pm$ 3.21            | 0 $\pm$ 3.41    | 7 $\pm$ 2.55   | -10 $\pm$ 6.36   | 7 $\pm$ 2.36   | 12 $\pm$ 7.28   |
| <i>Subject 3</i>  | 9 $\pm$ 3.14            | -1 $\pm$ 3.42   | 9 $\pm$ 2.65   | -2 $\pm$ 5.75    | 10 $\pm$ 2.14  | 5 $\pm$ 5.49    |
| <i>Subject 4</i>  | -3 $\pm$ 3.41           | -15 $\pm$ 4.45  | -2 $\pm$ 2.12  | -7 $\pm$ 8.16    | -3 $\pm$ 2.52  | 4 $\pm$ 6.74    |
| <i>Subject 5</i>  | 6 $\pm$ 2.22            | -3 $\pm$ 2.23   | 4 $\pm$ 1.78   | -5 $\pm$ 7.25    | 5 $\pm$ 3.25   | 10 $\pm$ 5.11   |
| <i>Subject 6</i>  | 4 $\pm$ 3.15            | -7 $\pm$ 3.63   | 3 $\pm$ 1.69   | -9 $\pm$ 8.05    | 5 $\pm$ 3.05   | 7 $\pm$ 5.54    |
| <i>Subject 7</i>  | 5 $\pm$ 2.27            | -3 $\pm$ 3.26   | 7 $\pm$ 2.25   | -2 $\pm$ 6.65    | 6 $\pm$ 2.36   | 11 $\pm$ 6.17   |
| <i>Subject 8</i>  | 11 $\pm$ 3.2            | -3 $\pm$ 4.62   | 10 $\pm$ 2.34  | -4 $\pm$ 7.45    | 8 $\pm$ 2.75   | 12 $\pm$ 4.32   |
| <i>Subject 9</i>  | -4 $\pm$ 3.12           | -10 $\pm$ 3.85  | -4 $\pm$ 2.63  | -9 $\pm$ 5.95    | -2 $\pm$ 2.65  | 5 $\pm$ 5.02    |
| <i>Subject 10</i> | 4 $\pm$ 3.62            | -5 $\pm$ 2.53   | 5 $\pm$ 1.95   | -5 $\pm$ 6.45    | 5 $\pm$ 3.12   | 9 $\pm$ 5.32    |
| <i>Average</i>    | 4.4 $\pm$ 2.87          | -3.7 $\pm$ 3.40 | 4.2 $\pm$ 2.15 | -6.60 $\pm$ 6.91 | 4.5 $\pm$ 2.68 | 9.30 $\pm$ 5.62 |

Table 3.3. Obtained TDs in various conditions (second iteration of the experiments)

|                   | TDs (ms); Mean± SD |           |             |            |          |          |
|-------------------|--------------------|-----------|-------------|------------|----------|----------|
|                   | Non-Smoking        | Smoking   | Wakefulness | Sleep      | Rest     | Run      |
| <i>Subject 1</i>  | 3 ±3.11            | -9 ±3.75  | 4±1.12      | -10±8.68   | 3 ±3.51  | 6 ±5.84  |
| <i>Subject 2</i>  | 5±2.25             | -3 ±3.44  | 7±2.60      | -2±6.23    | 6 ±2.50  | 11 ±6.60 |
| <i>Subject 3</i>  | 10±2.14            | -1±4.63   | 12±2.47     | -3±7.40    | 10±2.25  | 14±4.66  |
| <i>Subject 4</i>  | -2±3.52            | -12±3.24  | -2±2.58     | -11±5.63   | -2±2.85  | 4±5.23   |
| <i>Subject 5</i>  | 5±3.53             | -3±2.75   | 4±1.96      | -5±6.45    | 4±3 .05  | 9±5.21   |
| <i>Subject 6</i>  | 5 ±2.11            | -11 ±2.71 | 2±1.11      | -12±7.25   | 4 ±2.53  | 9 ±5.47  |
| <i>Subject 7</i>  | 7±3.45             | -3 ±3.12  | 5±2.35      | -9±6.75    | 6 ±2.56  | 10 ±7.14 |
| <i>Subject 8</i>  | 8±3.23             | -2±3.14   | 11±2.12     | -4±5.81    | 11±2.60  | 14±5.42  |
| <i>Subject 9</i>  | -2±3.27            | -13±4.01  | -3±2.23     | -6±8.98    | -4±2.52  | 3±6.61   |
| <i>Subject 10</i> | 4±2.36             | -4±2.22   | 5±1.48      | -4±7.35    | 4±3.19   | 8±5.24   |
| <i>Average</i>    | 4.3±2.89           | -6.10±3.3 | 4.5± 2.00   | -6.62±7.05 | 4.20±2.7 | 8.80±5.7 |

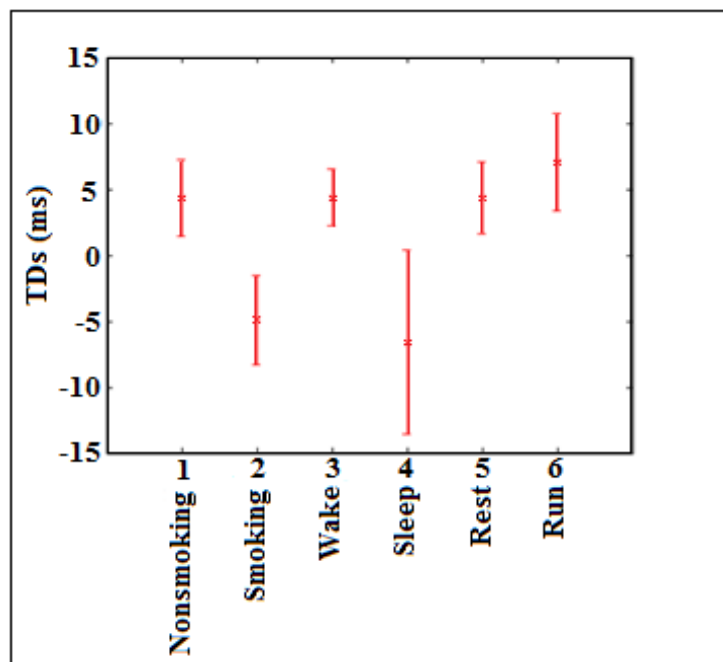


Figure 3.5. Error plot of quantitative analysis (means and SD)

Table 3.4. Results of t-test for the different experiments; study (2)

| Pair                      | Differences |        |   |         | <i>t</i> | <i>df</i> | <i>P</i> Value           |
|---------------------------|-------------|--------|---|---------|----------|-----------|--------------------------|
|                           | Mean        | SD     | 95%<br>Confidence Interval of the<br>Difference |         |          |           |                          |
|                           |             |        | Lower   | Upper   |          |           |                          |
| Nonsmoking-smoking (mean) | 10          | 4.2658 | 7.2535  | 11.2465 | 9.6973   | 19        | $8.614 \times 10^{-9}$   |
| Nonsmoking-smoking(SD)    | 0.2457      | 0.8887 | -0.8749   | -0.0431 | -2.3099  | 19        | 0.032                    |
| Wake-Sleep (mean)         | 10          | 3.9132 | 9.1186  | 12.781  | 12.514   | 19        | $1.2718 \times 10^{-9}$  |
| Wake-Sleep (SD)           | -4          | 1.2856 | -5.5082   | -4.3048 | -17.068  | 19        | $5.560 \times 10^{-12}$  |
| Rest-run (mean)           | -4          | 1.3416 | -5.3279   | -4.0721 | -15.667  | 19        | $2.555 \times 10^{-12}$  |
| Rest-run (SD)             | -3          | 1.3181 | -3.9014   | -2.6676 | -11.142  | 19        | $8.9477 \times 10^{-10}$ |

### 3.3. The Results of the Study (3)

The obtained TDs corresponded with the separate phases of each experiment of this study are given in Tables 3.5. Figure 3.6 (a) and (b) shows the mean and SD of TDs in the corresponding experiments. This figure shows that the pair of mean and SD reflects the difference of TDs associated with respiratory system variations and can be used to evaluate respiratory system.

Table 3.5. Obtained TDs in each experiment of the study (3)

|                   | TDs (ms); Mean± SD |            |                   |                |                                    |
|-------------------|--------------------|------------|-------------------|----------------|------------------------------------|
|                   | First Experiment   |            | Second Experiment |                |                                    |
| Situation         | Wake               | Deep Sleep | Normal Breathing  | Breath Holding | Starting to Normal Breathing Again |
| <i>Subject 1</i>  | 2.14±0.82          | 4.36±3.70  | 2.33 ±2.23        | 3.12±2.26      | 2.25 ±3.12                         |
| <i>Subject 2</i>  | -0.12±0.72         | 1.25±3.88  | 1.04±1.07         | 1.39±1.55      | 2.16±3.08                          |
| <i>Subject 3</i>  | 9.01± 2.17         | 10.22±12.3 | 8.11±2.04         | 9.19±2.40      | 8.15±3.59                          |
| <i>Subject 4</i>  | -0.12±1.04         | 1.25±6.02  | 0.2± 1.33         | 0.16±1.55      | 1.42± 3.86                         |
| <i>Subject 5</i>  | 2.4±1.98           | 3.22±11.89 | 2.11±2.10         | 2.90±2.51      | 2.14±3.56                          |
| <i>Subject 6</i>  | 1.9±0.99           | 4.54± 4.89 | 1.81± 1.44        | 2.93±1.48      | 2.64±2.31                          |
| <i>Subject 7</i>  | 7.74±2.7           | 9.45±13.19 | 5.86± 2.21        | 6.31±2.36      | 5.10±3.12                          |
| <i>Subject 8</i>  | -0.57±0.78         | 4.43± 4.07 | 0.11±2.05         | 0.89±2.55      | 0.19±3.22                          |
| <i>Subject 9</i>  | 4.04±2.0           | 12.52±7.56 | 3.55±2.29         | 3.22±2.52      | 4.28±3.64                          |
| <i>Subject 10</i> | 3.55±1             | 9.82±8.26  | 4.02±1.63         | 5.30±2.78      | 4.41± 2.57                         |
| <i>Subject 11</i> | -1.51±2.52         | 7.61±9.25  | -1.23±2.02        | 3.95±3.67      | 1.75±2.84                          |
| <i>Subject 12</i> | 3.42±0.79          | 7.29±3.29  | 2.26±0.89         | 4.26±2.06      | 4.0±1.90                           |
| <i>Subject 13</i> | 0.55±0.76          | 3.18±2.96  | 0.67± 0.77        | 2.01±2.01      | 1.54±1.31                          |
| <i>Subject 14</i> | 1.66±0.74          | 13.9±5.53  | 1.05 ±0.86        | 2.01±2.32      | 0.77±1.24                          |
| <i>Subject 15</i> | 3.69±2.11          | 7.87±6.87  | 3.57± 2.00        | 4.82±3.22      | 3.71±2.637                         |
| <i>Average</i>    | 2.51±1.46          | 6.29±6.89  | 2.36±1.63         | 3.56±2.56      | 3.14±2.90                          |

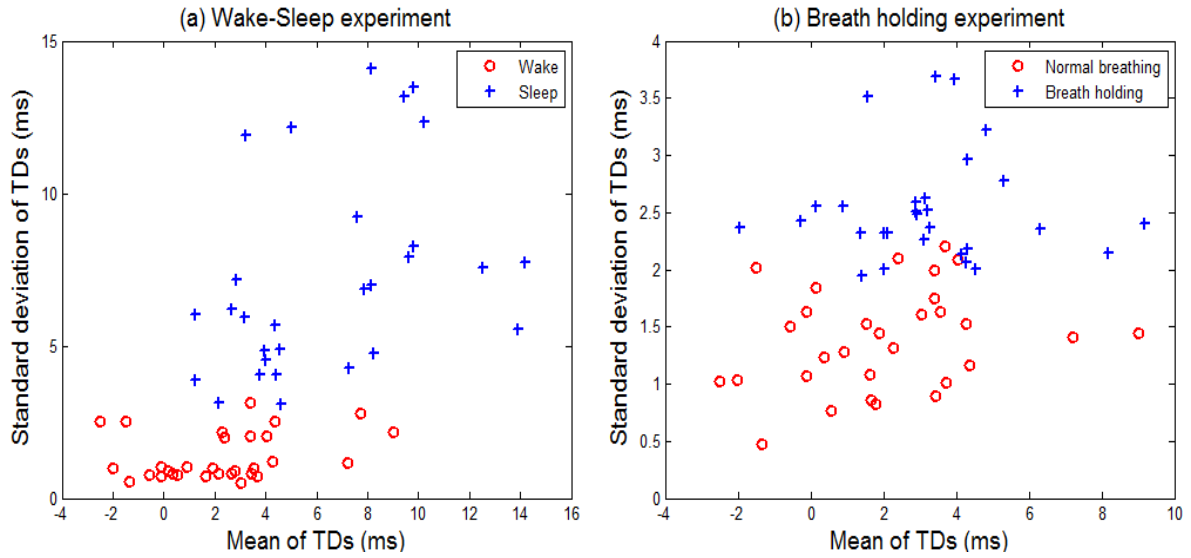


Figure 3.6. Means versus SD in (a) wake-sleep experiment (b) breath holding experiment

The results of the t-test for the mean and SD values of TDs in each of the corresponding segments of the experiments are shown in Tables 3.6 and 3.7. As seen in the Table 3.6,  $P$  value was less than 0.05 and that the 95% confidence interval of the difference for means was from -5.4208 to -3.1678 and for SDs was in the range of -6.9638 to -4.9009. These results confirm statistical differences both for the means and SDs between deep sleep and the wakefulness situations. In Table 3.7, it can be seen that the mean and SD of TDs also had statistical differences during the separate stages of the breath holding experiment so that  $P$  value was much less than 0.05 and the 95% confidence interval of the difference for means equaled from -1.7759 to -0.6587 and for SD was in the range of -1.3466 to -0.9265.

The box-and-whisker diagram of mean and SD related to the each experiment are illustrated in Figures 3.7 and 3.8. These figures also indicate that the differences between mean and SD of TDs obtained in separate phases of each experiment were significant. In the Figure 3.7., the first column is associated with wake situation and second column is for the deep sleep situation. In the Figure 3.8., the First column is related to normal breathing and second column is for the breath holding situation.

Table 3.6. The results of the t-test for the first experiment of study (3)

| Pair                 | Differences |        |   |         | <i>t</i> | <i>df</i> | <i>P</i> Value          |
|----------------------|-------------|--------|---|---------|----------|-----------|-------------------------|
|                      | Mean        | SD     | 95% Confidence Interval of the Difference |         |          |           |                         |
|                      |             |        | Lower                                     | Upper   |          |           |                         |
| Wake-Sleep<br>(mean) | -4.00       | 3.0168 | -5.4208                                   | -3.1678 | -7.79    | 29        | $1.344 \times 10^{-8}$  |
| Wake-Sleep<br>(SD)   | -5.00       | 2.7623 | -6.9638                                   | -4.9009 | -11.76   | 29        | $1.468 \times 10^{-12}$ |

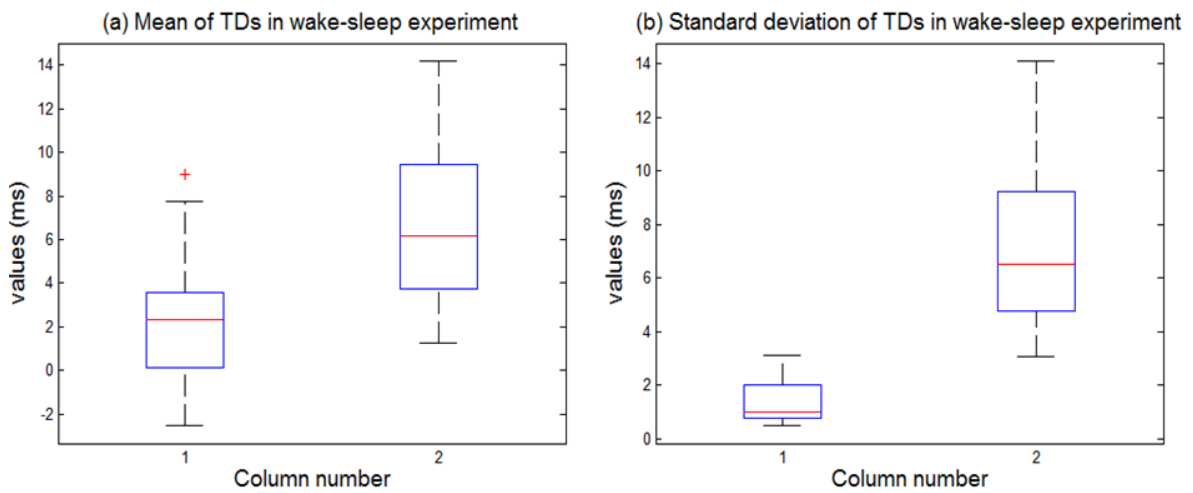


Figure 3.7. Box-and-whisker diagram obtained from (a) mean and (b) SD of TDs

Table 3.7. The results of the t-test for the second experiment of study (3)

| Pair                    | Paired Differences |        |   |         | <i>t</i> | <i>df</i> | <i>P</i> Value          |
|-------------------------|--------------------|--------|---|---------|----------|-----------|-------------------------|
|                         | Mean               | SD     | 95% Confidence Interval of the Difference |         |          |           |                         |
|                         |                    |        | Lower                                     | Upper   |          |           |                         |
| Normal-Hold breath mean | -1.00              | 1.4959 | -1.7759                                   | -0.6587 | -4.457   | 9         | $1.143 \times 10^{-4}$  |
| Normal-Hold breath SD   | -1.00              | 0.5625 | -1.3466                                   | -0.9265 | -11.06   | 29        | $6.311 \times 10^{-12}$ |

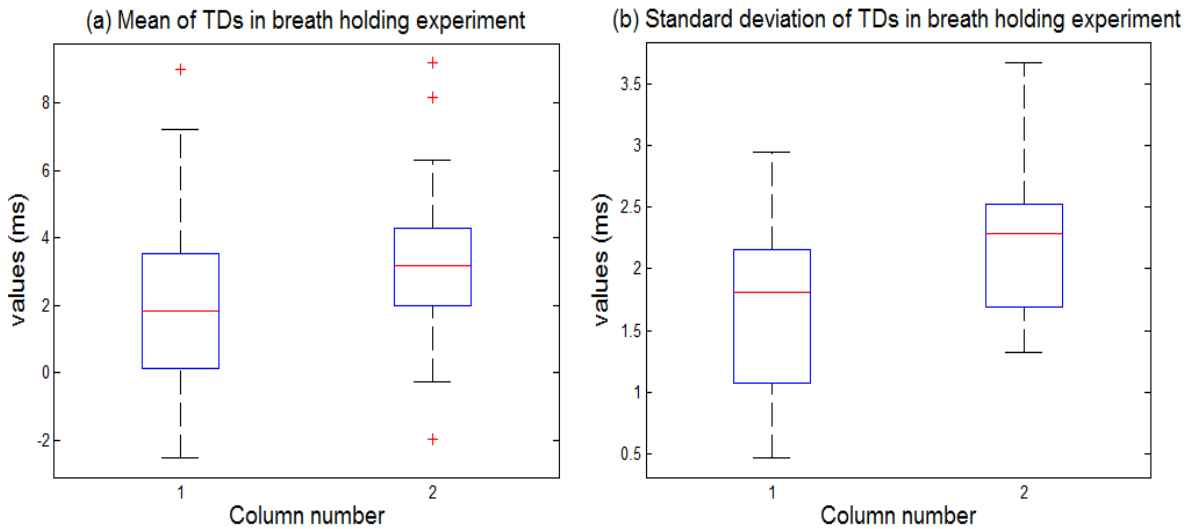


Figure 3.8. Box-and-whisker diagram of (a) mean (b) SD of TDs

### 3.4. The Results of the Study (4)

Table 3.8 represents mean, SD and standard error of the mean (SE) of TDs for the PPG pairs of Red-IR, Green-IR and Blue-IR separately. As seen in this table, in normal breathing phase (breathing spontaneously), the mean of TDs between the mentioned pairs of different PPGs were about 3.22ms, 8.12ms, 11.84ms, respectively. In the breath holding,



the mean of TDs were reduced. Besides, standard deviations of the TDs were increased in the breath holding relative to the breathing spontaneously.

Table 3.8. Mean, SD and SE of TDs obtained in study (4)

| PPG Pair        | TDs (ms)                    |      |       |                     |       |        |
|-----------------|-----------------------------|------|-------|---------------------|-------|--------|
|                 | Breathing Spontaneously(ms) |      |       | Breath Holding (ms) |       |        |
|                 | Mean                        | SD   | SE    | Mean                | SD    | SE     |
| <b>Red-IR</b>   | 3.22                        | 0.89 | 0.162 | -3.88               | 3.54  | 0.6463 |
| <b>Green-IR</b> | 8.12                        | 3.63 | 0.811 | 3.18                | 5.33  | 1.1918 |
| <b>Blue-IR</b>  | 11.84                       | 5.95 | 1.502 | 4.922               | 11.69 | 3.8352 |

The results of the t-test for each of PPG pairs are shown in Table 3.9. As seen in this table, *P* value for TDs of Red-IR PPG pair was  $7.1473 \times 10^{-9}$ . By conventional criteria, this difference is considered to be extremely statistically significant. For Green-IR PPG pair the *P*-value was 0.0015 that was considered to be very statistically significant. In the case of Blue-IR PPG, the *P* value calculated as 0.0241 that this value was considered to be statistically significant. The bar plot with error bars obtained from the mean and SE of TDs related to the each PPG pairs is illustrated in Figure 3.9. This figure also indicate that TDs were significantly different for normal conditions (breathing spontaneously) and biological challenging conditions (breathe holding). These results confirm that although all three PPG pair had significant biological related TD variations, but the greatest and the most significant TD variations were related to the red-IR PPG pair and TDs of blue-IR pair had the lowest response to biological variations.

Table 3.9. *P* value of the t-test for PPG pairs

| Biological Condition Pair              | Red-IR                  | Green-IR | Blue-IR |
|--|-------------------------|----------|---------|
| Breathing Spontaneously-Breath Holding | $7.1473 \times 10^{-9}$ | 0.0015   | 0.0241  |

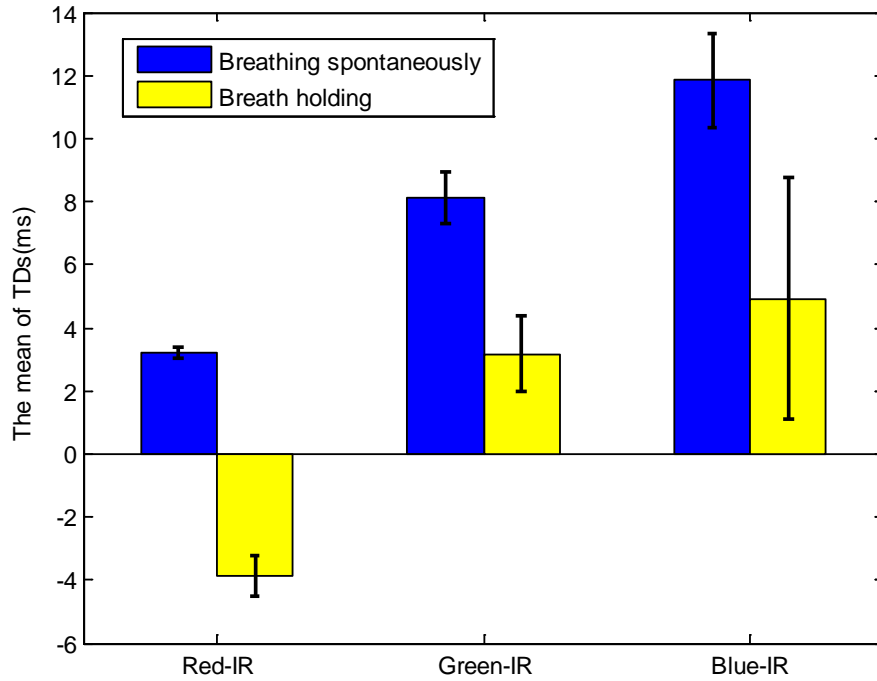


Figure 3.9. The mean of TDs for both breathing conditions

### 3.5. The Results of the Study (5)

Apnea detection results using *k*-NN and SVM classification algorithms are presented in this section. Firstly the data set was split to two equal parts of training and test data sets. In order to obtain more reliable classification results, training data set were randomly mixed and classification stages were repeated 10 separate times. The obtained classification results for separate data mixing stages have been presented with Table 3.10. As seen in Table, good classification results were obtained by using the used TD features and *k*-NN classification methods. The most accurate results have been achieved by leave one-out cross-validation approach.

Table 3.10. *k*-NNclassification results in 10 separate data mixing; study (5)

|                   | <i>k</i> -NN<br>K-fold               | <i>k</i> -NN<br>Leave One-Out          | <i>k</i> -NN<br>Random Subsampling   | SVM                                   |
|-------------------|--------------------------------------|--|--------------------------------------|---------------------------------------|
| Data Mixing       | Correct Rate,<br>FN, FP<br>%         | Correct Rate,<br>FN, FP<br>%           | Correct Rate,<br>FN, FP<br>%         | Correct Rate<br>FN, FP<br>%           |
| First             | 93<br>FN=3 FP=4                      | 94<br>FN=2 FP=4                        | 91<br>FN=2 FP=7                      | 89<br>FN=3 FP=8                       |
| Second            | 89<br>FN=5 FP=6                      | 96<br>FN=1 FP=3                        | 93<br>FN=2 FP=5                      | 91<br>FN=3 FP=6                       |
| 3 <sup>th</sup>   | 94<br>FN=2 FP=4                      | 94<br>FN=3 FP=3                        | 95<br>FN=2 FP=3                      | 88<br>FN=1 FP=11                      |
| 4 <sup>th</sup>   | 92<br>FN=3 FP=5                      | 97<br>FN=1 FP=2                        | 98<br>FN=0 FP=2                      | 88<br>FN=3 FP=9                       |
| 5 <sup>th</sup>   | 88<br>FN=3 FP=9                      | 98<br>FN=0 FP=2                        | 91<br>FN=3 FP=6                      | 91<br>FN=3 FP=6                       |
| 6 <sup>th</sup>   | 93<br>FN=3 FP=4                      | 95<br>FN=2 FP=3                        | 95<br>FN=1 FP=4                      | 87<br>FN=1 FP=12                      |
| 7 <sup>th</sup>   | 91<br>FN=2 FP=7                      | 95<br>FN=2 FP=3                        | 89<br>FN=4 FP=7                      | 90<br>FN=4 FP=6                       |
| 8 <sup>th</sup>   | 88<br>FN=3 FP=9                      | 93<br>FN=3 FP=4                        | 89<br>FN=1 FP=10                     | 88<br>FN=3 FP=9                       |
| 9 <sup>th</sup>   | 93<br>FN=2 FP=5                      | 98<br>FN=1 FP=1                        | 94<br>FN=2 FP=4                      | 91<br>FN=4 FP=5                       |
| 10 <sup>th</sup>  | 89<br>FN=4 FP=7                      | 95<br>FN=2 FP=3                        | 92<br>FN=3 FP=5                      | 88<br>FN=2 FP=10                      |
| <b>Average±SD</b> | 92.34±6.06<br>FN=3±0.94<br>FP=6±1.94 | 96.1±1.8<br>FN=1.7±0.94<br>FP=2.8±0.97 | 92.7±3.22<br>FN=2±1.15<br>FP=5.3±2.3 | 89.1±1.70<br>FN=2.7±1.0<br>FP=8.2±2.4 |

### 3.6. The Results of the Study (6)

$k$ -NN (K-fold cross-validation, leave one-out cross-validation and random subsampling classification) and SVM methods were examined for wake/sleep detection using the extracted three dimensional feature vectors (including  $A_{FWHM}$ ,  $\Delta tr$  and  $\Delta t$  features). The total number of features was two hundred points (100 wakes and 100 sleeps). All of the features were divided in two separate hundred folds of training (50 wakes and 50 sleeps) and test (50 wakes and 50 sleeps) sets. Figure 3.10 shows the feature spaces of training and test data sets. Like the study (5), training data set were randomly mixed and validation stages were repeated in 10 separate iterations. The obtained 10 distinct classification results using three separate  $k$ -NN methods are revealed with Table 3.11. The average $\pm$ SD of classification correct rates in the validation and test stages are revealed in Table 3.12. As seen in this Table, the results show that wake/sleep detection using the mentioned TD features was indeed feasible with a good accuracy. Tables 3.10 and 3.11 in addition to classification correct rate, indicate also samples that were classified as false negatives (FN) and false positives (FP). Classifications errors appear with FN and FP values.

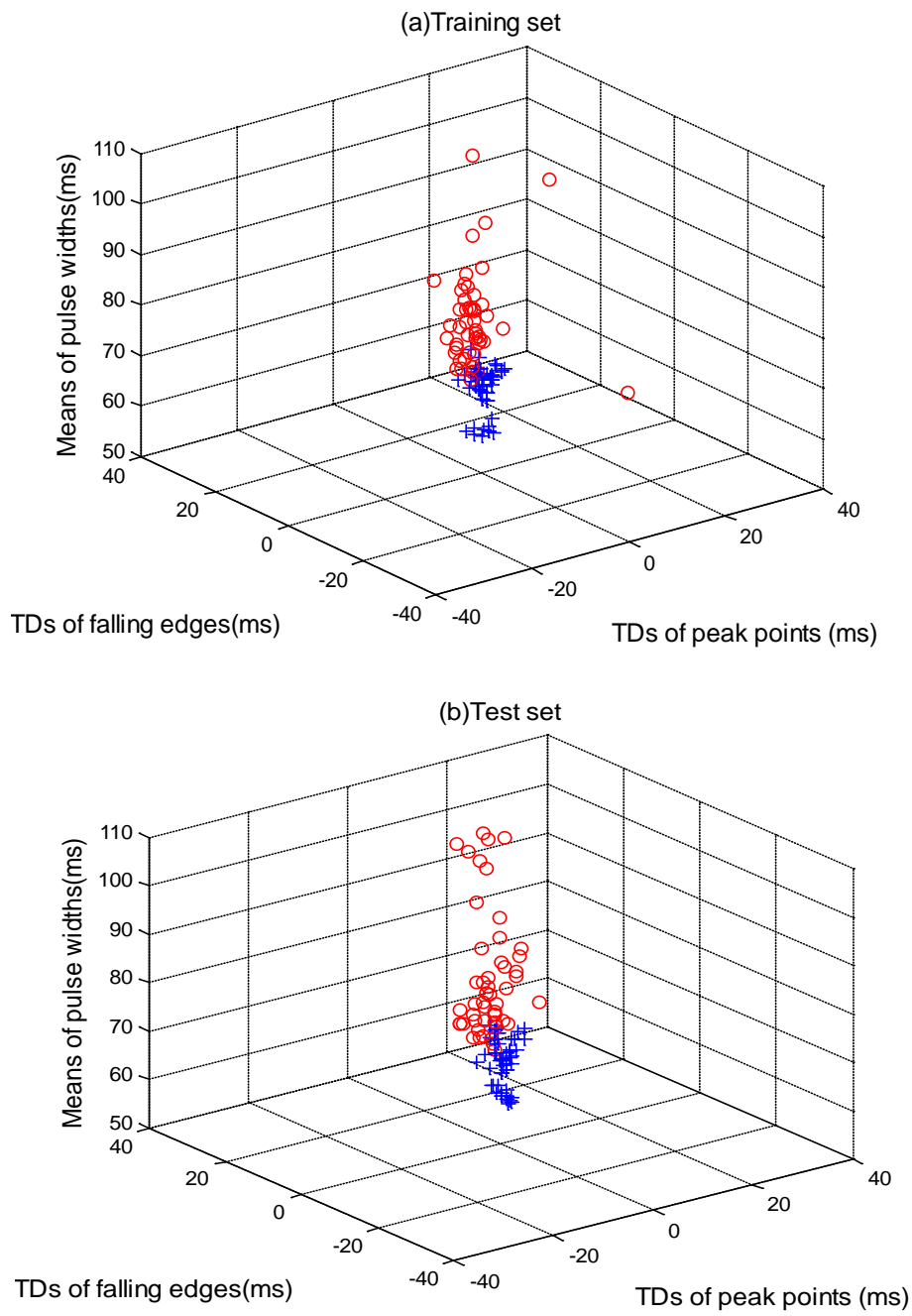


Figure 3.10. (a) Training and (b) test data sets

Table 3.11. *k*-NN and SVM classification results in 10 separate iterations; study(6)

|                        | <i>k</i> -NNK-fold                    | <i>k</i> -NN Leave One-Out            | <i>k</i> -NN Random Subsampling       | SVM                                   |
|------------------------|---------------------------------------|---------------------------------------|---------------------------------------|---------------------------------------|
| <b>Data Mixing</b>     | <b>Correct rate,<br/>FN, FP<br/>%</b> | <b>Correct rate,<br/>FN, FP<br/>%</b> | <b>Correct rate,<br/>FN, FP<br/>%</b> | <b>Correct rate,<br/>FN, FP<br/>%</b> |
| <b>First</b>           | 97<br>FN=3 FP=0                       | 96<br>FN=3 FP=1                       | 97<br>FN=2 FP=1                       | 90<br>FN=8 FP=2                       |
| <b>Second</b>          | 97<br>FN=2 FP=1                       | 97<br>FN= 2 FP=1                      | 96<br>FN=3 FP=1                       | 93<br>FN=5 FP=2                       |
| <b>3<sup>th</sup></b>  | 94<br>FN=5 FP=1                       | 96<br>FN= 4 FP=0                      | 94<br>FN=4 FP=2                       | 93<br>FN=6 FP=1                       |
| <b>4<sup>th</sup></b>  | 97<br>FN=2 FP=1                       | 97<br>FN=2 FP=1                       | 97<br>FN=2 FP=1                       | 93<br>FN=4 FP=3                       |
| <b>5<sup>th</sup></b>  | 97<br>FN=3 FP=0                       | 96<br>FN=3 FP=1                       | 97<br>FN=3 FP=0                       | 94<br>FN=4 FP=2                       |
| <b>6<sup>th</sup></b>  | 96<br>FN=4 FP=0                       | 97<br>FN=3 FP=0                       | 96<br>FN=3 FP=1                       | 91<br>FN=6 FP=3                       |
| <b>7<sup>th</sup></b>  | 97<br>FN=1 FP=2                       | 98<br>FN=0 FP=2                       | 97<br>FN=1 FP=2                       | 92<br>FN=3 FP=5                       |
| <b>8<sup>th</sup></b>  | 95<br>FN=5 FP=0                       | 97<br>FN=3 FP=0                       | 95<br>FN= 4 FP=1                      | 90<br>FN=8 FP=2                       |
| <b>9<sup>th</sup></b>  | 98<br>FN=2 FP=0                       | 99<br>FN=1 FP=0                       | 97<br>FN=2 FP=1                       | 91<br>FN=7 FP=2                       |
| <b>10<sup>th</sup></b> | 96<br>FN=1 FP=3                       | 98<br>FN=1 FP=1                       | 96<br>FN=1 FP=3                       | 93<br>FN=1 FP=6                       |

Table 3.12. Average±SD for *k*-NN classification results and the best *k* parameter

| <b>Validation Type</b>    | <b>The Best<br/><i>k</i></b> | <b>Validation<br/>Correct Rate%</b> | <b>Test<br/>Correct Rate%</b> |
|---------------------------|------------------------------|-------------------------------------|-------------------------------|
| <b>K-Fold</b>             | 5                            | 95±2.23                             | 96.4±1.183                    |
| <b>Leave One-Out</b>      | 3                            | 98.25±1.52                          | 97.8±1.17                     |
| <b>Random Subsampling</b> | 3                            | 94.13±2.48                          | 96.2±1.03                     |

### 3.7. The Results of the Study (7)

PTTs obtained by an ECG signal and different PPG signals in both conditions of normal breathing and breathe holding (apneatic breathing) are compared. Figure 3.11 show the bar graph for the means of PTTs and SE of means obtained from corresponding segments of the experiments. As seen in this figure, there is a meaningful difference between PTTs obtained in breathing spontaneously and breath holding conditions and also between PTTs obtained by IR, Red and Green PPG signals. The mean, SD and SE of PTTs obtained by ECG and PPGs with different wavelengths in different conditions are shown in Table 3.13. As seen in this Table, PTTs obtained by ECG and Green PPG was much different with PTTs achieved simultaneously by the same ECG and IR PPG signals. Also, there were slight difference between PTTs obtained simultaneously by ECG-IRPPG and ECG-RedPPG. Table 3.14 reveals the t-test's results separately for all of PTTs.

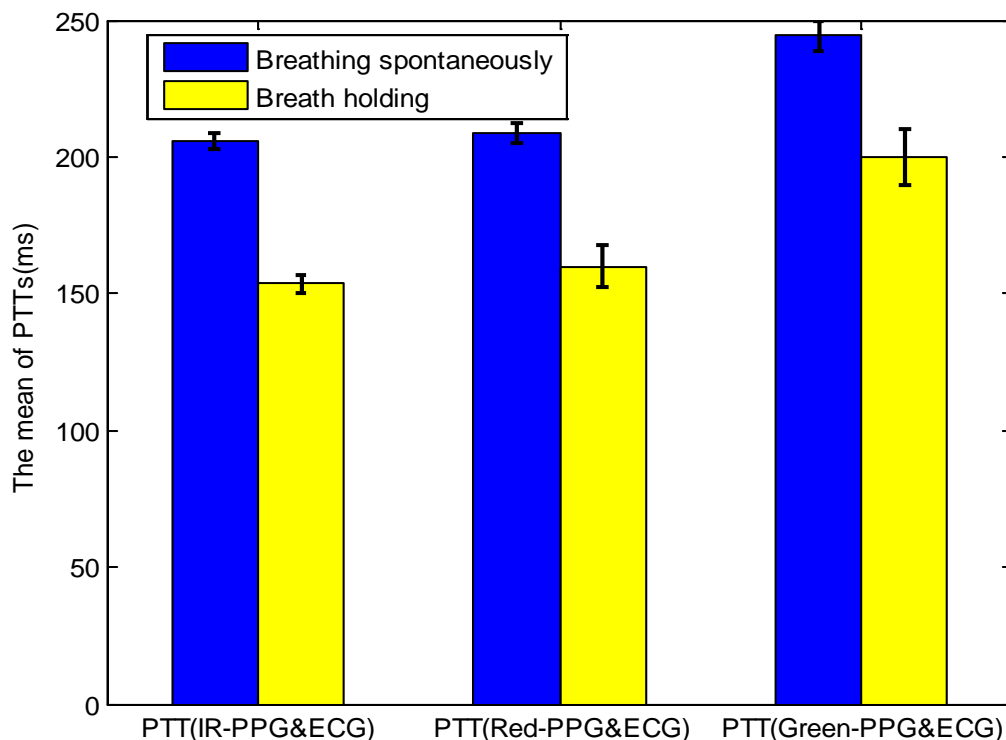


Figure 3.11. Error plot to compare PTTs obtained from ECG and different PPGs

Table 3.13. PTTs obtained by ECG and PPGs in different conditions

|                | PTTs (ms)               |      |       |                |       |         |
|----------------|-------------------------|------|-------|----------------|-------|---------|
|                | Breathing spontaneously |      |       | Breath holding |       |         |
| PTT Type       | Mean                    | SD   | SE    | Mean           | SD    | SE      |
| ECG& IR-PPG    | 205.928                 | 2.84 | 0.401 | 153.55         | 3.197 | 0.452   |
| ECG& Red-PPG   | 208.58                  | 3.70 | 0.523 | 160.07         | 7.83  | 1.1073  |
| ECG& Green-PPG | 244.21                  | 5.7  | 0.806 | 199.75         | 10.19 | 1.44207 |

Table 3.14. The t-test results to compare PTTs in normal and abnormal breathing

| PTT Type      | Differences |       |   |          | <i>t</i> | <i>df</i> | <i>P</i> value |
|---------------|-------------|-------|---|----------|----------|-----------|----------------|
|               | Mean        | SD    | 95% Confidence Interval of the Difference |          |          |           |                |
|               |             |       | Lower                                     | Upper    |          |           |                |
| ECG&IR-PPG    | 52.37       | 0.605 | 51.17788                                  | 53.57812 | 86.610   | 98        | <0.0001        |
| ECG&Red-PPG   | 48.51       | 1.225 | 46.0796                                   | 50.9404  | 39.608   | 98        | < 0.0001       |
| ECG&Green-PPG | 44.46       | 1.652 | 41.1815                                   | 47.73850 | 26.911   | 98        | < 0.0001       |



### 3.8. The Results of the Study (8)

Parts of the recorded concurrent ECG and dual-wavelength PPG signals before and during the exercise test are revealed in Figure 3.12 (a) and (b) respectively. As seen in the Figure, both of ECG and dual-wavelength PPG signals had a good quality and extraction of features could be carried out without a major problem; but during the exercise, big motion artifacts led to distortion of ECG signal and PTT extraction was indeed impossible. However, beat-to-beat PTT and TD features were calculated before the ending the test. The mean results of extracted PTTs and TDs before and after exercise can be seen in Table 3.15. As seen in this Table, strenuous physical activity PTTs reduced and TDs increased seriously.

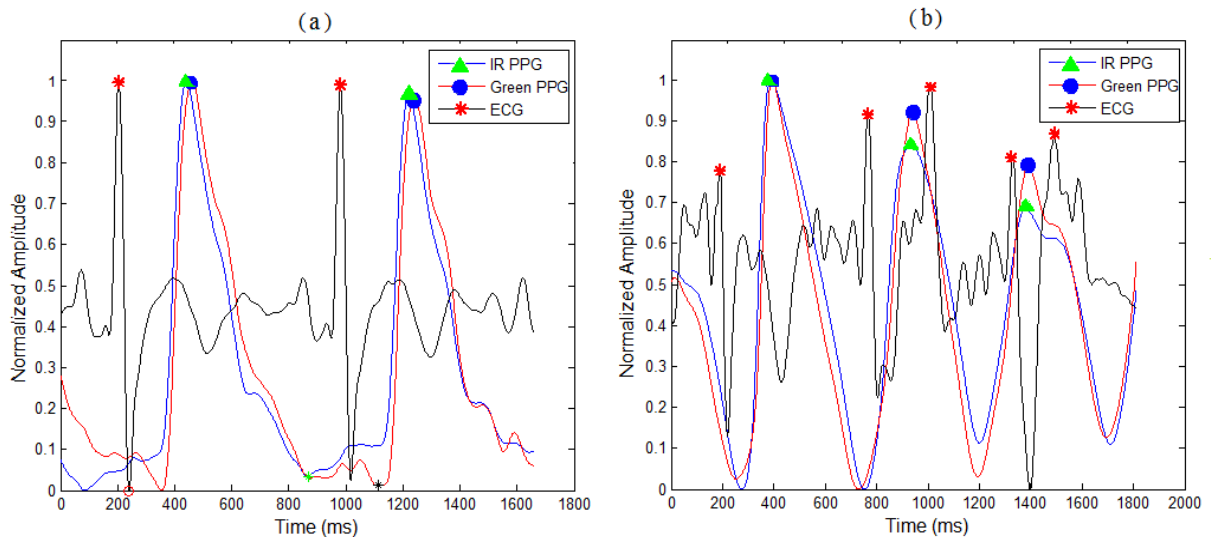


Figure 3.12. ECG and dual-wavelength PPG (a) before and (b) during exercise test

Table 3.15. The mean of PTTs and TDs (ms) obtained before and after the exercise test

| PTT Type     | Before the Test |      | After the Test |      |
|--------------|-----------------|------|----------------|------|
|              | PTTs            | TDs  | PTTs           | TDs  |
| ECG& IR-PPG  | 206.831         | 0.33 | 163.76         | 5.66 |
| ECG& Red-PPG | 210.75          | 0.33 | 162.28         | 5.66 |

#### 4. DISCUSSION

The possibility of the application of TDs obtained from dual-wavelength photoplethysmographic signals was studied during separate physiological challenging tests. In summary, it can be said, with respect to the results it was demonstrated that as long as physiological situation was stable, TD values had no serious variations. However, when the physiological conditions were changed, TD values were also significantly changed. This means the obtained TD series had a pattern related to physiological conditions that can be indicative of physiological variations. This earlier unreported phenomenon would have been a novel and interesting finding of this thesis.

Multi-wavelength PPG was considered with different methods by other researchers. Nonetheless, TDs are new issue in multi-wavelength PPG technology and variations of TDs with respect to bio-physiological conditions were not studied previously. The method presented in this thesis is compared with that of previous studies in the field of multi-wavelength PPG.

Some studies such as [7], [100] and [101] used the multi-wavelength PPG without considering TDs. The used parameter in those studies was the amplitude ratio of PPG signals. Multi-wavelength PPG was applied also by Spigulis *et al.* [102] for skin microcirculation assessment. In that study, different PPG signals have been simultaneously recorded in separate wavelengths. Results of that research showed that signal baseline responses at separate wavelengths were different. They concluded that a depth variety of the skin blood pulsation dynamics was caused to distinct baseline values. In that study there was also no mention of TD variations; but their results in the case of base line variation can supports our research.

Gailite *et al.* [103] employed multi-wavelength PPG, based on fiber-coupled laser irradiation and time-resolved spectrometric detection. They confirmed that PPG pulses that were recorded simultaneously at distinct wavelengths were different in waveform. The outcomes of those two researches can support our results in the case of TDs, with the exception that they also focused on baseline differences without considering TDs.

Other researches in the case of simultaneous different PPG signals obtained from a small hole of the skin were conducted by Asare *et al.* studies [46-48] in which multi-

wavelength PPG signals were analyzed with respect to blood microcirculation characteristics at different vascular depths. These studies reported the shape difference between simultaneous PPG signals. In the mentioned researches there was no TD extraction algorithm and no respect to the bio-physiological conditions.

In addition to the above mentioned studies, Kuzmina *et al.*[104] assembled and tested a fiber-optic spectrometry set-up for applications in skin diffuse laser fluorescence spectrometry and multi-wavelength photoplethysmography studies. Their results also showed differences in spectra of healthy and pathologic skin without mention of TDs and TD variations.

Natural fluorescence of blood has been introduced years ago [105]. Fluorescence feature of blood is due to the existence of some elements such as hemoglobin that they have an intrinsic fluorescence property [106]. Gao *et al.* [107] measured the fluorescence spectra of the whole blood and the hemoglobin. Outcomes of that research revealed that fluorescence spectrum was affected by the wavelength of emitting light and amount of the blood dissolved fluorophores. Considering the results of that research, variations of TDs in distinct biological situations and difference between TDs obtained from separate wavelength pairs (involved in the present study) may be interpreted by the blood fluorescence phenomenon.

Fluorescence is one of the optical processes arises from interaction of light with biological tissues [108]. It is a well-known optical effect that has been proved to be an intrinsic parameter of biological substrates and may aid in the characterization of the physiological states [109]. In fluorescence process, a fluorescent substance is excited by a light beam and then, absorbed light is emitted by the substance [110]. Existing of fluorescent substance molecules in the excited state before returning to the initial conditions takes certain duration called lifetime. Fluorescence lifetime is the time delay between the light absorbance and the emission. The lifetime is dependent on concentration of fluorescent substance and excitation light wavelength [111]. In the case of dual-wavelength PPG, fluorescent substances of blood were excited by Red and IR lights. Blood fluorescence property is due to the existence of some elements such as oxyhemoglobin that have intrinsic fluorescence property [106]. Light absorbance and fluorescence lifetime is changed considering to concentration of blood fluorescent substance (oxyhemoglobin) and is different for each wavelength. Concentration of the blood fluorescent substance is

changed when physiological situation is changed. For example, at bedtime, blood oxyhemoglobin is decreased relative to wakefulness [112]. Therefore, the time difference between unlike PPG signals may be described by fluorescence lifetime difference between two emitted lights and variations of the time difference can be attributed to concentration variations of blood oxyhemoglobin.

There are some studies in the case of apnea detection using PPG signals. In these researches simple PPG signals have been used with a single wavelength. Different features of PPG and various classification methods were proposed to classify two groups of normal breathing and apnea. For example, changes in the peak and valley amplitudes ( $\Delta P$  and  $\Delta V$ ) were used as features and artificial neural networks (ANN) was employed as classification algorithm in [113]. Obtained results of that study showed classification accuracy of 85.4%. In another study, time domain features, reflection index (RI) and stiffness index (SI), and frequency domain feature, power ratio (PR) were extracted from simple PPG and used along with support vector machine (SVM) classifier to identify apnea [114]. Average classification accuracy of 95% was achieved as the results of that research. Notice to the results of the study (5) of this thesis, it can be said that applying the time difference features could improve the apnea identification results.

In the case of wake/sleep detection there are many studies that used bio-signals such as Polysomnography (PSG), EEG and ECG. Use of PPG as a simple and inexpensive method in order to detect sleep stages was reported in a few studies. The most of those studies used HR and HRV as features to detect sleep. A recent study reported the averaged classification performance of 95% accuracy with the processing time of one minute by using wavelet-based HRV features [115]. The older methods based on FFT and HRV features, had 68.8% accuracy [115]. With respect to the existing studies in the literature, the results of the present thesis (study 6) showed that faster and more accurate classification results could be achieved by using TD features.

## 5. CONCLUSIONS AND FUTURE WORKS

This thesis uniquely presented a new strategy for the analysis of dual-wavelength photoplethysmographic signals in terms of bio-physiological conditions. An improved sensor system with a new design was developed for dual-wavelength photoplethysmography. The disadvantages of previous sensor systems (TDM based) come from switching and modulation processes were modified in the proposed system. The developed sensor system had the ability to select three different pairs of unlike PPG signals with distinct wavelengths. Low noise and no need for complex filtration were the good attributes of this system. Providing fully synchronized PPG signals to avoid any delay between the signals, was another advantage of the developed sensor system.

Performance of the both proposed and TDM sensor systems were evaluated based on time domain differences of separate PPG signals and it was demonstrated that the time-difference between PPG signals in two unlike wavelengths obtained by the proposed sensor system had very significant variations when the physiological conditions were changed. However in the TDM based system, significant bio-physiological related TD variations were not observed.

TDs were monitored and analyzed during different biological challenges such as smoking and running experiments in study (2). Experimental results showed that PPG TD series (time-difference pseudo-signal) may contain increasing, decreasing or strenuous oscillations that lead to different long-term patterns depending on the physiological conditions. The results of the corresponding experiments also confirmed the significance of bio-physiological related TD variations.

In the next step, TDs obtained from three different pairs of unlike PPG signals were compared. Based on the results, all of the three PPG pairs of Red-IR, Green-IR and Blue-IR had significant bio-physiological related TD variations, but the Red-IR pair was the most relevant case for biological applications. For this reason, in this thesis, PPG pair of Red-IR was selected for further analysis.

In the other studies of this thesis, significance of TD variations based on respiratory system was analyzed. The main conclusion of this study was that the TDs are indeed applicable for respiratory system analyses. Avoiding from the use of any nasal or face mask and their connected chemical sensors was the good attribute to use TDs for

evaluating respiratory system. The recording signals obtained from this study, were used also in order to fast detection of apnea using  $k$ -NN classification method. The results showed good capability of TDs for fast and accurate classification of normal and apneatic respiratory situations.

Another study of this thesis was to investigate possibility of using TD features for wake/sleep detection. Three different beat-to-beat TD features were extracted from the experimental recordings and  $k$ -NN algorithm was employed to classify wake/sleep. Obtained results revealed high capability of the obtained TD features to determine subjects' status. Use of just a finger connectable ring shaped PPG sensor to detect sleep, could be a very good attribute for the proposed method.

Last two studies were related to investigate PTT time series extracted from concurrent ECG and dual-wavelength PPG signals. Results of these studies showed that PTTs obtained by using two simultaneous PPG signals with different wavelengths and an ECG signal, were significantly different with each other and should be considered in applications such as blood pressure estimation to avoid from any mistake measurement results.

In summary, it can be said, with respect to the overall results of this thesis it was demonstrated that as long as physiological situation was stable, the TDs had no large variations. However, when the biological state was changed, the mean and standard deviations of TD values were significantly changed. This means that the obtained TD series had a pattern related to biological conditions that can be indicative of human physiology. It seems that TDs and their biology-related pattern can be used for important clinical applications. Good attribute of TDs was their independence from amplitude of PPG signals and light intensity variations. Due to this advantage, the presented approach may be used as an alternative to intensity-based multi-wavelength PPG applications in which they suffer from several drawbacks including susceptibility to light source or detector drift, changes in optical path, scattering and attenuation of excitation light.

Based on the results, we believe that TDs can have a potential for clinical and bio-physiological assessment applications such as anesthesia and drowsiness detecting, respiratory assessment or measuring of blood ingredients as a new helpful technology. Obtained results encourage more research and provide enough evidence that the proposed

method can have ability for clinical and physiological assessments as a new helpful technology.

As the feature works, the performance of the presented method could be further evaluated by conducting more different studies. Especially, the robust noise of TDM method can be further reduced and compared with the proposed method. In addition, the presented sensor system can be more developed to use for real time sleep or drowsiness detection, measuring different factors of blood and more accurate estimation of blood pressure. Predict the occurrence of apnea using presented TD features can be evaluated and studied as another feature work.

One of the main choices for the feature works is investigating and introducing of time difference variability (TDV) as an important indicator for prediction of sleep apnea and some other physiological disorders.

## 6. REFERENCES

1. Kamal, A.A., Harness, J.B., Irving, G. and Mearns, A.J., Skin photoplethysmography—a review, Comput Methods Programs Biomed, 28, 4 (1989) 257-269.
2. Anderson, R.R. and Parrish, J.A., The optics of human skin. J Invest Dermatol, 77, 1 (1981) 13-19.
3. Murray, W. and Foster, P.A., The peripheral pulse wave: information overlooked, Clin Mon, 12 (1996) 365–77.
4. Allen, J. and Murray, A., Age-related changes in peripheral pulse shape characteristics at various body sites, Physiol Meas, 24 (2003) 297–307.
5. Hertzman, A.B., Photoelectric plethysmography of the nasal septum in man. Proc Soc Exp. Biol Med, 3 (1937) 290–2.
6. Hertzman, A.B., The blood supply of various skin areas as estimated by the photoelectric plethysmograph, Am J Physiol, 124 (1938) 328-340.
7. Bagha, S. and Shaw, L., A real time analysis of PPG signal for measurement of SpO2 and pulse rate, International Journal of Computer Applications, 36,11 (2011) 0975 – 0980.
8. Nilsson, L., Johansson, A. and Kalman, S., Monitoring of respiratory rate in postoperative care using a new photoplethysmographic technique, J. Clin. Monit, 16 (2000) 309-315.
9. Nilsson, L., Johansson, I.A., Kalman, S., Respiratory variations in the reflection mode photoplethysmographic signal. Relationships to peripheral venous pressure, Med. Biol. Eng. Comput., 41 (2003) 249-254.
10. Gil, E., Orini, M., Bailon, R., Vergara, J.M., Mainardi, L. and Laguna, P., Photoplethysmography pulse rate variability as a surrogate measurement of heart rate variability during non-stationary conditions, Physiol Meas., 31,9 (2010) 1271-90.
11. Pilt, K., Ferenets, R., Meigas, K., Lindberg, L.G., Temitski, K. and Viigimaa, M., New photoplethysmographic signal analysis algorithm for arterial stiffness estimation. Scient. World J., 2013 (2013) Article ID 169035, 9 pages.
12. Lee, Q.Y., Redmond, S.J., Chan, G.S., Middleton, P.M. and Steel, E., Estimation of cardiac output and systemic vascular resistance using a multivariate regression model with features selected from the finger photoplethysmogram and routine cardiovascular measurements. Biomed. Eng. Online, 12 (2013).



13. Yao, J., Sun, X. and Wan, Y., A pilot study on using derivatives of photoplethysmographic signals as a biometric identifier, Conf Proc IEEE Eng Med Biol Soc., (2007) 4576-9.
14. Sukanesh, R. and Harikumar, R., Analysis of Photo-Plethysmography (PPG) signals with motion artifacts (gaussian noise) using wavelet transforms, Biomedical Soft Computing and Human Sciences, 16,1 (2010) 135-139.
15. Trafford, J.C., Cotton, L.T., Kitney, R.I., Lafferty, K. and Roberts, V., Modelling of the human vasomotor control system and its application to the investigation of arterial disease. IEE Proc A., 129 (1982) 646–50.
16. Larsen, P.D., Harty, M., Thiruchelvam, M. and Galletly, D.C., Spectral analysis of AC and DC components of the pulse photoplethysmograph at rest and during induction of anaesthesia, Int J Clin Monit Comput., 14 (1997) 89–95.
17. Okada, M., Kimura, S. and Okada, M., Estimation of arterial pulse wave velocities in the frequency domain: method and clinical considerations, Med Biol Eng Comput., 24 (1998) 255–60.
18. Nitzan, M., Boer, H., Turivnenko, S. and Sapoznikov, D., Power spectrum analysis of the spontaneous fluctuations in the photoplethysmographic signal. J Basic Clin Physiol Pharmacol., 5 (1994) 269–76.
19. Grohmann, G., Krauss, M., Lindloh, C., Pohlmann, G. and Eidner, G., NIR-photoplethysmography—a noninvasive method for the early diagnosis and control of circulation parameters in peripheral vascular diseases. Theory and Technical devices Perfusion, 9 (1996a) 268–77.
20. Grohmann, G., Krauss, M., Lindloh, C., Pohlmann, G. and Eidner, G., NIR-photoplethysmography—a noninvasive method for the early diagnosis and control of circulation parameters in peripheral vascular diseases, Bedside measurements Perfusion, 9 (1996b) 300–10.
21. Yan, Y.S., Poon, C.C. and Zhang, Y.T., Reduction of motion artifact in pulse oximetry by smoothed pseudo Wigner–Ville distribution, J Neuroeng Rehabil., 2, 3 (2005).
22. Banerjee, R., Sinha, A., Pal, A. and Kumar, A., Estimation of ECG parameters using photoplethysmography, Bioinformatics and Bioengineering (BIBE), IEEE (2013).
23. Allen, J. and Murray, A., Modelling the relationship between peripheral blood pressure and blood volume pulses using linear and neural network system identification techniques, Physiol Meas., 20 (1999) 287–301.

24. Allen, J. and Murray, A., Prospective assessment of an artificial neural network for the detection of peripheral vascular disease from lower limb pulse waveforms, Physiol Meas., 16 (1995) 29–38.
25. Millasseau, S., Guigui, F.G., Kelly, R.P., Prasad, K., Cockcroft, J.R., Ritter, J.M. and Chowienczyk, P.J., Noninvasive assessment of the digital volume pulse comparison with the peripheral pressure pulse, Hypertension, 36 (2000) 952–6.
26. Enriquez, R.H., *et al.* Analysis of the photoplethysmographic signal by means of the decomposition in principal components, Physiol Meas., 23 (2002) N17–N29.
27. Elgendi, M., On the analysis of fingertip photoplethysmogram signals, Current Cardiology Reviews, 8 (2012)14-25.
28. Bhattacharya, J. and Kanjilal, P.P., Analysis and characterization of photoplethysmographic signal, IEEE BME., 48 (2009) 5–11.
29. Christ, F., Abicht, J.M., Athelougou, M., Baschnegger, H., Niklas, M., Peter, K. and Messmer, K., Cardiovascular monitoring of elective aortic aneurysm repair using methods of chaos analysis, Int J Microcirc Clin Exp., 17 (1997) 374–84.
30. Lin, Y.D., Liu, W.T., Tsai, C.C. and Chen, W.H., Coherence Analysis between Respiration and PPG Signal by Bivariate AR Model, International Journal of Biological and Life Sciences, 5, 4 (2009) 197-202.
31. Bortolotto, L.A., Blacher, J., Kondo, T., Takazawa, K. and Safar, M.E., Assessment of vascular aging and atherosclerosis in hypertensive subjects: second derivative of photoplethysmogram versus pulse wave velocity, Am J Hypertens., 13 (2000) 165–71.
32. Ubeylia, E., Cvetkovicb, D. and Cosicb, I., Analysis of human PPG, ECG and EEG signals by eigenvector methods, Digital Signal Processing, 20 (2010) 956–963.
33. Cvetkovica, D., Ubeylib, E.D. and Cosica, I., Wavelet transform feature extraction from human PPG, ECG, and EEG signal responses to ELF PEMF exposures: A pilot study, Digital Signal Processing, 18, 5 (2008) 861–874.
34. Vincent, P. and Crabtree, Smith, P.R., Physiological Models of the Human Vasculature and Photoplethysmography, Electronics Systems and Control Division Research, (2003) 60-63.
35. Mandeep S. and Shivangi, N., Features Extraction in Second Derivative of Finger PPG Signal: A Review, IJCSC, 4, 2 (2013) 1-5.

36. Ubeylia, E., Cvetkovicb, D. and Cosicb, I., AR Spectral Analysis Technique for Human PPG, ECG and EEG, Signals Journal of Medical Systems, 32 (2006) 201-206
37. Suganthi, L., Manivannan, M., Kunwar, B.K., Joseph, G. and Danda, D., Morphological analysis of peripheral arterial signals in Takayasu's arteritis, J Clin Monit Comput., 29, 1 (2015) 87-95.
38. Linder, S.P., Hanover, N.H. and Wendelken, S., Using the Morphology of the Photoplethysmogram Envelope to Automatically Detect Hypovolemia, Computer-Based Medical Systems, 2006. CBMS 2006. 19th IEEE International Symposium on. Page 371.
39. Linder, S.P., Wendelken, S., Clayman, J., Steiner, P.R. and Mcgrah, S.P., Noninvasive detection of the hemodynamic stress of exercise using the photoplethysmogram, J Clin Monit Comput., 22, 4 (2008) 269-78.
40. Linder, S.P., Wendelken, S.M., We,i E. and McGrath, S.P., Using the morphology of photoplethysmogram peaks to detect changes in posture, J Clin Monit Comput., 20, 3 (2006) 151-8.
41. Kayikcioglu, T. and Aydemir, O., A polynomial fitting and k-NN based approach for improving classification of motor imagery BCI data, Pattern Recognition Letters, 31 (2010) 1207–1215.
42. Rubins, U., Finger and ear photoplethysmogram waveform analysis by fitting with Gaussians, Medical and Biological Engineering and Computing, 46, 12 (2008) 1271–1276.
43. Huotari, M., Vehkaoja, A., Maatta, K. and Kostamovaara, J., Photoplethysmography and its detailed pulse waveform analysis for arterial stiffness, Journal of Structural Mechanics, 44, 4 (2011) 345–362.
44. Huotari, M., Vehkaoja, A., Maatta, K. and Kostamovaara, J., Pulse waveforms are an indicator of the condition of vascular system, in: Proceedings of World Congress on Medical Physics and Biomedical Engineering, 39 (2012) 526–529.
45. Li, D., Zhao, H., Li, S. and Zheng, H., A New Representation of Photoplethysmography Signal. In: Wireless Algorithms, Systems and Applications, Cai, Z., C. Wang, S. Cheng, H. Wang and H. Gao (Eds.). Springer, Berlin, Germany, ISBN: 978-3-319-07781-9, (2014) 279-289.
46. Asare L., Kviesis-Kipge, E., Ozols, M., Spigulis, J. and Erts, R., Multi-spectral optoelectronic device for skin microcirculation analyses. Lithuanian Journal of Physics, 52 (2012a) 59-62.
47. Asare, L., Ozols, M., Rubins, U., Rubenis O. and Spigulis, J., Clinical measurements with multi-spectral photoplethysmography sensors. Proceedings

of the Biophotonics: Photonic Solutions for Better Health Care III, April 16-19, 2012, Brussels, Belgium.

48. Asare, L. and Spigulis, J., Analysis of Multi-spectral Photoplethysmograph Biosensors. *Novel Biophotonic Techniques and Applications II*, edited by I. Alex Vitkin, Arjen Amelink, Proc. of SPIE-OSA Biomedical Optics, SPIE, (2013) 8801 880106.
49. Lindberg, L.G., Ugnell, H. and Oberg, P.A., Monitoring of respiratory and heart rates using a fiberoptic sensor, Med Biol Eng Comput., 30, 5 (1992) 533-537.
50. Nilsson, L., Johansson, A. and Kalman, S., Monitoring of respiratory rate in postoperative care using a new photoplethysmographic technique, J Clin Monit Comput., 16, 4 (2000) 309-315.
51. Johansson, A., Oberg P.A. and Sedin, G., Monitoring of heart and respiratory rates in newborn infants using a new photoplethysmographic technique, J Clin Monit Comput. 15 (1999) 461-7.
52. Park, J.U., Lee, H.K., Lee, J., Urtnasan, E., Kim, H. and Lee, K.J., Automatic classification of apnea/hypopnea events through sleep/wake states and severity of SDB from a pulse oximeter, Physiological Measurement, 36, 9 (2015) 2009-2025.
53. Heck, A.F. and Hall, V.R., An on-line system for measurement of opacity pulse propagation times in atraumatic screening of patients for occlusive vascular disease, Med Instrum., 9, 2 (1975) 88-92.
54. Osmundson, P.J., O'Fallon, W.M., Clements, I.P., Kazmier, F.J., Zimmerman, B.R. and Palumbo, P.J., Reproducibility of noninvasive tests of peripheral occlusive arterial disease, J Vasc Surg., 2, 5 (1985) 678-683.
55. Kvernebo, K., Megerman, J., Hamilton, G. and Abbott, W.M., Response of skin photoplethysmography, laser Doppler flowmetry and transcutaneous oxygen tensiometry to stenosis-induced reductions in limb blood flow, Eur J Vasc Surg., 3, 2 (1989) 113-120.
56. Allen, J., Oates, C.P., Lees, T.A. and Murray, A., Photoplethysmography detection of lower limb peripheral arterial occlusive disease: a comparison of pulse timing, amplitude and shape characteristics. Physiol Meas., 26, 5 (2005) 811-821.
57. Allen, J., Overbeck, K., Stansby, G. and Murray, A., Photoplethysmography assessments in cardiovascular disease. Measurement & Control., 39, 3 (2006) 80-83.
58. Chowienczyk, P.J., Kelly, R.P., MacCallum, H., Millasseau, S.C., Andersson, T.L., Gosling, R.G., Ritter, J.M. and Anggard, E.E. Photoplethysmographic

assessment of pulse wave reflection: blunted response to endothelium-dependent beta2-adrenergic vasodilation in type II diabetes mellitus, J Am Coll Cardiol., 34, 7 (1999) 2007-2014.

59. Gopaul, N.K., Manraj, M.D., Hebe, A., Lee Kwai Yan, S., Johnston, A., Carrier, M.J. and Anggard, E.E., Oxidative stress could precede endothelial dysfunction and insulin resistance in Indian Mauritians with impaired glucose metabolism, Diabetologia, 44, 6 (2001) 706-712.
60. Cooke, E.D., Bowcock, S.A. and Smith, A.T., Photoplethysmography of the distal pulp in the assessment of the vasospastic hand, Angiology, 36, 1 (1985) 33-40.
61. Avnon, Y., Nitzan, M., Sprecher, E., Rogowski, Z. and Yarnitsky, D., Different patterns of parasympathetic activation in uni- and bilateral migraineurs, Brain, 126 (2003) 1660-1670.
62. Avnon, Y., Nitzan, M., Sprecher, E., Rogowski, Z. and Yarnitsky, D., Autonomic asymmetry in migraine: augmented parasympathetic activation in left unilateral migraineurs, Brain, 127 (2004) 2099-2108.
63. Komatsu, K., Fukutake, T. and Hattori, T., Fingertip photoplethysmography and migraine, J Neurol Sci., 216, 1 (2003) 17-21.
64. Shi, P., Peris, V.A., Echiadis, A., Zheng, J., Zhu, Y. and Yeng, P., Non-contact reflection photoplethysmography towards effective human physiological monitoring, J. Med. Biol. Eng. 30, 3 (2010) 161-167.
65. Azmal, G.M., Al-Jumaily, A. and Al-Jaafreh, M., Continuous measurement of oxygen saturation level using photoplethysmography signal, Biomedical and Pharmaceutical Engineering, 2006. ICBPE 2006. International Conference on, (2006) 504-507.
66. Hertzman, A.B. and Dillon, J.B., Distinction between arterial, venous and flowcomponents in photoelectric plethysmography in man, Am J Physiol., 130 (1940a) 177-185.
67. Twersky, V., Multiple scattering of waves and optical phenomena, J Opt Soc Am., 52 (1962) 145-171.
68. Twersky, V., Absorption and multiple scattering by biological suspensions, J Opt Soc Am., 60, 8 (1970) 1084-1093.
69. De Kock, J.P. and Tarassenko, L., Pulse oximetry: theoretical and experimental models, Med Biol Eng Comput., 31, 3 (1993) 291-300.

70. Mendelson, Y., and Ochs, B.D., Noninvasive Pulse Oximetry Utilizing Skin Reflectance Photoplethysmography, IEEE transactions on bio-medical engineering, 35, 10 (1988) 798-805.
71. Mendelson, Y., Kent, J.C., Yocum, B.L. and Birle, M.J., Design and Evaluation of a New Reflectance Pulse Oximeter Sensor, Medical instrumentation, 22, 4 (1988) 167.
72. Lee, J., Matsumura, K., Yamakoshi, K., Rolfe, P., Tanaka, S. and Yamakoshi, T., Comparison between red, green and blue light reflection photoplethysmography for heart rate monitoring during motion, Conf Proc IEEE Eng Med Biol Soc. 2013 (2013) 1724-7.
73. Nogawa, M., Kaiwa, T., and Takatani, S., A Novel hybrid reflectance pulse oximeter sensor with improved linearity and general applicability to various portions of the body, Engineering in Medicine and Biology Society, Proceedings of the 20th Annual International Conference of the IEEE, 4 (1998) 1858-1861.
74. Gibbs, P. and Asada, H.H., Reducing motion artifact in wearable bio-sensors using MEMS accelerometers for active noise cancellation, American Control Conference, 3 (2005) 1581–1586.
75. Li, Q., and Clifford, G.D., Dynamic time warping and machine learning for signal quality assessment of pulsatile signals, Phys. Meas., 33,9 (2012) 1491–1501.
76. Goldman, J.M., Petterson, M.T., Kopotic, R.J., and Barker, S.J., Masimo signal extraction pulse oximetry, Journal of Clinical Monitoring and Computing, 16 (2000) 475–483.
77. Lee, B., Kee, Y., Han, J. and Yi, W.J., Adaptive comb filtering for motion artifact reduction from PPG with a structure of adaptive lattice IIR notch filter, Conf Proc IEEE Eng Med Biol Soc. 2011 (2011) 7937-40.
78. Ram, M.R., Madhav, K.V., Krishna, E.H. and Komalla, N.R., A Novel Approach for Motion Artifact Reduction in PPG Signals Based on AS-LMS Adaptive Filter, Instrumentation and Measurement, IEEE Instrumentation and Measurement, 61, 5 (2012) 1445–1457.
79. Lee, H.W., Lee, J.W., Jung, W.G. and Lee, G.K., The Periodic Moving Average Filter for Removing Motion Artifacts from PPG Signals, International Journal of Control, Automation and Systems, 5, 6 (2007) 701-706.
80. Couceiro, R., Carvalho, P., Paiva, R.P., Henriques, J. and Muehlsteff, J., Detection of motion artifact patterns in photoplethysmographic signals based on time and period domain analysis, Physiol Meas., 35, 12 (2014) 2369-88.

81. Tamura, T., Maeda, Y., Sekine, M. and Yoshida, M., Wearable Photoplethysmographic Sensors—Past and Present, Electronics, 3 (2014) 282-302.
82. Hamamatsu, K.K., S8753 Datasheet, (2002).
83. Polo, O., Tafti, M., Hamalainen, M., Vaahtoranta, K. and Alihanka, J., Respiratory variation of the ballistocardiogram during increased respiratory load and voluntary central apnoea, Eur Respir J., 5 (1992) 257-262.
84. Segal, S. and Lavie, P., Sleep and Breathing in Sleep in Children with Breath-Holding Spells, Neuropsychobiology, 12 (1984) 209–210.
85. Rassovsky, Y., K. Abrams and M.G. Kushner, Suffocation and respiratory responses to carbon dioxide and breath holding challenges in individuals with panic disorder, J. Psychosomatic Res., 60 (2006) 291-298.
86. Parkes, M.J., Breath-holding and its breakpoint, Exp. Physiol., 91 (2006) 1-15.
87. Klocke, F.J. and Rahn, H., Breath holding after breathing of oxygen, J. Applied Physiol., 14 (1959) 689-693.
88. Rourke, M.O. and Taylor, M., Vascular impedance of the femoral bed, Circ Res., 18 (1996) 126-139.
89. Lee, H.W., Lee, J.W., Jung, W.G. and Lee, G.K., The periodic Moving Average Filter for removing motion artifacts from PPG signals, International Journal of Control, Automation, and Systems, 5, 6 (2007) 701-706.
90. Gholamhosseini, H., Nazeran, H. and Reynolds, K.J., ECG noise cancellation using digital filters. in: 2nd International Conference on Bioelectromagnetism, Melbourne AUSTRALIA, February 1998.
91. Bhattacharya, J., Kanjilal, P.P. and Muralidhar, V., Analysis and characterization of photo-plethysmographic signal, IEEE Transaction on BioMedical Engineering, 48, 1 (2001) 5-23.
92. Lo, T.Y. and Tang, P.C., A fast band pass filter for ECG processing, IEEE Engr in Med and Bio Soc 4th Annual Inter. Conference, (1982) 20-21.
93. Tan, L., Digital signal processing fundamentals and applications. Digital Signal Processing Systems, Basic Filtering Types, and Digital Filter Realizations Book Chapter from Digital signal processing fundamentals and applications, Academic Press is an imprint of Elsevier, (2008).
94. Zhanga, F., Chena, S., Zhanga, H., Zhangb, X. and Lia, G., Bioelectric signal detrending using smoothness prior approach, Medical Engineering & Physics, 36 (2014) 1007–1013.

95. Tarvainen, M.P., Ranta-aho, P.O., and Karjalainen, P.A., An Advanced Detrending Method With Application to HRV Analysis, IEEE Transaction on biomedical engineering, 49, 2 (2002) 172-175.
96. Faber, D.J., Aalders, M.C.G., Mik, E.G., Hooper, B.A., Gemert, M.J.C. and Leeuwen, T.G., Oxygen saturation dependent absorption and scattering of whole blood, Proc. SPIE 5316, Coherence Domain Optical Methods and Optical Coherence Tomography in Biomedicine, 78 ( 2004).
97. Aksoy, S. and Haralick, R.M., Feature normalization and likelihood-based similarity measures for image retrieval. Pattern Recognition Letters, 22 (2001) 563-582.
98. Shin, H.S., Lee, C. and Lee, M., Adaptive threshold method for the peak detection of photoplethysmographic waveform, J. Computers in Biology and Medicine, 39 (2009) 1145-1152.
99. Lao, C.K., Portable heart rate detector based on photoplethysmography with android programmable devices for ubiquitous health monitoring system, IJATES, 2 (2013).
100. Phillips, J.P., Langford, R.M., Chang, S.H., Maney, K., Kyriacou P.A., and Jones, D.P., An esophageal pulse oximetry system utilizing a fiber-optic probe. J. Phys. Conf. Ser., 178, 1 (2009).
101. Kyriacou, P.A., Powell, S., Langford, R.M. and Jones, D.P., Investigation of esophageal photoplethysmographic signals and blood oxygen saturation measurements in cardiothoracic surgery patients, Physiol. Meas., 23 (2002) 533-545.
102. Spigulis, J., Gailite, L., Lihachev, A. and Erts, R., Simultaneous recording of skin blood pulsations at different vascular depths by multiwavelength photoplethysmography. APPLIED OPTICS, 46, 10 (2007) 1754-9.
103. Gailite, L., Spigulis, J. and Lihachev, A., Multilaser photoplethysmography technique, Lasers Med Sci., 23 (2008) 189–193.
104. Kuzmina, I., Lihachev, A., Gailite, L., Lasma and Spigulis, J., Compact multi-functional skin spectrometry set-up. Advanced Optical Materials, Technologies, and Devices, edited by Steponas Asmontas, Jonas Gradauskas Proc. of SPIE, (2007) 6596: 65960T.
105. Fuerst, D.E. and Jannach, J.R., Autofluorescence of eosinophils: a bone marrow study. Nature, 205 (1965) 1333-1334.
106. Parul, D.A., *et al.*, Time-resolved fluorescence reveals two binding sites of 1, 8-ANS in intact human oxyhemoglobin. Journal of Photochemistry and Photobiology B: Biology, 58 (2000) 156–162.



107. Gao, S., Lan, X., Liu, Y., Shen, Z., Lu1, J. and Ni1, X., Characteristics of blood fluorescence spectra using low-level, 457.9-nm excitation from Ar+ laser. Chin. Opt. Lett., 2, 3 (2004) 160-161.
108. Ghervase, L., Savastru, D., Dontu, S., Forsea, A.M. and Borisova, E., Characterization of Human Skin by Fluorescence, Exemplified by Dermatofibroma, Keratoacanthoma, and Seborrheic Keratosis, Analytical Letters, 48 (2015).
109. Monici, M., Pratesi, R., Bernabei, P.A., Caporale, R., Ferrini, P.R., Croce, A.C., Balzarini, P. and Bottiroli, G., Natural fluorescence of white blood cells: spectroscopic and imaging study, Photochem Photobiol B., 30, 1 (1995) 29-37.
110. Wolfbeis, O.S., Fluorescence Spectroscopy in Biology. Springer book series on Fluorescence, (2004).
111. Kaplanova, M. and Parma, L., Effect of excitation and emission wavelength on the fluorescence lifetimes of chlorophyll, a Gen Physiol Biophys., 3 (1984) 127-34.
112. Morgenthaler, T.I., Kapen, S., Lee-Chiong, T., Alessi, C., Boehlecke, B., Brown, T., Coleman, J., Friedman, L., Kapur, V., Owens, J., Pancer, J. and Swick, T., Practice parameters for the medical therapy of obstructive sleep apnea, SLEEP, 29 (2006) 1031-1035.
113. Knorr-Chung, B.R., McGrath, S.P. and Blike, G.T., Identifying airway obstructions using photoplethysmography (PPG), Journal of Clinical Monitoring and Computing, 22 (2008) 95–101.
114. Pradhapan, P., Swaminathan, M., Salila Vijayalal Mohan, H.K. and Sriraam, N., Identification of apnea during respiratory monitoring using support vector machine classifier: a pilot study, J Clin Monit Comput., 27, 2 (2013) 179-85.
115. Li, G. and Chung, W.Y., Detection of driver drowsiness using wavelet analysis of heart rate variability and a support vector machine classifier, Sensors, 13,12 (2013) 16494-16511.

## 7. APPENDIX

Program codes that were prepared using MATLAB<sup>®</sup>R2012b are presented in this section.

Program code 1: The program to record signals using audio dual-channel codec.

```
% Description: This program was developed
% to record signals via dual-channel audio
% codecs or sound cards
% Sampling rate, bit rate, the number of channels
% and time duration of the recordings can bet selected
% by this code.
% the recordings are saved as a wav file in the end of
% running this program
recObj = audiorecorder(1000,16,2);
recordblocking(recObj,60);
myRecording = getaudiodata(recObj);
wavwrite(myRecording,1000,16,'Name');
```

Program code 2: The program for filtering, DC component cancelling and normalization of PPG signals and extraction of TD features from them.

```
% Description: This program was developed
% for filtering, DC component cancelling, normalization
and %peak detection of PPG signals and extraction of TD
features %from them

clc;clear all;close all;

ppg = wavread('Name.wav');

Red=ppg(:,2); %Extract out each of the signals
IR=ppg(:,1);
```

```

%Band
filter*****pass
****

a=[1,-2.81157367732469,2.64048349277834,-
0.828146275386261];

b=[9.54425084237281e-
05,0.000286327525271184,0.000286327525271184,9.54425084237281
e-05];

Red2=filtfilt(b,a,Red);
IR2 =filtfilt(b,a,IR);

%Detrend
filter*****

Red2 = detrend(Red2);
IR2 = detrend(IR2);

%%%%%%%%%5

%dc          canceling          &          normalize
*****

Red3 = Red2 - mean (Red2 ); % cancel DC components
IR3 = IR2 - mean (IR2 ); % cancel DC components

Red=(Red3-min(Red3))/(max((Red3))-min((Red3)));%
normalize first channel to one

IR=(IR3-min(IR3))/(max((IR3))-min((IR3))); %
normalize second channel to one

PPg(:,1)=Red;PPg(:,2)=IR;

from=1;
to=size(IR);
figure;plot(from:to,IR(from:to),'r');
figure;plot(from:to,Red(from:to),'r',from:to,IR(from:to))
;

Red=Red(from:to);IR=IR(from:to);

```

```

%Peak detecting of REd and IR
peperatly*****
*****

    [maxtab, mintab] = peakdet(Red, 0.15);
    Redh=maxtab(:,1);Redlow=mintab(:,1);
hold on; plot(mintab(:,1), mintab(:,2), 'b*');
plot(maxtab(:,1), maxtab(:,2), 'b^');
    [maxtab, mintab] = peakdet(IR, 0.15);
    IRh=maxtab(:,1);IRlow=mintab(:,1);
hold on; plot(mintab(:,1), mintab(:,2), 'g*');
plot(maxtab(:,1), maxtab(:,2), 'g^');
    heart_rate=length(maxtab);

%%%%%%%%%%%%%%%%%%%%%%%%%%%%%%%%%%%%%%%%%%%%%%%%%%%%%%%%%%%%%%%%%%%%%%%%%%
%%%%%%%%%%%%%%%%%%%%%%%%%%%%%%%%%%%%%%%%%%%%%%%%%%%%%%%%%%%%%%%%%%%%%%%%%%

    from=IRlow(1);
    to=IRlow(2);
    n= max(IR(from:to))- max(Red(from:to));IR=IR-n;
    m=min(IR(from:to))- min(Red(from:to));Red=Red+m;
    rRed1=Red(from:to);
    rIR1=IR(from:to);
    K_Red=(rRed1-min(rRed1))/(max((rRed1))-min((rRed1)));
    K_IR=(rIR1-min(rIR1))/(max((rIR1))-min((rIR1)));

figure(44);plot(from:to,K_IR,'r',from:to,K_Red,'linewidth',2)
;
    grid;

    l1=length(Redh);l2=length(Redlow);l3=length(IRh);l4=length
h(IRlow);
    leng=[l1 l2 l3 l4];leng=min(leng);

%%%%%%%%%%%%%%%%%%%%%%%%%%%%%%%%%%%%%%%%%%%%%%%%%%%%%%%%%%%%%%%%%%%%%%%%%%
%%%%%%%%%%%%%%%%%%%%%%%%%%%%%%%%%%%%%%%%%%%%%%%%%%%%%%%%%%%%%%%%%%%%%%%%%%

    for i=2:leng-1

        az=IRlow(i);

```



```

for i=2:leng-1
az=IRlow(i);
ta=IRlow(i+1);
IR1=IR(az:ta);Red1=Red(az:ta);
IRdamane1=(max(IR1));IRdamane=IRdamane1(1);
Reddamane1=find(max(Red1));Reddamane=Reddamane1(1);
damane(i)=IRdamane-Reddamane;
end
damane(1)=[];
for i=2:leng-1
az=IRlow(i);
ta=IRlow(i+1);
IR1=IR(az:ta);Red1=Red(az:ta);
IRfaz1=find(max(IR1)-0.13<IR1&IR1<max(IR1)-
0.11);IRfaz=IRfaz1(1);IRdef=IRfaz1(end);
Redfaz1=find(max(Red1)-0.13<Red1&Red1<max(Red1)-
0.11);Redfaz=Redfaz1(1);Reddef=Redfaz1(end);
fark(i)=IRfaz-Redfaz;
def(i)=IRdef-Reddef;
end

fark=fark';fark(1)=[];def=def';def(1)=[];
figure(66);plot(Peak,'b');grid;hold on; plot(Peak,'.r');
figure(660);plot(Far,'b');grid;hold on;
plot(Far,'.r');hold on
plot(damane*8,'g')
figure(86);plot(def,'b');grid;hold on; plot(def,'.r');
pah1(1)=[];pah2(1)=[];defpah(1)=[];
figure(861);plot(pah1,'b');grid;hold on; plot(pah1,'.r');
figure(862);plot(pah2,'b');grid;hold on; plot(pah2,'.r');
figure(863);plot(defpah,'b');grid;hold on;
plot(defpah,'.r');
figure(77);plot(damane);hold on;plot(damane,'.r');

```

```
Mean=mean(fark);
Std=std(fark);
```

Program code 3: The program to execute t-test on the extracted TD features.

```
% Description: This program was developed
% to execute t-test on the extracted TD features
clc;clear all; close all
load fark.mat;
boxplot([fark(:,1),fark(:,2)])
[h0,p0,ci0,stats0]=ttest(fark(:,1),fark(:,2))
```

Program code 4: The program for  $k$ -NNclassification by three separate training methods along with the data permutation in order to repetition of experiments.

```
% Description: This program was developed
% to classify the extracted data using Random
subsampling,
% K-fold and Leave-one-out methods
clear all
close all
clc
load normalbreath100.mat;
load holdbreath100.mat;
    VB(:,1)=holdbreath(:,1);VB(:,2)=holdbreath(:,2);
VM(:,1)=normalbreath(:,1);VM(:,2)=normalbreath(:,2);

%Mster Mixing*****
                                r=randperm(100);
                                VM=VM(r,:);
                                VB=VB(r,:);

figure(1);plot(VM(:,1),VM(:,2),'or'
,VB(:,1),VB(:,2),'+', 'linewidth',2)
```

```

xlabel('Mean of TDs (ms)','FontSize',14);
ylabel('Standard deviation of TDs (ms)','FontSize',14);
title('Data set','Color','k','FontSize',14)
legend('Normal breathing','Apneatic situation');

%*****
*****

    Train(1:50,:)=VM(1:50,:);Train(51:100,:)=VB(1:50,:);
    TEST(1:50,:)=VM(51:100,:);TEST(51:100,:)=VB(51:100,:);
MixVM(1:50,:)=VM(1:50,:);
MixVB(1:50,:)=VB(1:50,:);

TEST1(1:50,:)=VM(51:100,:);TEST2(1:50, :, :)=VB(51:100, :, :);

%Validation Mixing*****

                                r=randperm(50);
                                MixVM=MixVM(r, :);
                                MixVB=MixVB(r, :);

                                TEST1=TEST1(r, :);
                                TEST2=TEST2(r, :);

%*****
*****

    figure(2);plot(MixVM(:,1),MixVM(:,2),'or'
,MixVB(:,1),MixVB(:,2),'+', 'linewidth',2)
    xlabel('Mean of TDs (ms)','FontSize',14);
    ylabel('Standard deviation of TDs (ms)','FontSize',14);
    title('Train set','Color','k','FontSize',14)
    legend('Normal breathing','Apneatic situation');

```



```

    figure(3);plot(TEST1(:,1),TEST1(:,2),'or'
,TEST2(:,1),TEST2(:,2),'+', 'linewidth',2)
    xlabel('Mean of TDs (ms)', 'FontSize',14);
    ylabel('Standard deviation of TDs (ms)', 'FontSize',14);
    title('Test set', 'Color', 'k', 'FontSize',14)
    legend('Normal breathing', 'Apneatic situation');

%knn
N1=50;
N2=50;
    tlabel=[zeros(1,N1) ones(1,N1)]'; %test datalar için
doğruluk tablosu
    slabel=[zeros(1,N1/2) ones(1,N1/2)]'; %test datalar için
doğruluk tablosu

    class =
knnclassify(Train,TEST,tlabel,11, 'cosine', 'nearest');%class =
knnclassify(XX,YY,t_d,15, 'cosine', 'random');
    classperf(class,tlabel)

%Random
subsampling*****
    SubtrainM(1:25,:)=MixVM(1:25,:);
    SubtrainB(1:25,:)=MixVB(1:25,:);
    %figure(2);plot(SubtrainM,SubtrainB, '+')

    ValidationM(1:25,:)=MixVM(26:50,:);
    ValidationB(1:25,:)=MixVB(26:50,:);

    Mtest(1:50,:)=VM(51:100,:);
    Btest(1:50,:)=VB(51:100,:);
    K=1:2:15;
    ValidationTruetable=zeros(50,length(K));

```

```

for k=1:2:15;
for i=1:50
distance=zeros(50,2);
distance(1:25,2)=1;
distance(26:50,2)=0;
if i<=25
        distance(1:25,1)=sqrt((SubtrainM(:,1)-
ValidationM(i,1)).^2+(SubtrainM(:,2)-ValidationM(i,2)).^2);
        distance(26:50,1)=sqrt((SubtrainB(:,1)-
ValidationM(i,1)).^2+(SubtrainB(:,2)-ValidationM(i,2)).^2);
    else
        distance(1:25,1)=sqrt((SubtrainM(:,1)-
ValidationB(i-25,1)).^2+(SubtrainM(:,2)-ValidationB(i-
25,2)).^2);
        distance(26:50,1)=sqrt((SubtrainB(:,1)-
ValidationB(i-25,1)).^2+(SubtrainB(:,2)-ValidationB(i-
25,2)).^2);
    end

    distance=sortrows(distance);
        M=0;
        B=0;
for jj=1:k
if distance(jj,2)==1
            M=M+1;
else
            B=B+1;
end
end

if i<=25 && M>B
ValidationTruetable(i,k)=1;
end
if i>25 && M<B
ValidationTruetable(i,k)=1;
end
end
end

```

```
V(k)=length(ValidationTruetable(ValidationTruetable(:,k)=
=1));
```

```
end
```

```
Random_susampling_validationsuccess=V(:,:).*2;
    [maximum
Bestk]=max(Random_susampling_validationsuccess)
    r=Random_susampling_validationsuccess;r=[r(:,1) r(:,3)
r(:,5) r(:,7) r(:,9) r(:,11) r(:,13) r(:,15)];
    Random_susamplingValidation_STD=std(r)
    Random_susamplingValidation_Mean=mean(r)
```

```
%K-foldclassifier*****
```

```
trainM(1:50,:)=MixVM(1:50,:);
trainB(1:50,:)=MixVB(1:50,:);
```

```
J=5:5:50;
for j=1:length(J)
    SubtrainM=trainM;SubtrainB=trainB;
    Validation(1:5,:)=trainM(j:j+4,:);
    Validation(6:10,:)=trainB(j:j+4,:);
    ValidationM=Validation(1:5,:);
    ValidationB=Validation(6:10,:);
    SubtrainM(j:j+4,:)=[];
    SubtrainB(j:j+4,:)=[];
    %*****
```

```
    K=1:2:15;
    ValidationTruetable=zeros(10,length(K));
    for k=1:2:15;

    for i=1:10
```

```

distance=zeros(90,2);
distance(1:45,2)=1;
distance(46:90,2)=0;
if i<=5

distance(1:45,1)=sqrt((ValidationM(i,1)-
SubtrainM(:,1)).^2)+((ValidationM(i,2)-SubtrainM(:,2)).^2);

distance(46:90,1)=sqrt((ValidationB(i,1)-
SubtrainM(:,1)).^2)+((ValidationB(i,2)-SubtrainM(:,2)).^2);
else
            distance(1:45,1)=sqrt((ValidationM(i-
5,1)-SubtrainB(:,1)).^2)+((ValidationM(i-5,2)-
SubtrainB(:,2)).^2);
            distance(46:90,1)=sqrt((ValidationB(i-
5,1)-SubtrainB(:,1)).^2)+((ValidationB(i-5,2)-
SubtrainB(:,2)).^2);
end
distance=sortrows(distance);
            M=0;
            B=0;
for jj=1:k
if distance(jj,2)==1
            M=M+1;
else
            B=B+1;
end
end

if i<=5&& M>B
ValidationTruetable(i,k)=1;
end
if i>5 && M<B
ValidationTruetable(i,k)=1;
end
end

Ktruelist(j,k)=length(ValidationTruetable(ValidationTruet
able(:,k)==1));

```

end

end

```

    ValidationTrue= Ktruelist;
    K_FOLD_Validation=sum(ValidationTrue)

```

```

    %*****Leave
Out *****
    %*****
    ***

        K=1:2:15;

        Truetable=zeros(100,length(K));
    for k=1:2:15;

        for i=1:100
            distance=zeros(100,2);
            distance(1:50,2)=1;
            distance(51:100,2)=0;
            vt=Train(i,:);
                distance(:,1)=sqrt((vt(1)-
Train(:,1)).^2)+((vt(2)-Train(:,2)).^2);
            distance(i,:)=[];
            distance=sortrows(distance);
                M=0;
                B=0;
            for jj=1:k
                if distance(jj,2)==1
                    M=M+1;
                else
                    B=B+1;
                end
            end
        end
    end

```

```

    if i<=50&& M>B
    Truetable(i,k)=1;
    end
    if i>50 && M<B
    Truetable(i,k)=1;
    end
    end

    LeaveOneOutvalidationtruelist(k)
=length(Truetable(Truetable(:,k)==1));
    end

        LeaveOneOutvalidationtruelist;

    [LeaveOneOutmaximumvalidation
Bestk]=max(LeaveOneOutvalidationtruelist)

    %*****
    *****TEST*****
    *****

    TRAIN=Train;

    TesttrueTable=zeros(100,1);
    FinalK=15;
    for ii=1:100
    dist=zeros(100,2);
    dist(1:50,2)=1;
    dist(51:100,2)=0;

    vt=TEST(ii,:);
        dist(:,1)=sqrt((vt(1)-TRAIN(:,1)).^2+(vt(2)-
TRAIN(:,2)).^2);
    dist=sortrows(dist);
        M=0;

```

```

        B=0;
    for jj=1:FinalK
    if dist(jj,2)==1
            M=M+1;
    else
            B=B+1;
    end
    end

    if M>B&&ii<=50
    TesttrueTable(ii,1)=1;
    end
    if M<B&&ii>50
    TesttrueTable(ii,1)=1;
    end
    end

    [Testsuccess
]=size(TesttrueTable(TesttrueTable(:,1)==1));

    feature1=VB';feature2=VM';
    mse = mse_classifier(feature1,feature1)
    mse(3)=0;
    syms x1x2real
    digits(5);
    eq3 = mse(1) + mse(2)*x1 + mse(3)*x2; teste3=vpa(eq3);

    feature2=-feature2;
    lbx1=min([feature1(2,:) feature2(2,)]);
    ubx1=max([feature1(2,:) feature2(2,)]);
    lbx2=min([feature1(1,:) feature2(1,)]);
    ubx2=max([feature1(1,:) feature2(1,)]);
    hold on

```

```
Test=TEST;
x1=Test(:,1);
x2=Test(:,2);
    Successtable=zeros(100,1);
for i=1:100
gg(i)= mse(1) + mse(2)*x1(i) + mse(3)*x2(i);

    g=gg;

if i<=50&&g(i)>0
Successtable(i,1)=1;
end
if i>50&&g(i)<0
Successtable(i,1)=1;
end
end
    Testsuccess=sum(sum(Successtable))

mean(K_FOLD_Validation)*2
```



## **CURRICULUM VITAE**

He was born in Tabriz on 16.05.1975. He completed high school in Tabriz Ashtab high school. In 1993 entered the Department of Electrical and Electronics Engineering of Tabriz Azad University. He worked at NCR Corporation of Iran branch during 1997-2010. In 2010, he received a master's degree in computer architecture from Tabriz Azad University. He started his Ph.D. program in 2011 in Karadeniz Technical University, Trabzon/Turkey. In 2013 he won a scholarship and began to work as researcher and education officer in Seraj Higher Education Institute of Tabriz/Iran.

### **Accepted and published papers:**

1. Vahdani-Manaf, N., Kayıkçıoğlu, T., Development of a novel physiological analysis method based on two wavelength photoplethysmography signals time difference variations, *Journal of Medical Imaging and Health Informatics* Vol. 6, 1-8, 2016.
2. Vahdani-Manaf, N., Kayıkçıoğlu, T., An improved method for dual-wavelength photoplethysmography with the ability to extract time difference features, *Second International Congress on Technology, Communication and Knowledge (ICTCK 2015)*, held on November 11-12 Mashhad Branch, Islamic Azad University.
3. Vahdani-Manaf, N., Kayıkçıoğlu, T., Comparison of time difference variations of photoplethysmographic signals with different wavelengths, *IEEE Signal Processing and Communications Applications Conference (SIU)*, 2015 23th, pp: 1134-1137.
4. Vahdani-Manaf, N., Kayıkçıoğlu, T., İki dalga boylu fotopletismograf işaretlerinin zaman farkı değişim analizi, *IEEE Signal Processing and Communications Applications Conference (SIU)*, 2014 22th, pp: 2241-2244.